The Pennsylvania State University

The Graduate School

School of Science, Engineering, and Technology

ANN-BASED PSS DESIGN FOR REACTIVE POWER REGULATION USING SYNCHRONOUS CONDENSER

A Thesis in

Electrical Engineering

by

Mohammed Abdullah Hatatah

Submitted in Partial Fulfillment
of the Requirements
for the Degree of

Master of Science

August 2015

The thesis of Mohammed Abdullah Hatatah was reviewed and approved* by the following:

Peter Idowu
Professor of Electrical Engineering
Thesis Adviser

Seth Wolpert
Associate Professor of Electrical Engineering

Scott Van Tonningen
Senior Lecturer in Electrical Engineering

Sedig Agili
Professor of Electrical Engineering
Chair of Graduate Program

*Signatures are on file in the Graduate School.

ABSTRACT

of

ANN-BASED PSS DESIGN FOR REACTIVE POWER REGULATION USING SYNCHRONOUS CONDENSER

by

Mohammed Hatatah

The behavior of the electric system requires a balanced operation between resources and customer demand including various electrical losses. As loads change, the reactive power requirements of the power system change. Since the reactive power cannot be transferred over long distances, voltage control has to be affected by using special equipment to keep sufficient levels of voltage in the power system network. The right selection of equipment for controlling reactive power and voltage stability are among the major challenges of system engineering [1]. With today's modern equipment designs and the modern control techniques, it is appropriate to again examine synchronous condensers as a reactive power solution. A synchronous condenser can work and support the system with an effective reactive power under low voltage conditions. In addition, it can raise the short circuit level of the system.

Stabilization is one of the most significant aspects in power system dynamics. The power system stabilizer (PSS) has become the primary means for supplying supplementary excitation signals to regulate reactive power delivery. In this thesis, the artificial neural network (ANN) was used to create a power system stabilizer. A three-layer feed-forward neural network PSS (FNNPSS) was employed. The back-propagation algorithm was used for the purpose of training. The main contribution of the control scheme is that it can improve the learning process by using the generalization property of the ANN. The test system (IEEE 9-bus) and the ANN-based PSS synchronous condenser were simulated in the MATLAB/SIMULINK environment. Results revealed that a system with ANN-based PSS can stabilize the system under various parameters in the power system.

TABLE OF CONTENT

LIST OF FIGURES

LIST OF TABLES

ACKNOWLEDGEMENTS

First of all, I would like to thank my advisor, Prof. Peter Idowu, for his constant guidance, encouragement and support. He has always gone above and beyond what I could expect. I have learned so much not only in the Electrical Engineering but also in the style of teaching and doing research.

I would like to thank all the committee members for all the suggestions and guidance.

I also wish to acknowledge the financial support from the Ministry of Higher Education, Saudi Arabia.

I would also like to thank my sisters for their encouragement and support throughout my Master's degree.

Lastly, and most importantly, I give my sincere appreciation to my parents for their unconditional support and making me a better person.

My deepest gratitude goes to my beloved wife and my children for their constant love and encouragement.

DEDICATION

To

My Beloved Family

Chapter 1

Introduction

1.1 Reactive Power Regulating

Alternating current (AC) is provided in a waveform of 60Hz. Reactive power is supplied when the current waveform is out of phase with the voltage, as a result of inductive or capacitive loads. The current lags voltage using an inductive load, while it leads voltage using a capacitive load. Current is in phase with voltage for a resistive load like an incandescent light bulb. Reactive power is highly essential in supplying the electric and magnetic fields in capacitors and inductors [1].

The behavior of the electric system requires a balanced operation between resources and customer demand including various electrical losses. Any abnormal loading of a generator may result in massive and costly damage. As loads change, the reactive power requirements of the power system change. Since the reactive power cannot be transferred over long distances, voltage control has to be affected by using special equipment located throughout the system to keep sufficient levels of voltage in the power system network. This has been occurring since the first power systems started. Increasing requirements, in regards to both the supply reliability and quality of supplied power, require the use of more modern compensators that are faster, more reliable, and have a broader range of applications. The right selection of equipment for controlling reactive power and voltage stability is one of the major challenges of system engineering [1][2]. These challenges gave birth to several methods to compensate reactive power.

The analysis of voltage limits and collapse is carried out throughout everyday operation analysis. In the events of voltage interruption or voltage collapse or when these are expected to occur, the operator starts to apply either no-cost or off-cost controls to maintain the voltages needed for system stability. No-cost control is the control that relates to the supplier, such as switching capacitors and reactors in/out of service, modifying and changing the output of the compensator, changing the generator's reactive output, fixing the tap position of the transformer, and finally switching lines or cables out of service—an aspect that is typically pre-analyzed for high voltage control. Secondly, the operator looks at off-cost control that relates to customer side, such as restricting non-firm transmission transactions to any market participant or re-dispatching generation. One final solution could be 'load shedding' if all the other control procedures fail. The synchronous condenser is what will be carefully discussed here as compensation equipment.

In recent decades, there has been significant progress in terms of equipment designed to enhance the voltage stability in power systems. This is due to the improvement of power supply systems worldwide, requiring better ways of controlling power flows and voltage levels. With the modern equipment designs existing today, and the modern techniques available for controls, it is appropriate to again examine synchronous condensers as a reactive power solution.

1.2 Reactive Power Control

Synchronous compensators have played a vital role in the voltage and reactive power control in a power system. A synchronous condenser is a simple synchronous machine with a slight difference that it is not intended to derive any mechanical load. Instead, it is connected to the power system, and then it runs freely without any mechanical load. In fact, it receives or provides the system with reactive power, according to the requirement of AC system, thus adjusting the system voltage within specified limits. After the synchronous condenser has been synchronized, its field current is controlled through an automatic control system, which in turn changes the reactive power in the system. With the synchronous condensers being employed in both the distribution and the transmission systems, not only would the system's stability be improved, but also its capability to transfer the active power would be enhanced.

A synchronous condenser is not aimed at converting electric energy to mechanical or vice versa. It utilizes the property of a synchronous motor which is explained through the V-curve. The V-curve is used to show the change in the armature current I_S as the field excitation current I_E of the machine is changed as shown in Figure 1.1. A synchronous motor takes a leading VA when its field excitation current is above a certain value and it takes a lagging VA when the field current is below such a value. Therefore, a synchronous compensator is a useful tool that can adjust the voltage level and act as a load compensator. First, it enhances the power factor by rendering or receiving the reactive power. In addition, the compensator removes the harmonics that form in the AC system through several factors such as nonlinear electrical loads [4].

As shown in Figure 1.1, when a synchronous motor runs in an overexcited region, it has at a leading power factor pf, thus supplying reactive power to the grid. However, when it runs in an under-excited region, it has a lagging power factor pf, thus absorbing reactive power from the system. Thus, a synchronous condenser is a highly useful tool for reactive power control, as well as an efficient component that can improve the stability of the power system network [6]. Note that P_s/P_N represents the per-unit power output.

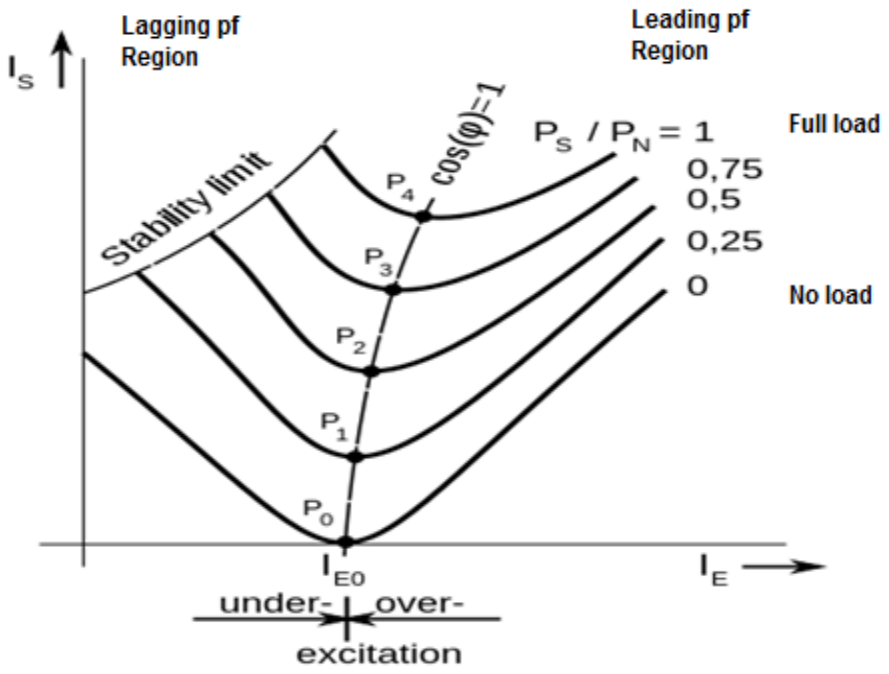

Figure 1.1: V-Curve for a synchronous condenser [3].

A brief review of the different devices being employed for reactive power control helps in the understanding of the performance characteristics of a synchronous condenser.

i. Static VAR Compensation (SVC)

The SVC is a set of electrical devices that is considered fast-acting reactive power controlled equipment. It functions to regulate the voltage, power factor, and harmonics in order to stabilize the system. If the load of a power system is capacitive (leading power factor), the SVC acts swiftly to absorb the reactive power, thus lowering the grid voltage. In case of an inductive (lagging power factor) load, its capacitor bank is automatically added to the system through thyristor switching, thus supplying reactive power to the system, and maintaining the voltage at its present value. Its advantage over the synchronous condenser is that its switching time is much shorter. Unlike synchronous condensers, the SVC does not have any rotating parts. Its disadvantages include the inherent ability to add harmonics to the system. Therefore, a harmonic filter has to be installed. However, the most serious drawback is that the maximum reactive current decreases linearly with the system voltage because the SVC becomes a fixed capacitor when the maximum reactive output is reached [5].

ii. Static Synchronous Compensation (STATCOM)

The STATCOM is a member of the family of Flexible AC Transmission Systems (FACTS). It is mainly a reactor with a voltage source behind it. It is used for voltage stability and power factor improvement in the power system. It can act as a sink or source of reactive power. Its advantage over the SVC is that it introduces fewer harmonics in the system. A STATCOM is considered better than an SVC as its reactive current can remain constant at reduced voltage levels [6]. In addition, it is current limited, so its reactive power output capability responds linearly with voltage.

iii. Synchronous Condenser (SC)

Several advantages can be observed with synchronous condensers compared to other equipment. First, its reactive current is independent of system voltage since the excitation system can control the internal voltage. In addition, it provides reactive power even in the event of a fault, since its output reactive current can be maintain under low voltage conditions [6]. Secondly, improving the system stability and power quality is solely dependent on the synchronous condenser's ability to raise the short circuit current in local faults. The transient reactance of the SC will be electrically parallel with the system equivalent impedance, which reduces the short circuit impedance. For instance, in a three-phase fault at a local transmission bus, the short circuit current is determined by dividing the internal voltage E by the sum of the subtransient reactance X''_d and the transformer leakage reactance X_t. Figure 1.2 is a simplified diagram that corresponds to (1.1).

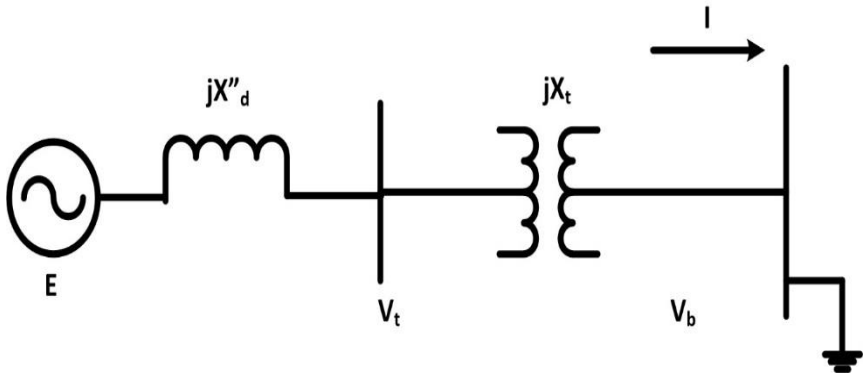

Figure 1.2: Synchronous condenser short circuit current.

$$I = \frac{E}{jX''_d + jX_t} \qquad (1.1)$$

In the case of no reactive power output, both the terminal voltage V_t and the internal voltage E will be equal to 1.0 p.u. Reactive power will be delivered to the system during maximum overexcited operation and the internal voltage E will be greater than 1.0 p.u. Hence, the short circuit current is increased.

Minimizing the reactance of both the synchronous condenser and the transformer will demonstrate the effectiveness of the condenser. Since the subtransient reactance is fixed in p.u. on the synchronous condenser MVA base, reducing the transformer leakage reactance is the only option. To give an example, consider the two following transformers, one with X_t = 0.12 and one with X_t = 0.06 p.u. connected to a synchronous condenser that has X''_d = 0.15 p.u. and an internal voltage E of 1.0 p.u. The short circuit current for the first transformer is 3.70 p.u. while the short circuit for the second one is 4.76 p.u. In general, it is more financially feasible to reduce transformer reactance to obtain a better short circuit current than to increase the condenser rating.

One of the most important features of synchronous condensers is that they act as a sink for harmonics [6]. In addition, high inertia is another interesting feature offered by the synchronous condenser. Their disadvantages include higher energy losses and longer response time. Modern control systems using a microprocessor-based controller can help improve upon the time response disadvantage [7][14].

Table 1.1 shows a comparison of synchronous condensers with other competing technologies based on different functional characteristics.

Table 1.1: Comparison of Synchronous Condenser with Other Competing Technologies [3-12].

Functional Characteristics	**SVC**	**STATCOM**	**Synchronous Condenser**
Solution type	Steady-state and Dynamic	Steady-state and Dynamic	Steady-state and Dynamic
Continuous VARS output	Leading/Lagging	Leading/Lagging	Leading/Lagging
Inherent transient overload rating	No	No	Up to 8x nominal
Real power output	None	None	None
Response to transient event	Sub-cycle	Sub-cycle	Sub-cycle
Response to severe voltage dips	No	Sub-cycle	Sub-cycle
Harmonic compensation required	Yes	Yes	No
Output dependent on bus voltage	Decreases with square of voltage	Decreases linear with voltage	Independent of bus voltage
Inertia adds to system stability	No	No	Yes

As synchronous condensers have been used for many years, several studies have been performed regarding their performance characteristics. Different operation modes have been studied and a large number of articles have been published in international journals to show the important role of synchronous condensers in the power industry.

Power system stabilizers (PSSs) are being widely used for synchronous machines. One of these stabilizers is the conventional power system stabilizer (CPSS), which is a fixed parameter analogue type of device introduced in 1950s. The CPSSs are being widely employed in the power system for dynamic system stability. However, the CPSS has some

inherent drawbacks. As the CPSS is a linear controller, it cannot be operated efficiently for different operating conditions as its quality of performance represses [17][18][19].

In the seventies, the inertia of an HVDC transmission system was one of the most important topics under study. Since inertia is the ability of something to retain its state under disturbances, the inertia of a system can be regarded as a system's ability to preserve the voltage at the inverter bus during any disturbance that it may encounter. In addition, inertia helps machines to maintain their speed and system frequency. Synchronous condensers provide frequency stability, and they depend upon the energy that is stored in the rotor [3][12][13].

Later on, power system stability was improved by using semiconductor technology such as SVC and STATCOM. Several studies have been performed to demonstrate the differences between conventional synchronous condensers and FACT devices, based on their characteristics of overload capability, low voltage output, short circuit strength and inertia. Results have shown that their characteristic performances are different since electronic solutions are possible. Each of these technologies has its own advantages and disadvantages [4][5][6].

Many non-conventional, environmentally friendly methods have been employed for electric power generation, such as wind turbine farms and solar plants. Extensive research has been carried out on these techniques so that the conventional energy sources can be replaced with renewable ones. However, these plants have their own operational characteristics, which are distinct from the generation of conventional energy. They are connected to a converter bus that has very low inertia. Moreover, energy production derived from these plants is a stochastic process, due to variable wind speed and irradiation. High inertia is always preferred in transmission systems especially if the system has a low number of conventional units. Synchronous condensers have the ability to provide dynamic voltage support. However, since these condensers are mainly synchronous motors, they consume active power as well. The active power usage is usually 3% of the rating of a synchronous condenser. For instance, a 50 MVAR synchronous condenser will consume 1.5 MW of active power [3][15].

Excitation controllers have been greatly utilized within power systems for years. The principal purpose of these controllers is to obtain a satisfactory voltage profile for the consumer. They also manage reactive power flow within the network [46][50][73]. Conventional excitation systems are linear controllers, having fixed gains because their gain values are determined at some particular operating condition. The gain of these systems become a problem when the operation condition changes from one point to another point. In some cases, a value of gain settings which are proper for one operating condition

may be unsatisfactory for another condition [9][73]. Thus, the controller must be able to work with different ranges of operating conditions and to provide a suitable performance when operating conditions of the power system change.

Planning departments in various electric utility organizations, such as Vermont Electric Power Company (VELCO) have carried out important studies on synchronous condenser-based reactive power devices [7]. Other papers provide performance considerations of different compensator technologies [5][29]. Some utilities also study isolated systems to enhance system reliability and improve the power factor, such as the case of Jeju Island [8].

With the modern machine design today, and the modern techniques available for control, it is appropriate to again examine synchronous condenser as a dynamic power solution. Table 1.2 shows various evolution of compensation devices.

Table 1.2: History of Compensator Technology.

Compensator	**Function of compensation**	**References**
Synchronous Condenser	Regulating of power since 1920's	2, 3
Synchronous Condenser	Power system stabilizer CPSS was introduced in 1950's	16, 17, 18, 19
Synchronous Condenser	HVDC transmission system during 1970's	3, 12, 13
Flexible AC Transmission System (FACTS)	SVC and STATCOM around the year 1980	4,5,6, 26, 27
Synchronous Condenser	Renewable energy, such as wind turbine farms and solar plants.	1, 3, 6, 15
Synchronous Condenser	A number of control methods such as Adaptive PSS, Fuzzy Logic Based PSS, and Neural Network-Based PSS.	21, 22, 23, 24, 33, 34, 35, 36, 37, 38, 39, 40.

One of the innovative control techniques is artificial neural networks (ANNs) that aim to have a satisfactory performance through intensive interconnection of basic computational factors [21]. ANNs take their structure from the brain. ANNs are a biologically motivated computational model consisting of neurons that are connected to specific weights in order to create a network's structure. The weights and connections have an important role in a neural network. Thus, they are known as the memory of the system and can be enhanced with more training [77]. Several training techniques are assigned to the network's structure. Better models can be achieved by developing the training techniques [78].

The key factor of ANNs is their generalization ability as solutions to various problems. The generalization refers to the behavior of networks in the new situations. The generalization ability of a network can be enhanced by using small networks as much as possible. This is only one method provide the generalization ability to the network [79].

Several methods can be used to accomplish generalization ability. Cross validation is one method. This approach is repeated throughout the learning stage until the error lessens for both training and test set data. Finally, the optimal network is selected [79][81].

Another method which can be used is multi-objective optimization which uses several cost functions in place of using the sum of the squared error of the network data [80]. The approach balances these cost functions [82]. The performance function is modified by adding a factor to the cost function, representing the mean of the sum of the squares of the network [83].

Siraj and Osman suggested a method for increasing the generalization of the network. Their approach used multiple classifier systems. Managing the advantages of different classifiers enhance the generalization ability of the network [84].

Hua et al. proposed a new function for a hidden layer to improve the generalization ability, which was created by using two terms, the fuzzy entropy and the cross entropy [85].

1.3 Different Types of Stabilizers

Excitation controllers have been greatly utilized within power systems for years. The principal purpose of these controllers is to obtain a satisfactory voltage profile for the consumer. They also manage reactive power flow within the network.

1.3.1 Power System Stabilizer (PSS)

Conventional power system stabilizers (CPSSs) have been enhancing the dynamic stability of power systems for a long time. The primary function of the PSS is to include some damping in the generator rotor oscillations by incorporating its excitation in the auxiliary stabilizing signal. In order to provide the damping, the stabilizer must produce a component of electrical torque, which is in phase with the rotor speed deviation. A simple PSS can be designed through two identical stages, lead/lag network, which is represented by K_{STAB} and two-time constants T_1 and T_2. A washout block of time constant T_w is also connected as shown in Figure 4.1.

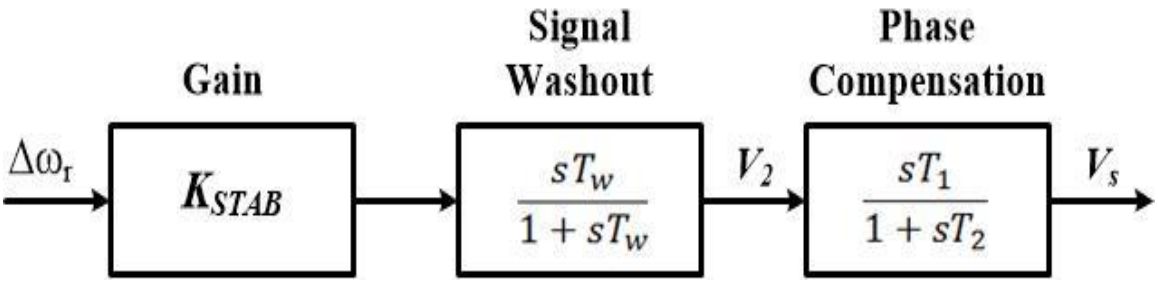

Figure 1.3: Block diagram of conventional PSS.

In Figure 4.1, the phase compensation block provides the phase lead, which compensates for the phase lag between the exciter input and the generator torque output. The signal washout block is a type of high pass filter that has the time constant T_w, thus removing the signal having frequency below ω_r and allowing the signals of frequency higher than ω_r, thereby removing the DC component from the signal. If the washout is not used in this situation, the PSS will then modify the terminal voltage for even a slight change in the rotor speed. Now, the PSS will only respond when a reasonable change in speed occurs. The value of gain K_{STAB} corresponds to the amount of damping introduced in the system. Ideally, this gain should be set in a way to include maximum damping, but it is restricted by some other considerations.

On the other hand, CPSS has its own disadvantages; some of these problems are presented below:

i. Linear model accuracy for the power system.
ii. Parameter accuracy for that model.
iii. Efficient tuning of the CPSS parameters.
iv. Interaction between different machines.
v. Tracking of the non-linearity of the system.

Extensive research has been performed to counteract these problems [17]. A great number of tuning techniques have been utilized in order to efficiently tune the parameters of the CPSS [18]. The interaction between CPSSs within systems of multi-machines has been analyzed as well [19]. In order to counteract the problem of parameter tracking, the theory of variable structure control was applied to create the CPSS [20].

1.3.2 Adaptive Power System Stabilizer

Adaptive control theory presents feasible solutions to the aforementioned obstacles associated with the CPSS. Both the input and output of the generating unit are sampled at each sampling interval. Then a mathematical model is acquired by a specific on-line identification tool so as to symbolize the dynamic behavior of a generating unit at that particular instant of time. It is also predictable that the mathematical model, acquired with each sampling process, can track the modifications within the system.

The control signal needed for the generating unit is created according to the identified model after the process of model identification. There are many control strategies, among which are the Pole Assignment (PA) and Pole Shifting (PS) methods [33]. Such control strategies are typically designed by accepting the identified model as the actual mathematical description of the generating unit [34][35]. However, due to the fact that the power system is a nonlinear continuous system of high order, it is difficult for the discrete identified model of low order to thoroughly explain the dynamic behavior of a power system. As a consequence, a discrete model of high order is utilized to stand for the power system. It consumes a great amount of computing time. The computing time of an adaptive PSS is almost proportional to the square of the order of the discrete model utilized in the identification process. Extended computing time restricts the control effect. This has a more powerful impact when the oscillation frequency is extremely high. There has to be a co-ordination between the discrete model order and the computing time of the parameter identification and optimization.

1.3.3 Fuzzy Logic-Based PSS

The Fuzzy Logic Control (FLC) is one of the most innovative methods that has been utilized lately in a number of controller designs. These systems are rule-based ones where a group of fuzzy rules symbolizes the mechanism of control decision in order to amend the effects of specific causes derived from the system [36]

The following features are associated with FLC [37] [38]:

i. Model-free based: In contrast to other conventional control methods, this tool does not need the exact mathematical model of the system.

ii. Robust nonlinear controller: FLC presents different methods to employ basic but robust solutions that can serve a broad range of system parameters. It can also handle significant disturbances.

iii. Development time reduction: FLC performs on two different levels of abstraction—the symbol level and compiled one. The symbol level is used for explaining the strategies of application engineers, while on the other hand, electronics engineers are very familiar with the compiled level. Due to the fact that there is a definite translation between these two levels, an FLC can be useful in counteracting communication obstacles.

iv. Knowledge-based: Fuzzy control resembles the strategy of the agent controlling a certain process. Therefore, control strategy simulates human thinking. Similarly, the experience of a human operator can be performed through an automatic control method, rather than the reluctant response of a human controller.

Designing FLC-based stabilizers has been a highly active area of study. Adequate results have been acquired [39][40]. Even though FLC presents an acceptable method to deal with sophisticated, ill-defined and nonlinear systems, there is a disadvantage associated with it, which is the parameter tuning of the controller. There is not yet a single systematic method for the designing of the FLC. However, the most direct strategy is to identify the Membership Functions (MFs) and decision rules in a subjective manner, through examining an operating system or existing controller. Thus, it is necessary to find an effective method of tuning the MFs and decision rules, so that the output error can be minimized and for the performance index to be maximized, as well.

1.3.4 Neural Network-Based PSS

Artificial Neural Networks (ANNs) aim to provide satisfactory performance through intensive interconnection of basic computational factors [21]. The structure of the ANNs relies on the current knowledge of biological nervous systems.

ANNs include a variety of advantages [21]:

i. The ability to synthesize sophisticated and transparent mappings.
ii. Swiftness caused by a parallel mechanism.
iii. The tolerance to robustness and fault.
iv. The ability to adapt to new environments.

Results of research carried out on the application of ANN in power system stability has been stated in [22][23][24]. The effective way with which ANNs can handle and manage unfamiliar systems with uncertainty makes ANNs a strong candidate for further research. On the other hand, there are some disadvantages associated with conventional ANNs, some of which are described below:

i. Black-box features: It is a complicated task for an outside watcher to comprehend or change the process of decision making of a network. This is because preliminary values for the parameters are arbitrarily selected.
ii. Extended training time: ANNs may need an extended training time to reach the required level of performance. The bigger the size of the ANN and the more sophisticated the mapping needed performing, the longer the training time necessary will be for the process.

1.4 Problem Statement

Voltage stability is associated with the way a power system maintains satisfactory voltage levels for all the nodes under regular, common and contingent conditions. A power system is believed to have the problem of voltage instability if a disturbance results in a consistent and uncontainable reduction in voltage level. Voltage instability progress is mainly the result of a disturbance or change in the conditions of operation. This can trigger increased need for reactive power [9] [30].

Reactive power support voltages have to be managed for reliable consistent operation of power system. There have been serious worldwide blackouts associated with lack of reactive power. One of these blackouts was the blackout of August 2003, which occurred

in the United States and Canada as shown in Figure 1.4 [41]. A great number of the incidents of voltage collapse have taken place across the world as presented in Table 1.3

Figure 1.4: Display of the black-out on August 14, 2003 [41].

Table 1.3: Voltage Collapse Incidents.

Date	**Location**	**Duration**
April 13, 1986	Winnipeg, Canada	1 second
Nov. 30, 1986	Brazil, Paraguay	2 seconds
May 17, 1985	South Florida	4 seconds
Aug. 22, 1987	Western Tennessee	10 seconds
Dec. 27, 1983	Sweden	55 seconds
May 21, 1983	Northern California	2 minutes
Sep. 2, 1982	Florida	1-3 minutes
Aug. 4, 1982	Belgium	4.5 minutes
May 20, 1986	England	5minutes
Jan. 12, 1987	Western France	7 minutes
July 23, 1987	Tokyo	20 minutes
Aug. 22, 1970	Japan	30 minutes
Sep. 22, 1970	New York State	Several hours
Aug. 14, 2003	Several States of United States of America and part of Canada.	Some power was restored in hours and many others got it back two days later

Under market environment, the rise of load demand and power transfer encourage the interconnected power system to perform under extremely difficult conditions. It is possible for a voltage collapse to take place within a heavily–loaded system. It has been a significant operational concern when generation re-dispatch is required to handle the obstacle. This is associated with the dispatching of a bulk unit and the cost of total production.

In this research, we want to design a power system stabilizer for a synchronous condenser, based on artificial neural network (ANN-based PSS), to regulate reactive power delivery and to demonstrate the effectiveness of the controller on the IEEE 9-bus system. In addition, we want to develop a better understanding of reactive power control with the help of the customized performance function of the artificial neural networks for the power stabilization system. Moreover, we aim to maintain the voltage within acceptable levels set by the American National Standard for Electric Power Systems and Equipment (ANSI) which specifies service voltage limits should fall between 97.5 % and 105 % of nominal voltage.

As the IEEE 9-bus system was utilized as a system model, bus no. 5 was chosen to connect the synchronous condenser. This particular decision was made according to a study of the eigenvalue capabilities of the IEEE 9-bus system that show bus no. 5 to be weak compared to the other buses.

As mentioned a neural network is capable of learning and performing more efficiently than the conventional excitation system. The neural network used in the training process encompasses several characteristics. The artificial neural network (ANN) is composed of processing networks arranged in a layer sequence. There are three layers, namely the input layer, the hidden layer and the output one. A three-layer feed-forward neural network (FNN) is employed [71]. In fact, the FNN is a static mapping technique. For dynamic problems, a great number of neurons are needed for the dynamical responses in the time domain.

General tasks are planned as follows:

i. Modeling an IEEE 9-bus system, then implementing it in the simulation program MATLAB/SIMULINK.
ii. Verifying results for IEEE 9-bus system with another case simulated in PowerWorld environment, and modal analysis.
iii. Designing an artificial neural network scheme for excitation system.
iv. Comparing the performance of a conventional excitation system with an ANN-Based PSS. Then, comparing the response of an ANN-based PSS with a SVC device.

The Power system model and synchronous condenser along with the control scheme will be simulated in the MATLAB/SIMULINK environment. Finally, all the studies and simulations will be presented in a final report of the thesis project including all the details and descriptions.

1.5 Motivation

On August 14, 2003, as shown in Figure 1.4, a severe blackout struck several U.S states. The blackout had severe effects on the North Eastern interconnection as 63 GW of the load was disconnected from the distribution feeders. This was approximately 11% of the total load distribution in that area. Many states, including New York, Michigan, Ohio and part of Pennsylvania, were affected by this massive blackout. Because of the cascading loss of major tie lines in Michigan and Ohio, large amounts of reverse power flow were serving loads in the Michigan and Ohio system and caused heavy loading in that area. This resulted in a power outage in the area supplied by these lines [1].
This blackout affected a population in several states. Had the blackout lasted for several more hours, the effect on people would have been more severe. The impact of this blackout motivated me to study this event and contribute to the work of others in this field.

1.6 Thesis Structure

Chapter 1: Reactive Power Compensation, Reactive Power Control and problem statement;

Chapter 2: Power System Model, Power System Stability and Reactive Power Management;

Chapter 3: Test System Description and Modeling of Synchronous Condensers;

Chapter 4: ANN-based Power System Stabilizer Design;

Chapter 5: Observing and comparing the performance of an ANN-Based PSS;

Chapter 6: Conclusions and Suggestions.

Chapter 2

Reactive Power Control

In practical power systems, system voltage needs to be continuously monitored in order to minimize the effects of change in load, generator and the network structure. Power system voltage control has become a very important concern. In 1994, Kundur identified voltage control as: "voltage at the terminals of all equipment in the system should be kept within acceptable limits, to avoid malfunction of and damage to the equipment" [9]. By keeping the voltage within the acceptable limits of a system, system stability can be enhanced and more active power can be transferred through the same transmission system. In addition, the active, as well as reactive power losses can be minimized by reducing the reactive power flow in the power system. Consequently, complex control schemes are needed for the design.

2.1 Power System Model

A power system is a complex network of electrical components, which aims to transfer electric power from generating stations to the end user. A power system network comprises three-phase alternators connected to the distribution feeders through three-phase transmission lines, and operating at 60 Hz (or 50 Hz) frequency. It is developed according to the geography and the user's load requirements, and is adjusted based on increased demands. A power transmission network can be modeled as:

$$I = YV \qquad (2.1)$$

Where: I represents the current, V represents the voltage and Y is the admittance of system.

It is normally assumed that all three phases are balanced so only a single phase is represented. A large power system may have thousands of generators connected together to form an interconnected system, and the size of (2.1) will consequently change. The current injections are taken as positive if they are supplied to the power network by the generators, but considered negative when the current is reversed to the generator. However, it is more convenient to represent this in terms of the power injections S while the mesh network can be represented as (2.2), instead of (2.1),

$$S = g(V) \qquad (2.2)$$

Where g is a non-linear function relating the system node voltages to the power injections *S*.

Hence, the steady-state representation of the power system will have a large number of non-linear algebraic equations representing the system's components and associated constraints [1][3].

Most of the generators and some of the loads are rotating machines that rotate steadily at 60Hz. In other words, the electric field in these rotating machines is 60 Hz while the mechanical rotor speed depends upon the design being employed in each machine. The synchronous machine rotates at speeds that are multiples of 60 Hz depending upon the number of poles as shown in (2.3).

$$f_e = \frac{P}{120}\, n_m \qquad (2.3)$$

Where: f_e is the electrical frequency, Hz; n_m is the rotor speed of the machine, rpm; P is the number of poles.

The system's operation changes because the consumer's load demand varies throughout the year. The demand can even become quite inconsistent from one day to another. Thus, the power system is constantly under perturbations. If the disturbance is significant, i.e. an outage of a large generating unit, sudden load changes, transmission line faults and line switching, the system will be unable to retain its synchronism and some of the machines within that system will deviate significantly from 60 Hz. A major disturbance on the system can also be identified as the one during which the nonlinear equations representing the system dynamics cannot be linearized for analysis. In the same manner, a minor disturbance is the one during which these nonlinear equations can be validly linearized. A change in the gain of the automatic voltage regulator (AVR) in the excitation system of a large generating station operating in a huge power system is an example of a minor disturbance. If a power system is in a steady-state operation and a minor disturbance occurs, but the system retains its state, that system is then known as steady-state stable. However, if such a disturbance is major and the system adjusts itself to some other stable state rather than the original one, that power system is transiently stable. The analysis of power system transient stability has become more important to study than others in order to avoid the disruption of power supply to the customer upon any large disturbance. Therefore, power systems are designed and operated with the factor of reliability as a top priority.

The rotating machine dynamics can be modeled as:

$$M\omega' + D\delta' = P_a = P_m - P_e \qquad (2.4)$$

Where δ is the angular displacement of the rotor from a synchronously rotating reference axis, while ω=δ' is the deviation of the synchronous speed. M and D, being constants, are rotational inertia and damping of the machine. Pa is the accelerating power, which is equal to the difference between mechanical and electrical power.

Equation (2.4) can also be written in terms of the first two differential equations [2]. This type of modeling will be an approximate since Pe is the real power injection at the electrical node, instead of the complex power *S* that is used in (2.2). Moreover, the terminal voltage of the generator is dependent on the speed of the rotating shaft. Hence, when the system is more prone to variation in rotor speeds as in the case of wind turbine generators, a more experienced assembly, known as power system stabilizers (PSS), is usually employed. On the other hand, the governor of the turbine system controls the mechanical power P_m. Thus, at least two differential equations are needed to represent the rotating machine dynamics and if modeling the exact dynamics of rotating machinery is needed, dozens of differential equations will then be required. Hence, during practical cases, the variable is incorporated according to the general requirements, depending upon how sophisticated the control of the machine is. Finally, the power system, while incorporating all the dynamics, can be represented as follows:

$$X' = f(X) \qquad (2.5)$$

Where X represents variables such as the rotor angle, rotor speed, terminal voltage and internal variables of the machine, exciter and governor.

The terminal voltage is the same as the node to which the generator is connected. Also, P_e that is used in (2.4) is the real component of the complex power *S* used in (2.2). Hence, (2.2) represents the static network while (2.5) represents the machine dynamics, which are connected through both the power injection and voltage at the generator nodes.

2.2 Reactive Power Management

Voltage control, i.e. keeping voltage within limits, in electrical systems is very important for the proper operation of the equipment connected to the system. It is also critical for an efficient transfer of electric power through the transmission lines, and to avoid voltage collapse and disturbances. Certain cases, such as increase in load, less generation, or transmission facilities, cause the drop in voltage. This is accompanied by the decrease in reactive power in the system, i.e., voltage drops when reactive power in the system decreases. However, reactive power must be available all along to transmit the electric power to the end user. As soon as voltage decreases, the current in the transmission line increases to maintain the power supply to the end user. If the current increases dramatically, transmission lines go off line, overloading other lines, which can cause cascading failures. If the voltage drops dramatically, some generators will disconnect.

With the increase in the transmission current, the reactive power utilization in the system increases too, which further reduces the reactive power and thus the voltage of the system. If this decrement in voltage continues, the stress on the transmission lines will continue to increase, which will result in an automatic outage of the lines loaded at their threshold. As a result, voltage collapse will occur, causing a blackout. Hence, the reactive power is a very important factor to maintain in the interconnected power system for the proper operation and transmission of electric power [2][3].

A simplified model of a power transmission system is displayed by a single transmission line having inductance X_L with two power grids connected at the buses 1 and 2, as shown in Figure 2.1(a). Their nominal voltages are 22 kV and 11 kV, respectively. The phasor diagram is shown in Figure 2.1(b), where $\delta=\delta_1-\delta_2$ is the angle between the two power grid bus voltages.

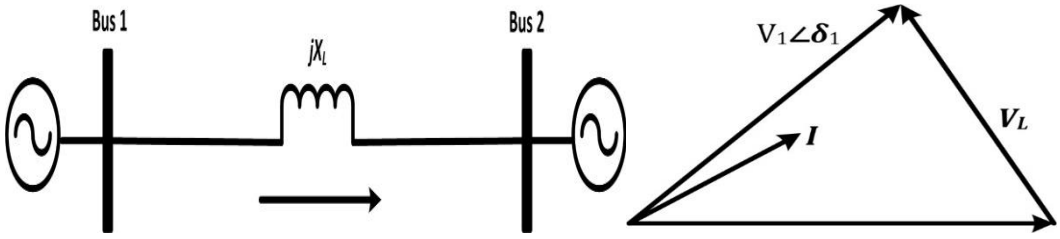

Figure 2.1: Power transmission system (a) Simplified model (b) Phasor diagram.

The magnitude of the transmission line current is given by:

$$I = \frac{V_L}{X_L} = \frac{|V_1 \angle \delta_1 - V_2 \angle \delta_2|}{X_L} \quad (2.6)$$

(The transmission line is assumed to be lossless and the line resistance is ignored.)

The magnitude of complex current flow at the bus 1 is given by:

$$I_{d1} = \frac{V_2 sin\delta}{X_L} \quad , I_{q1} = \frac{V_1 - V_2 cos\delta}{X_L} \quad (2.7)$$

And the active and reactive power can be written as:

$$P_1 = \frac{V_1 V_2 sin\delta}{X_L} \quad , \quad Q_1 = \frac{V_1 (V_1 - V_2 cos\delta)}{X_L} \quad (2.8)$$

In the same way, the complex currents at bus 2 can be written as given by (2.9):

$$I_{d2} = \frac{V_2 sin\delta}{X_L} \quad , \quad I_{q2} = \frac{V_2 - V_1 cos\delta}{X_L} \quad (2.9)$$

Also both the active and reactive power at bus 2 are given by (2.10):

$$P_2 = \frac{V_1 V_2 sin\delta}{X_L} , \quad Q_2 = \frac{V_2 (V_2 - V_1 cos\delta)}{X_L} \quad (2.10)$$

Equations (2.6) to (2.10) show that active and reactive power/current can be controlled by changing the voltage, transmission line reactance, and adjusting the phase angle between the sending and receiving end.

Note that the reactive power will have maximum value when the phase angle reaches δ = 90°. In practice, the phase angle is normally kept less than 90°, as shown in Figure 2.2, so that the system can bear the transient and oscillatory disturbances [3].

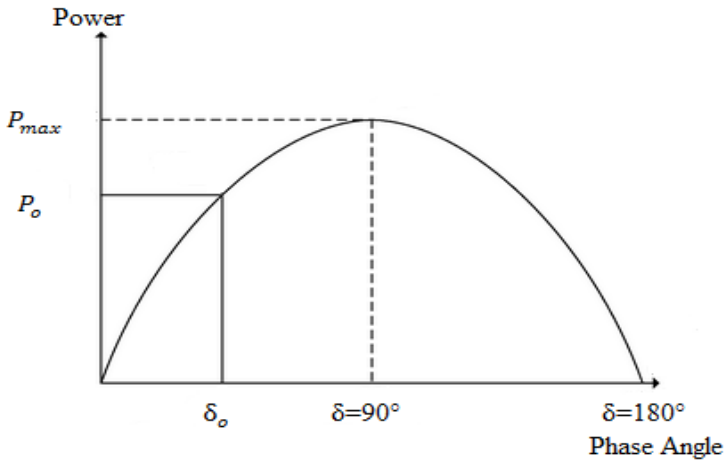

Figure 2.2: Power angle curve.

2.3 Power System Stability

A great number of modern-day power systems are similarly interconnected as thousands of power generating stations, so that the quality and reliability of electric power supply to the customer can be enhanced. When generators are operated with reciprocating turbines, a sustained oscillation in their frequency occurs due to the oscillations in the mechanical torque supplied to the rotor of a generator. These periodic variations in the voltage and frequency are transmitted to the motors connected in the power system at the user's end. With the interconnection of so many generators together, the problem of power system stability and synchronism is also heightened. Thus, system stability has gained extremely critical importance during the design and extension of an interconnected system across vast geographical regions.

Over the years, extensive efforts have been made to improve system stability. Various methods have been developed and employed while the method of excitation control has become very popular. This is due to the following:

i. Electrical control systems are more economical than mechanical systems and even more sophisticated control schemes can be implemented
ii. Time constants of the electrical control systems are much shorter than those of the mechanical systems, i.e. the response time is very short

iii. Additional equipment can be easily attached and operated at a much lower cost, compared to other methods (capacitor switching and resistance braking)

Moreover, it is well known that voltage stability is a dynamic state phenomenon. The dynamic analysis reveals the use of a model described by nonlinear differential and algebraic equations, such as generator dynamics, induction motor loads and tap changing transformers. However, dynamic studies are time-consuming in terms of computer speed and the specific engineering requirements for analysis. Thus, the dynamic simulation applications are limited to the examination of specific voltage collapse situations, such as the transient state in a specific place. Moreover, dynamic simulation can be used for the coordination of protection systems and voltage controls [44].

Chapter 3

Test System Model

In this chapter, the test model IEEE 9-bus system will be presented. The IEEE 9-bus system is implemented into the MATLAB/SIMULINK and verified with another case simulated in the PowerWorld environment. The method for identifying the weakest bus will be explained in order to determine where the synchronous condenser should be connected. Then, the synchronous condenser model will be demonstrated. Also, the design of the excitation system will be illustrated.

3.1 Test System Description

In the test system in Figure 3.1, equivalence method, the process of reducing all buses, is utilized to minimize simulation time. This is beneficial when studying a large power system having hundreds of thousands of electrical components connected together so that the number of components can be reduced for analysis purposes. However, this simplified model has a disadvantage: it can only be used for the analysis study for which it has been reduced. The model system has approximately the same characteristics as the original one, plus the fact that it saves time. Therefore, engineering insight is needed to optimize the relationship between the equivalent model size and accuracy of simulation results.

In 1949, Ward introduced the first equivalence method, which is still widely used. Another classical method of equivalence, known as Radial, Equivalent and Independent (REI) was developed [9]. The PowerWorld simulator utilizes the Ward-type technique.

There are two types of equivalencing: static and dynamic. Static equivalence is the network reduction for planning and development and monitoring the system online. On the other hand, dynamic equivalence is used for modeling the synchronous machines for the purpose of studying the transient stability behavior of the original system. Dynamic equivalence also includes the modeling of loads [9].

The test system under study is the IEEE 9-bus system, which represents the western system coordinating council (WSCC). This 9-bus system has three generators and three loads as illustrated in Figure 3.1. In the WSCC system, bus no. 5 has a load of 125+j 50 MVA, while bus no. 6 has a load of 90+j 30 MVA and finally a bus no. 8 has a load of 100+j35 MVA. The generators and lines data are given in Appendix A.

Generators 2 and 3 are supplying 163 MW and 85 MW power respectively in the base case loading conditions. The MVA Base is 100 MVA, the KV base is 230 KV and the system frequency is 60 Hz.

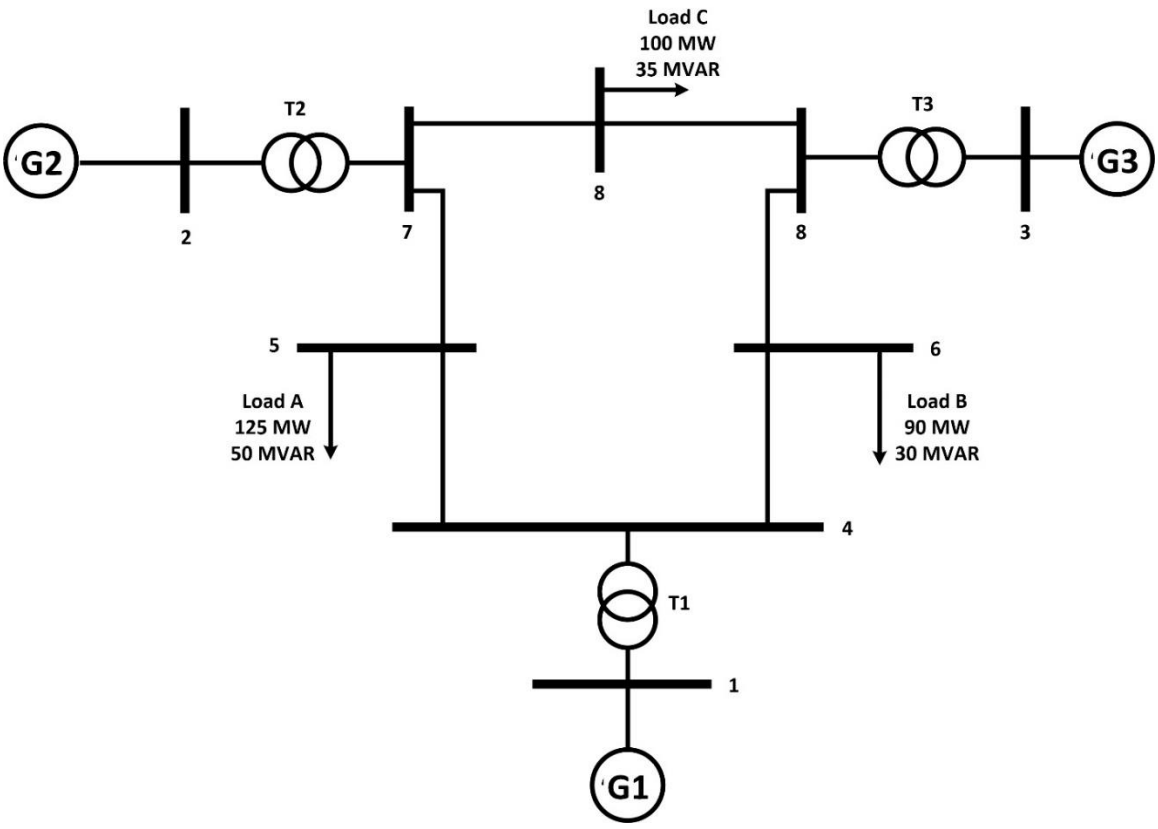

Figure 3.1: IEEE 9-bus system.

Minimum eigenvalues, associated with instability, have to be taken into consideration and treated more seriously. The most suitable definition of which bus takes part in the determined modes become highly critical. This typically requires a participation factor tool to identify those buses that are of the weakest nature and having a negative impact on the chosen modes [70]

The method of modal analysis is implemented in the IEEE 9-bus system. The voltage profile of buses is shown in the simulation of load flow. In addition, the least eigenvalue of the reduced Jacobian matrix is identified. After that, load buses of the weakest nature, contribute to a voltage collapse, are detected by the computation of the participating factors. The results are then described in Figure 3.2 and Figure 3.3.

Figure 3.2 illustrates the voltage profile of all buses of WSCC, 3-Machine 9-Bus system, that are acquired through the load flow. As shown, all the bus voltages are within the allowed level (± 5%). Bus no. 5, as presented, has the least voltage value compared to the other available buses.

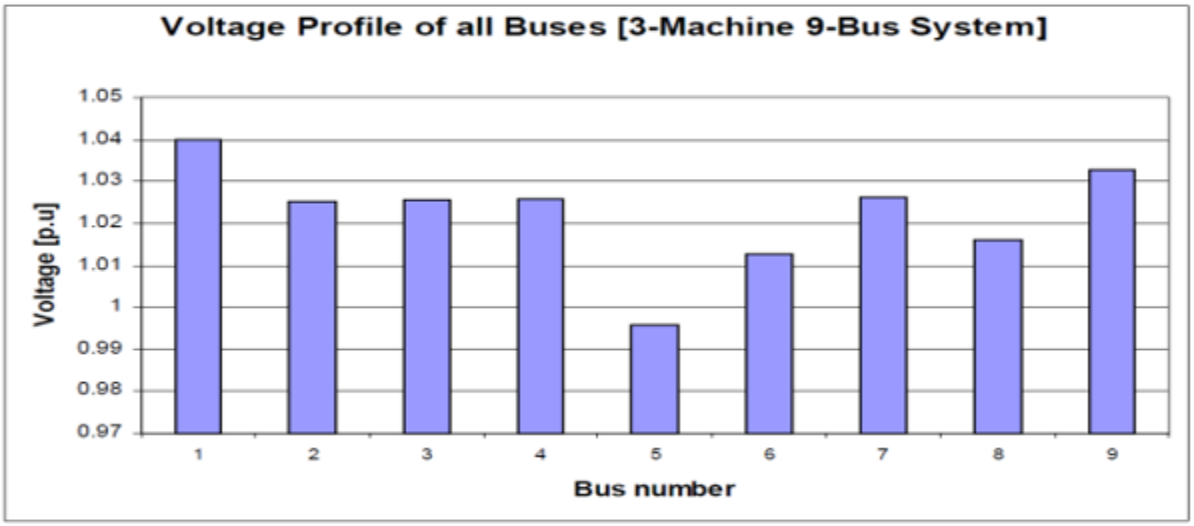

Figure 3.2: Voltage profile of all buses of IEEE 3-machine 9-bus system.

Due to the fact that there are nine buses, one is a swing bus and two of them are generator buses (PV). The overall number of the eigenvalues of the reduced Jacobian matrix JR will be six as described in Table 3.1. It is worth mentioning that all the eigenvalues are positive, which is an indication of the stability of the system.

Table 3.1: IEEE 3-Machine 9-Bus System Eigenvalues [45].

#	1	2	3	4	5	6
Eigen value	51.0938	5.9589	46.6306	12.9438	14.9108	36.3053

Note that for all the small eigenvalues, bus participation factors identify the area close to voltage instability. From Table 3.1, it can be seen that the minimum eigenvalue 5.9589 is the most critical mode.

The next step is to calculate the participating factor for this mode and the result is shown in Figure 3.3. This Figure shows that bus no. 5 has the highest participation factor to the critical mode. The largest participation factor (0.3) at bus no. 5 indicates that this bus is the most critical bus contributing to the voltage collapse.

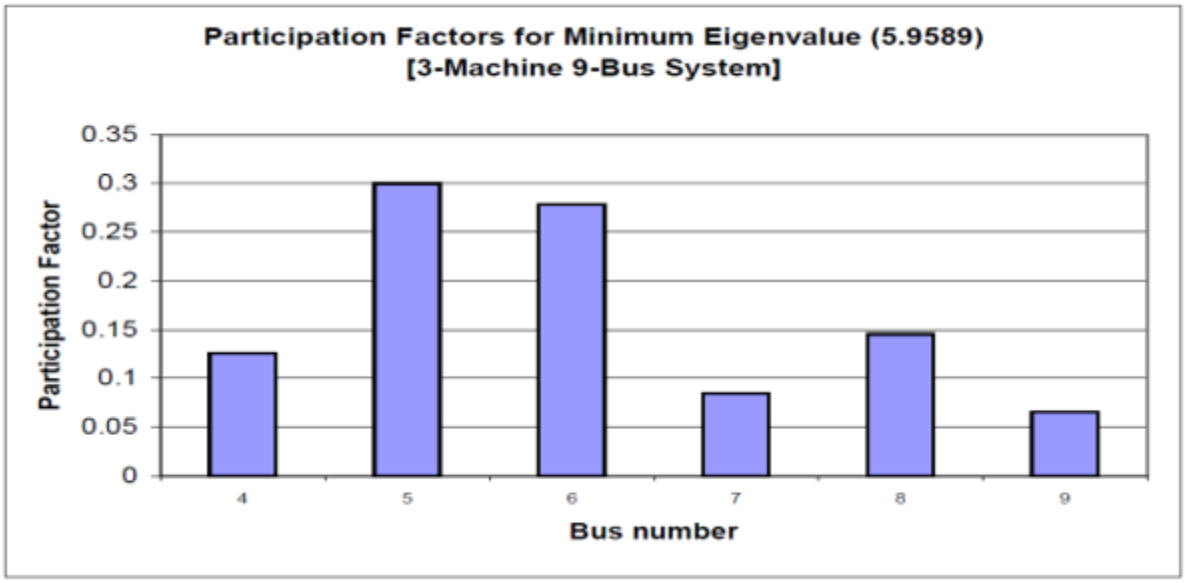

Figure 3.3: Participating factors of all buses for most critical mode of IEEE 3-machine 9-bus system [45].

By using Q-V curves, it is possible to know the maximum reactive power that can be added to the weakest bus before reaching the minimum voltage limit or voltage instability. In addition, the calculated Mvar margins relate to the size of the compensator in the load area.

So, bus no. 5 was chosen to connect the synchronous condenser. As mentioned above, this particular decision was made according to a study of the eigenvalue capabilities of the IEEE 9-bus system that shows bus no. 5 to be weak compared to the other buses. To be consistent with other generators, the synchronous condenser that has approximately the same MVA rating as the other generators, which is 100 MVA, was chosen. We have connected the condenser to bus no. 5 through a 13.8 / 230 KV transformer.

3.2 Modeling of Synchronous Condensers (SCs)

Figure 3.4 illustrates a simplified model of the SC and its control. The amount of reactive power is determined by the internal voltage of the generator, which is proportional to the excitation current. Thus, by changing the excitation current, the amount of reactive power flow between the SC and the power system network can be varied to maintain the terminal bus voltage.

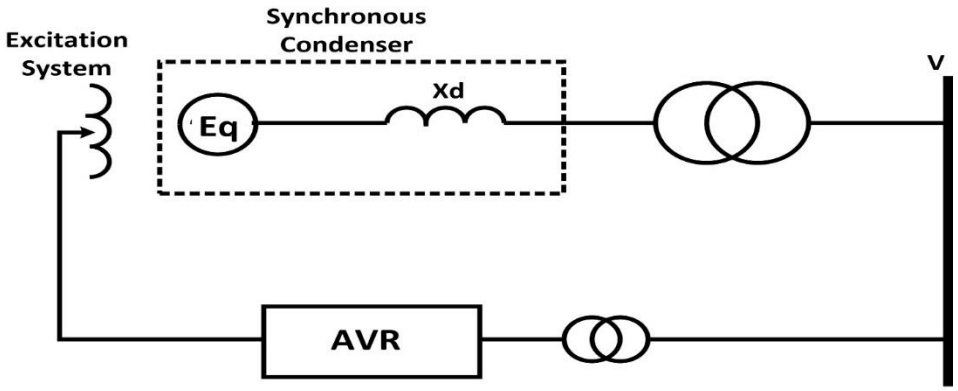

Figure 3.4: Synchronous condenser circuit and VI characteristics.

In steady state conditions, the SC can be considered as a voltage source that keeps the bus voltage constant before its reactive power limit is reached. During a voltage droop – the intended loss in output voltage from a device as it drives a load – , the SC regulates the bus voltage in a slight slope with respect to the reactive current. When the reactive power limit is reached, the SC can be modeled as a current source. The current limit is applied by introducing an overcurrent relay. This is a balanced model where the relay trips if a large amount of current persists for a longer period of time. During the transient overcurrent, this relay is not considered as it is set to operate after a particular time following a fault's event. This relay operation time is slightly longer than that of the transient fault current. Thus, the excitation ceiling determines the synchronous condensers output during transients. Sometimes, however, its output could be higher than the assigned steady state rating.

Figure 3.4 clarifies and elaborates on the above philosophy. It can also be explained by considering the equivalent model of the SC connected to the power system as illustrated in Figure 3.5, and giving the current equations from the SC to the system bus *Vs* as follows:

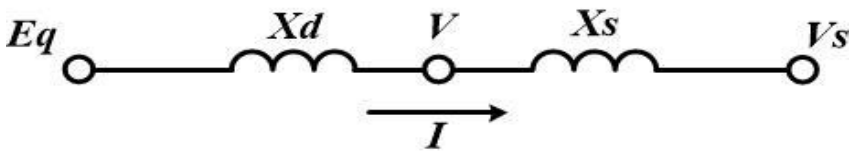

Figure 3.5: Equivalent circuit of a SC connected to a system.

$$I = \frac{E_q - V}{X_d} \quad (3.1)$$

$$I = \frac{V - V_s}{X_s} \quad (3.2)$$

Where

E_q = the excitation voltage for SC

V = terminal voltage of SC

V_s = system voltage

X_d = Equivalent impedance of SC

X_s = impedance between the SC and the system

Combining (3.1) and (3.2), we get

$$E_q = V\left(1 + \frac{X_d}{X_s}\right) - \frac{X_d}{X_s} V_s \quad (3.3)$$

The primary function of SC is to maintain the bus terminal voltage V by changing the excitation voltage E_q whenever the system voltage V_s changes. Equation (3.3) shows that the excitation voltage E_q will increase whenever the system voltage Vs decreases and vice versa.

The working mechanism of the SC can be explained during different dynamic situations with the help of Figure 3.6. Suppose the SC is initially working at point (A). When the system voltage V_s decreases, the SC will increase the excitation voltage E_q, thus supplying reactive power to the system.

Then the operating point will be at (B). At this point, the value of capacitive current is denoted as I_{cs}. It is also the limiting value of the current in the steady state region. After crossing this value of the current, it will no longer be termed as steady state.

Now, if the system voltage continues to decrease, the operating point will be shifted to point (C) where the current will be larger than I_{cs}. The SC can work only for a short period of time in the transient region since the overcurrent, which is installed with the SC, will trip after a certain time interval.

If the system voltage further decreases for a short interval of time, the excitation voltage E_q will increase further until it reaches the maximum value $E_q(max)$. The SC can no longer sustain the drooping voltage beyond this point (D). At the maximum value of Eq, the corresponding reactive current will be at I_{ct} which is the limiting value of a transient

capacitive current. It is evident from (3.3) that if the system voltage decreases further beyond point (D) (after the maximum value of Eq has been attained), the terminal voltage will have to decrease.

The operation time of SC beyond point (B), such as (C), (D), and (E) can be determined from the time-delaying characteristics of the overcurrent relay. Similarly, the behavior of the SC, when it operates to absorb the reactive power, can be analyzed. Figure 3.6 shows that the transient current limit I_{ct} for SC is significantly higher than the steady state current limit I_{cs}.

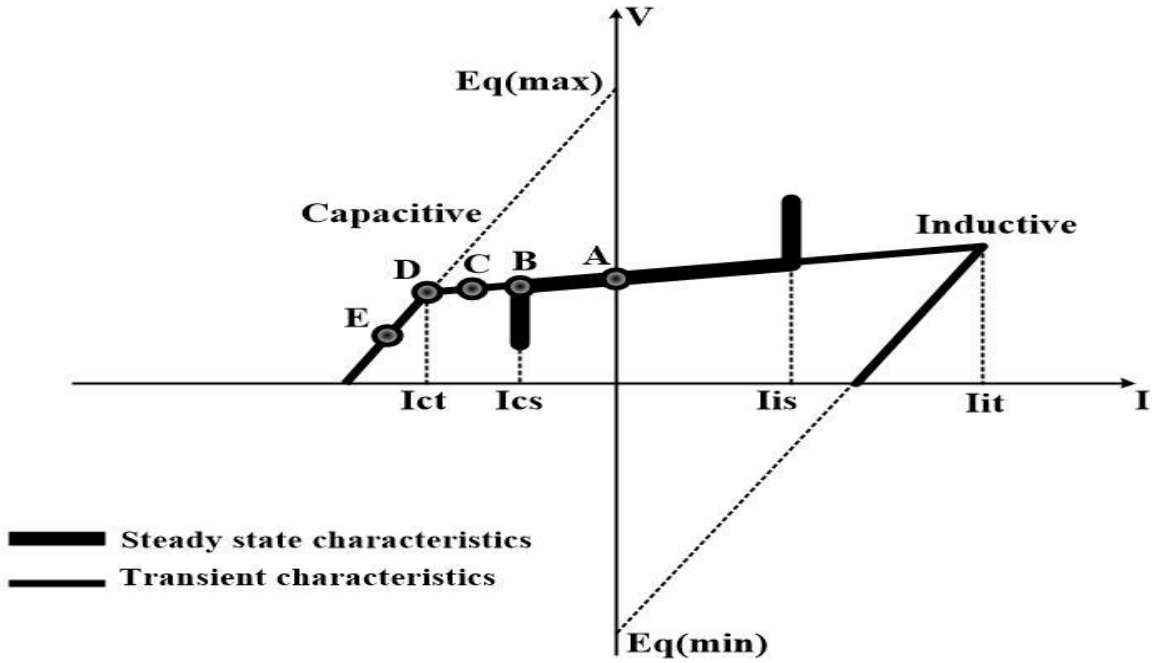

Figure 3.6: Operation V-I characteristics of a SC.

The following subsections clarify the modeling of the traditional synchronous condensers and superconducting synchronous condensers.

3.2.1 Traditional Synchronous Condenser

The operation of synchronous condensers is similar to large electrical motors as shown in Figure 3.7. After synchronization, the field excitation is controlled to either add or absorb the reactive power, depending on the requirement of the system. An automatic exciter can also be used if the system requires a continuous reactive power control. If the system requires a reactive power supply, the field excitation of a synchronous condenser is increased. On the other hand, during reactive power absorption, the field excitation is consequently decreased. Synchronous condensers can also be used to control system voltage, especially in starting large motors.

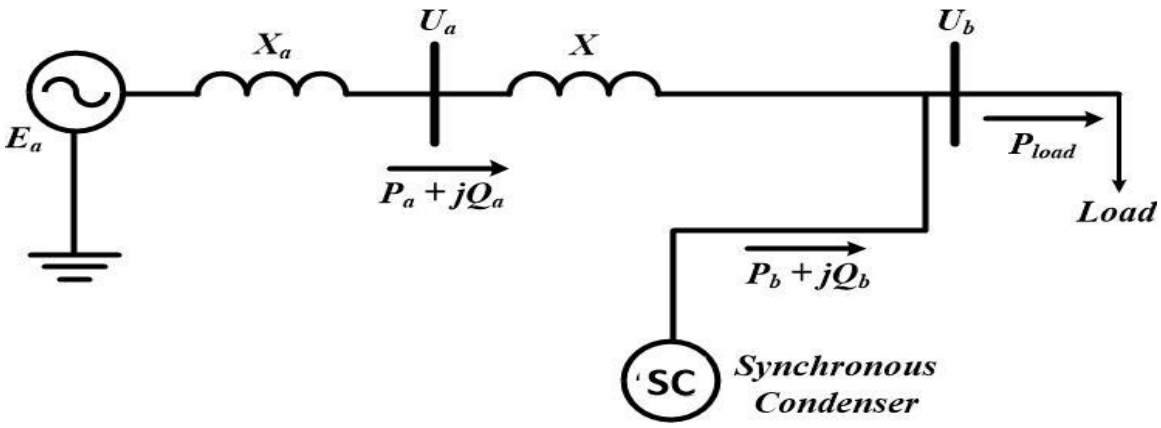

Figure 3.7: Single phase grid connected to synchronous condenser.

According to [46], synchronous condensers have certain disadvantages, including higher energy losses and a longer response time.

3.2.2 Superconducting Synchronous Condenser

According to [47], with the development of high temperature superconductors, the technology of large electric machines is revolutionized. The use of high temperature superconductors (HTS) in electric machines can make them smaller, lighter, more efficient and less expensive. One prototype is shown in Figure 3.8.

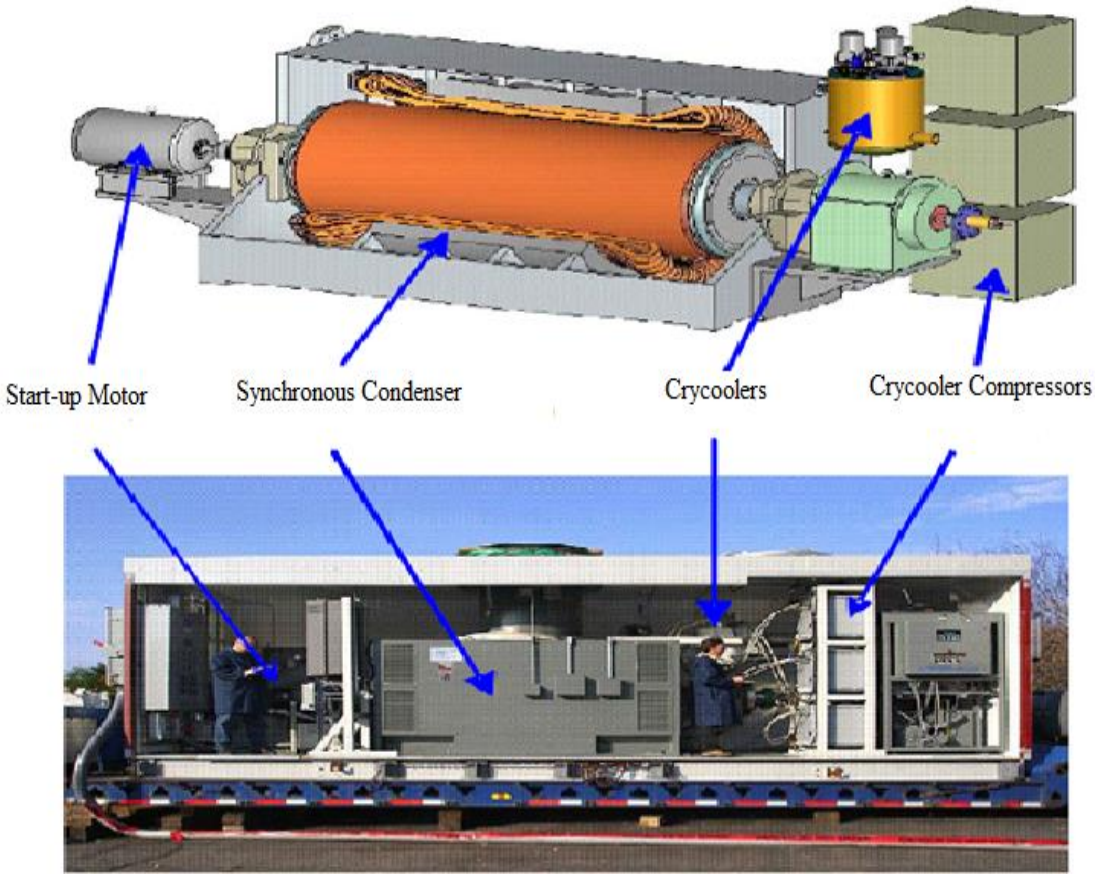

Figure 3.8: Prototype of dynamic synchronous condenser (Photo courtesy of American superconductor).

The development of high temperature superconductor (HTS) wire technology resulted in superconducting electromagnets, which have revolutionized this field due to their efficient response during high-temperature applications. These high temperature superconducting electromagnets can be utilized as less expensive and more efficient cooling systems. These advantages make HTS more technically and economically feasible than lower temperature superconductor LTS wire technology based motors and generators.

A HTS technology based winding is shown in Figure 3.9.

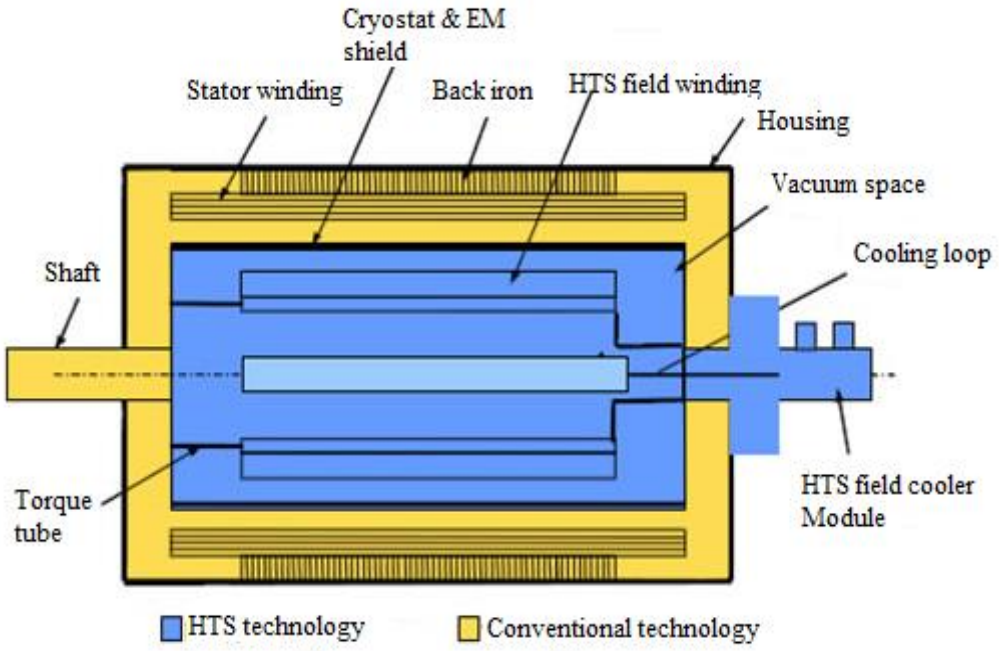

Figure 3.9: HTS superconductor generator (Design courtesy American superconductor).

Only the field winding of the machine uses a 35-40K crycooler subsystem based on the HTS technology. Crycooler modules are placed on the stationary frame and a cooling gas, normally Helium, is used for rotor components. The stator winding uses the slightly modified conventional copper winding. Due to the high magnetic field imposed by the HTS winding, the stator winding is not placed inside the iron core teeth.

According to [48], due to the problem of saturation caused by the high magnetic field generated by the HTS synchronous condenser winding, conventional magnetic iron core is not used in this situation. The magnetic field value, due to the HTS winding, is around 1.5-2.0 T which is double the value of a magnetic field generated by conventional winding. This high magnetic field can cause saturation and excessive heating in iron teeth. Only the stator yoke uses the magnetic iron to provide shielding. The absence of iron in most of the circuits can cause the low synchronous reactance, which is almost 0.3-0.5 per unit. As far as transient system faults are concerned, the HTS-based SC machines are more robust than the traditional SC if both of them have the same transient and sub-transient reactance. This lower synchronous reactance also allows for the lower load angle operation of these HTS-based SC machines.

3.3 Modeling of the Excitation System

On an industrial level, DC excitation systems have been broadly used. A type of DC1A excitation system is connected to the synchronous condenser. As shown in the figure 3.10, the exciter can be either separately excited or self-excited. Excitation system stabilization is confirmed with the help of field voltage signals [9].

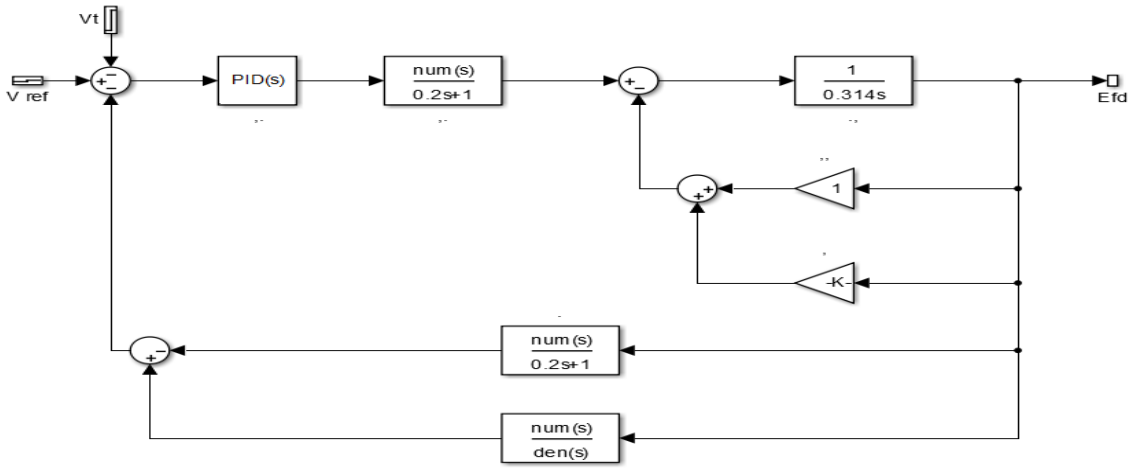

Figure 3.10: IEEE excitation system- DC1A type.

To improve the stability of the system and enable increase in the gain, a proportional-integral-derivative (PID) controller was used, which can increase the speed of the controller response. PID controller is used when dealing with higher order capacitive processes (processes with more than one energy storage) when their dynamic is not similar to the dynamics of an integrator. With four machines and several lines, it is hard to linearize the IEEE 9-bus system to get a reasonable gain. Each component has multiple equations that have to be solved before we can linearize the system. We assumed that we have a single machine that is connected to an infinite bus to get the gain value and PID values. Then we can check the stability of the system by using root locus method.

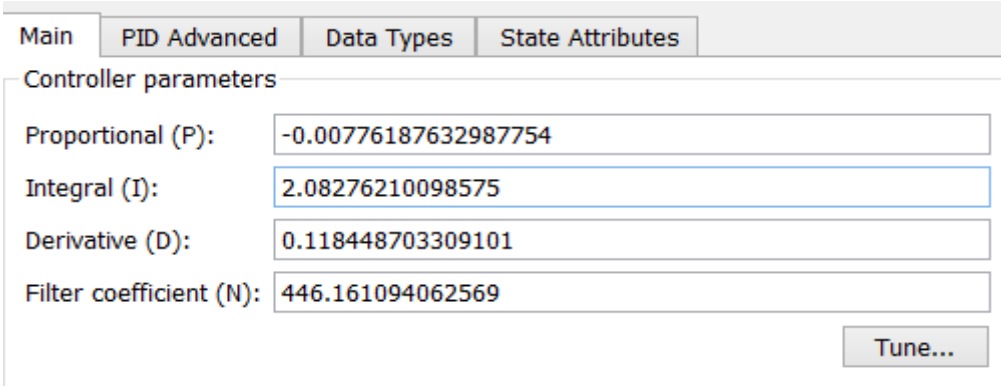

Figure 3.11: PID values.

The simple AVR system of the machine has the following parameters of DC1A:

Amplifier:	K_A	τ_A= 0.2
Exciter:	K_E= 1	τ_E= 0.314
Generator:	K_G= 1	τ_G= 1
Sensor:	K_R= 0.063	τ_R= 0.35

The open loop transfer function of the AVR system is:

$$KG(s)\,H(s) = \frac{0.063\,K_A}{(1+0.2\,s)(1+0.314\,s)(1+s)(1+0.35\,s)} \quad (3.4)$$

$$= \frac{0.063\,K_A}{0.022\,s^4+0.265\,s^3+1.11\,s^2+1.86\,s+1} \quad (3.5)$$

$$= \frac{2.86\,K_A}{s^4+12.04\,s^3+50.4\,s^2+84.5\,s+45.5} \quad (3.6)$$

The characteristic equation is given by

$$1+ KG(s)\,H(s) = 1+ \frac{2.86\,K_A}{s^4+12.04\,s^3+50.4\,s^2+84.5\,s+45.5} = 0 \quad (3.7)$$

$$s^4 + 12.04\,s^3 + 50.4\,s^2 + 84.5\,s + 45.5 + 2.86\,K_A = 0 \quad (3.8)$$

The Routh-Hurwitz array for this polynomial is then

s^4	1	50.5	$45.5 + 2.86\,K_A$
s^3	12.04	84.5	0
s^2	43.48	$45.5 + 2.86\,K_A$	0
s^1	$71.9 - 0.79\,K_A$	0	0
s^0	$45.5 - 2.86\,K_A$	0	0

From the s^1 row, $71.9 - 0.79\,K_A = 0$, we see that for control system stability, K_A must be less than 91, and also, from the s^0 row, $45.5 - 2.86\,K_A$, K_A must be greater than -15.9.

For K_A = 91, the auxiliary equation from the s^2 row is

$$43.48\,s^2 + 45.5 + 2.86 * 91 = 0 \qquad (3.9)$$

Or $s = \pm j\,2.64$, we have a pair of conjugate poles on the *jw* axis, and the control system is marginally stable.

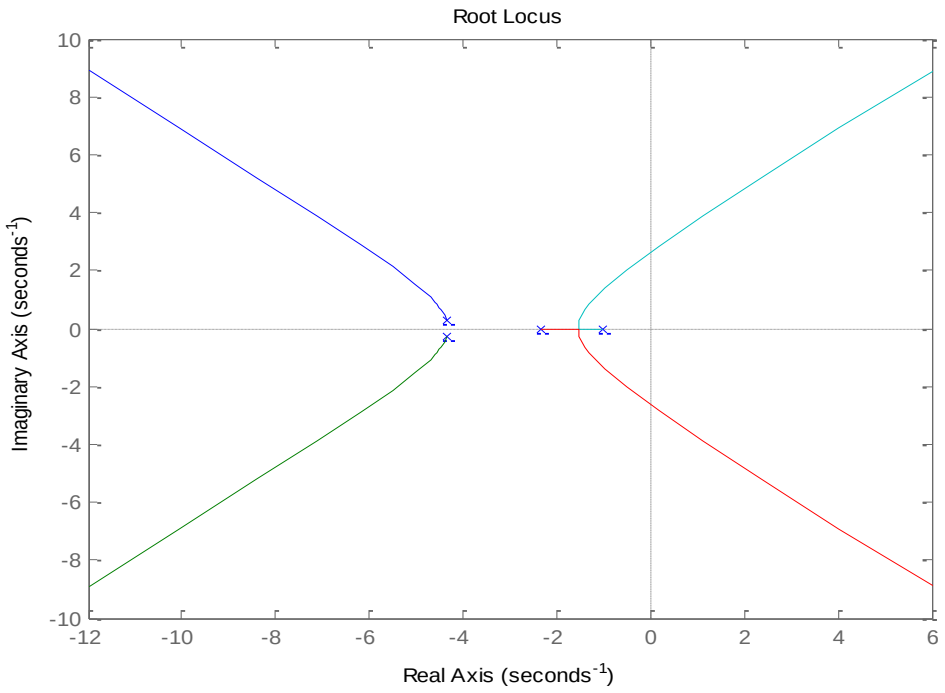

Figure 3.12: Root-locus plot for the excitation system.

As shown in figure 3.12, the loci intersect the *jw* axis at $s = \pm j\,2.64$ for K_A = 91. Thus, the system is marginally stable for K_A = 91.

The closed loop transfer function is

$$\frac{V_t\,(s)}{V_{ref}\,(s)} = \frac{15.9\,K_A\,(s+2.86)}{s^4+12.04\,s^3+50.4\,s^2+84.5\,s+45.5+2.86\,K_A} \qquad (3.10)$$

3.4 Modeling of the Static Var Compensation (SVC)

SVCs are used in power systems for several applications such as enhancement of transient stability, increasing the power-transfer capability and prevention of voltage instability. A classic static var compensation (SVC) comprises the following major components: coupling transformer, thyristor valve, capacitor bank and reactor. With suitable organization of the capacitor switching and reactor control, the reactive power output can be varied between the capacitive and inductive ratings of the equipment, illustrated in Figure 3.13. SVC regulates the voltage of the transmission system at a selected bus. If the voltage bus begins to fall below its range, the SVC will inject reactive power into the system. On the other hand, if the bus voltage increases, the SVC will inject less; in other words, the SVC will absorb more reactive power. The SVC has no capacitive overcurrent ability and its reactive power output is proportional to the square of the voltage magnitude [5].

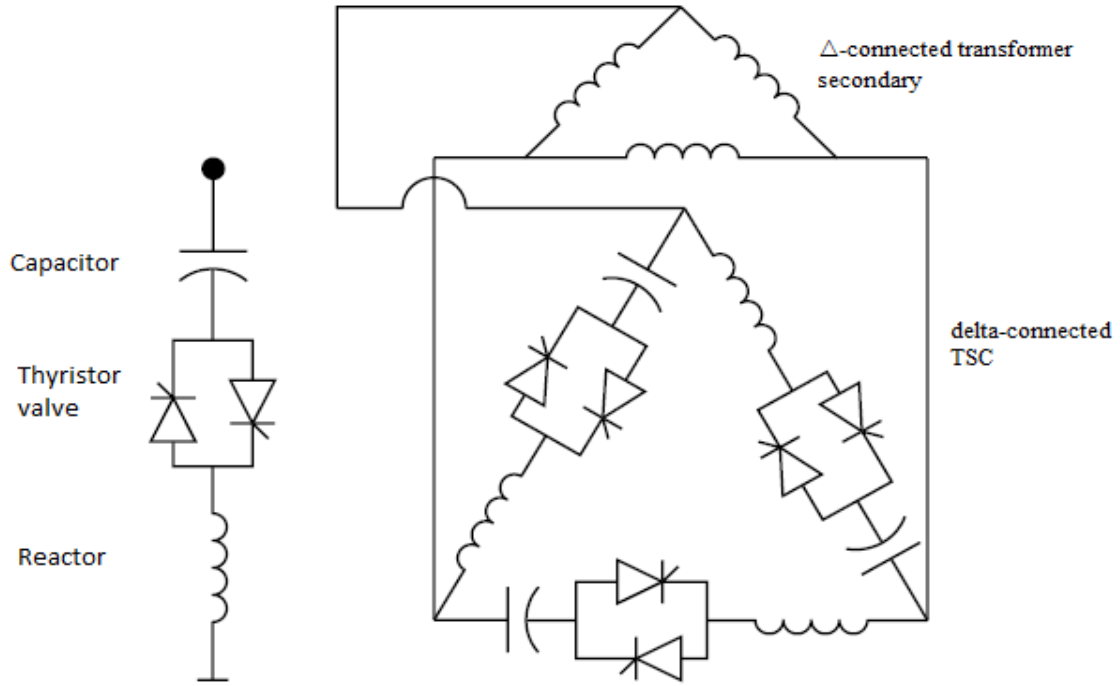

Figure 3.13 (a) a single-phase TSC branch; (b) a 3-phase delta-connected TSC supplied by a 3-phase ∆-connected transformer secondary.

The SVC has different configurations such as thyristor-controlled reactors (TCRs) and thyristor-switched capacitors (TSCs). In deciding to use TSC instead of TCR, there are advantages and disadvantages that should be considered based on the application.
The primary advantage of the TCR is that it has a lower capital cost resulting from the absence of the thyristor switches. The other cost related advantage is lower operating costs. However TCR generates harmonics which have to be eliminated so filters would have to be installed for this job. Another disadvantage of the TCR is a slower response speed. The TCR switches close in two cycles and open in eight cycles, compared to one cycle or less with TSC switches [86].

Because TSC current is sinusoidal and free from harmonics, filters are not needed. This is one of the main reasons why some SVCs have been designed with TSCs only [86]. Table 3.2 illustrates the differences between TSC and TCR. Three-phase TSC consists of three single-phase TSCs connected in a delta, as shown in Figure 3.13(b).

Table 3.2: Comparison of Different Reactive Compensators [86].

Feature	**Synchronous Condenser**	**TSC**	**TCR**
Response time	Slow	Fast	Slow
Voltage control	Very good	Good	Good
Harmonic generation	None	None	Yes
Overload capability	Very good	None	Limited
Rotating inertia	Yes	No	No
Sensitive to frequency deviations	Yes	No	No

The primary concern is a SVC with high response time and good voltage control. In addition, since the synchronous condenser has no harmonic generation, we chose a TSC that has no harmonic generation (see Figure 3.14).

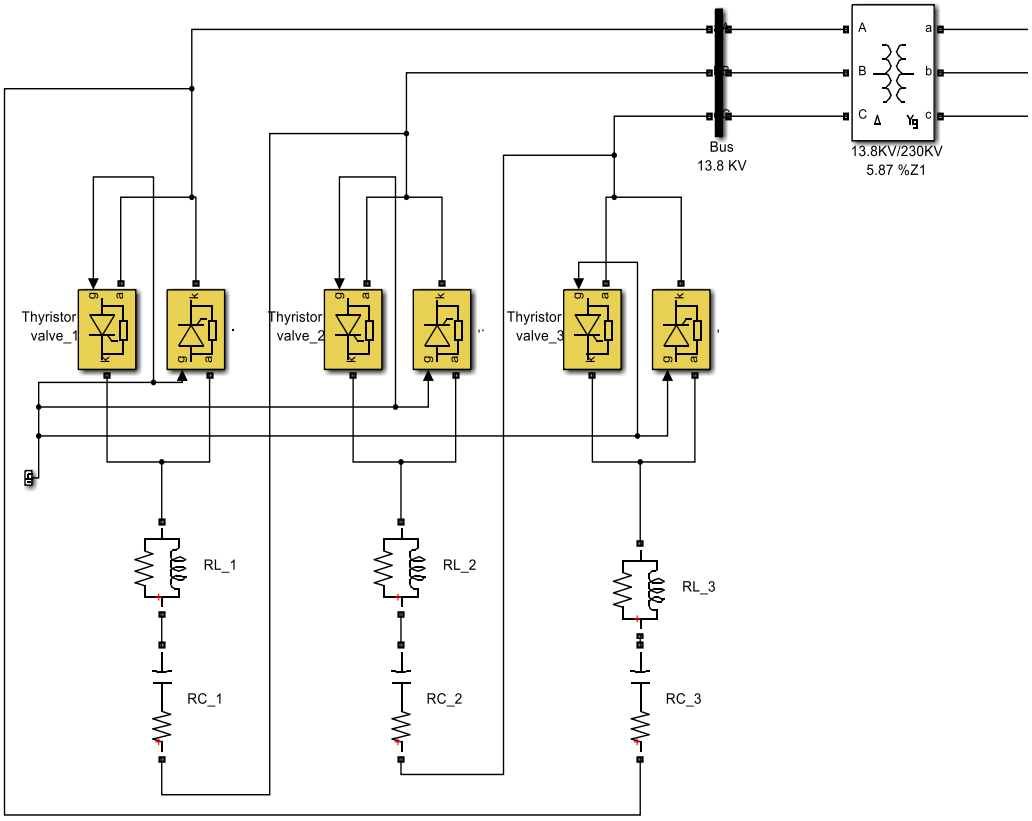

Figure 3.14: SVC model.

Chapter 4

Design of the Power System Stabilizer

The stability of power systems against disturbances taking place within a power system has been analyzed by a considerable number of engineers for decades. One method of power system stabilizer in this area of study has been the classical power system stabilizer (CPSS).

In the CPSS structure, the gain of PSS is modified according to a certain situation then left as constant. However, it is evident that the operating point of the power system varies based on load changes. Therefore, the PSS may lose its capability in sustaining the important characteristic of stability. Besides, any adjustment in the parameters of the automatic voltage regulator (AVR), or automatic governor control (AGC) can result in a severe change in the state of the system. Moreover, it is probable that the PSS will not be effective then. In order to counteract this obstacle, a number of techniques are presented, such as the fuzzy sets [36][40]. Fuzzy techniques have certain disadvantages associated with them, such as an inappropriate response when parameters are altered, as well as low potential for training. If these drawbacks can be eliminated, dynamic behaviors will be further enhanced. In this respect, other techniques based on artificial neural networks (ANN) can be used [21][24].

This chapter will discuss the PSS, which is created with the help of an appropriate neural network. This technique has its own advantages in regard to the potential of being trained, due to its non-sensitive nature to the power system variations of parameters.

4.1 Introduction to the Artificial Neural Network

4.1.1 Basic Elements of ANN

Artificial neural networks (ANNs) are the computational models that have been developed by the inspiration of the human central nervous system. Similar to the human nervous system, the neuron is the basic building block of the ANNs. Neurons are information processing units represented by a circle, known as nodes in the ANN. The building blocks of a single neuron can be modeled as shown in Figure 4.1.

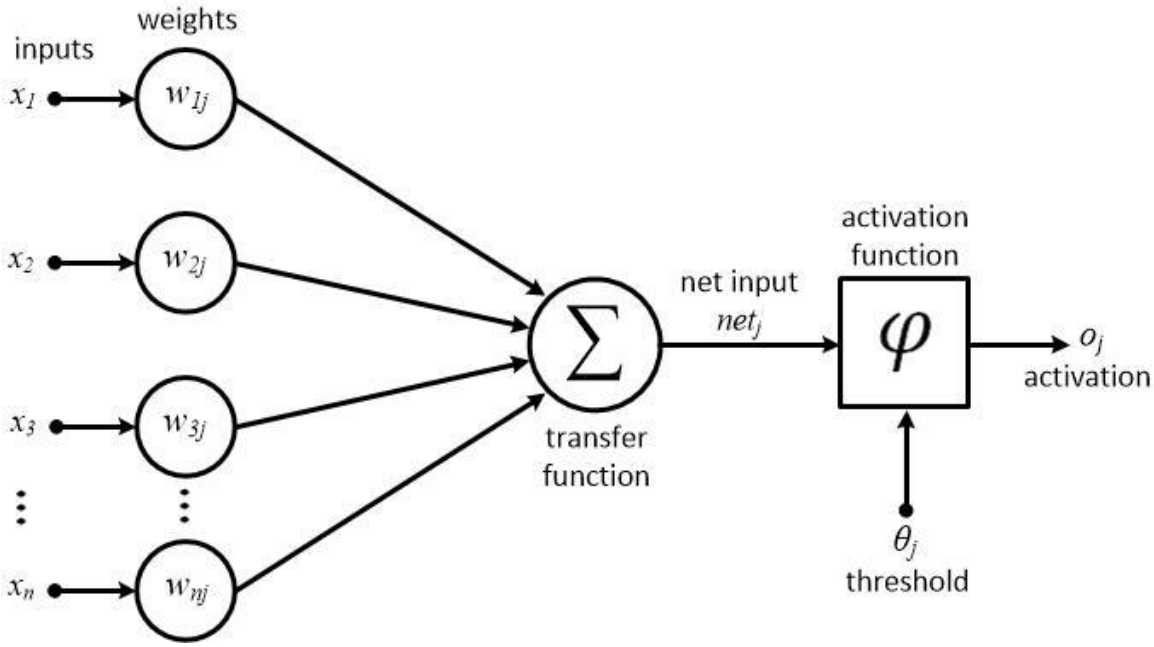

Figure 4.1: Non-linear model of a neuron.

The neuron model has three basic units that are further explained below:

First, there is a set of connecting links, each of which is characterized by its effective weight. A signal x_i is fed to synapse $w_{j,}$ where j represents its synapse number and w is the effective weight. A summing point or adder is indicated where each weighted synapse is collected. Finally, in order to limit the output of a neuron, an activation signal is introduced. This limiting signal is within the range of [0 - 1] or alternatively [-1 - 1].

As shown in Figure 4.1, the model may also sometimes include a threshold signal to limit the input of the activation signal introduced earlier. Mathematically, a neuron model can be given by the following pair of equations:

$$u_k = \sum_{j=1}^{p} w_{kj}\ x_j \quad (4.1)$$

$$y_k = \phi(u_k - \theta_k) \quad (4.2)$$

Where:

x1, x2. . . ,xp: Input signals ,

wk1, wk2, . . .,wkp: Synaptic weights of neuron k ,

uk: Linear Output ,

θk: Threshold ,

ϕ(.): Activation Function , and

y_k: Output signal of the neuron

There are three basic types of activation function, which are presented as follows:

1. The Threshold Function:

$$\phi(v) = \begin{cases} 1 & if\ v \geq 0 \\ 0 & if\ v < 0 \end{cases} \quad (4.3)$$

2. The Piece-wise Defined Function:

$$\phi(v) = \begin{cases} 1 & if\ v \geq 1/2 \\ v & if\ \frac{1}{2} > v \geq -1/2 \\ 0 & if\ v < -1/2 \end{cases} \quad (4.4)$$

3. Sigmoid Function:

$$\phi(v) = \frac{1}{1+ e^{-av}} \quad (4.5)$$

Where *a* is the slope of Sigmoid Function

The manner by which the neurons are connected together can be classified into two categories. First, there is a feed-forward network, where the output of one layer becomes the input of a subsequence layer, thus making up the whole neural structure, as shown in Figure 4.2.

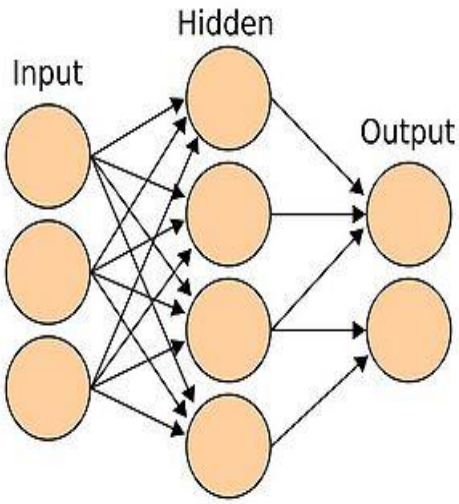

Figure 4.2: Feed-forward neural network with one hidden layer.

It is indeed a feed-forward as all the connections are in the forward direction. The network usually consists of an input layer, one or more hidden layers and an output layer. The inclusion of one or more hidden layers in the network enables the network to extract higher order statistics. Source nodes provide the network with the input signal while the output nodes constitute the overall output response of the network. In addition, the network can be fully or partially connected. Secondly, there are the recurrent networks, which differ from the feed-forward network in the fact that the former must have at least one feedback loop as shown in Figure 4.3. This feedback loop has a profound impact on the capability of the network and its overall performance. Besides, a feedback loop involves one or more unit-delay elements, which help the network to be dynamic.

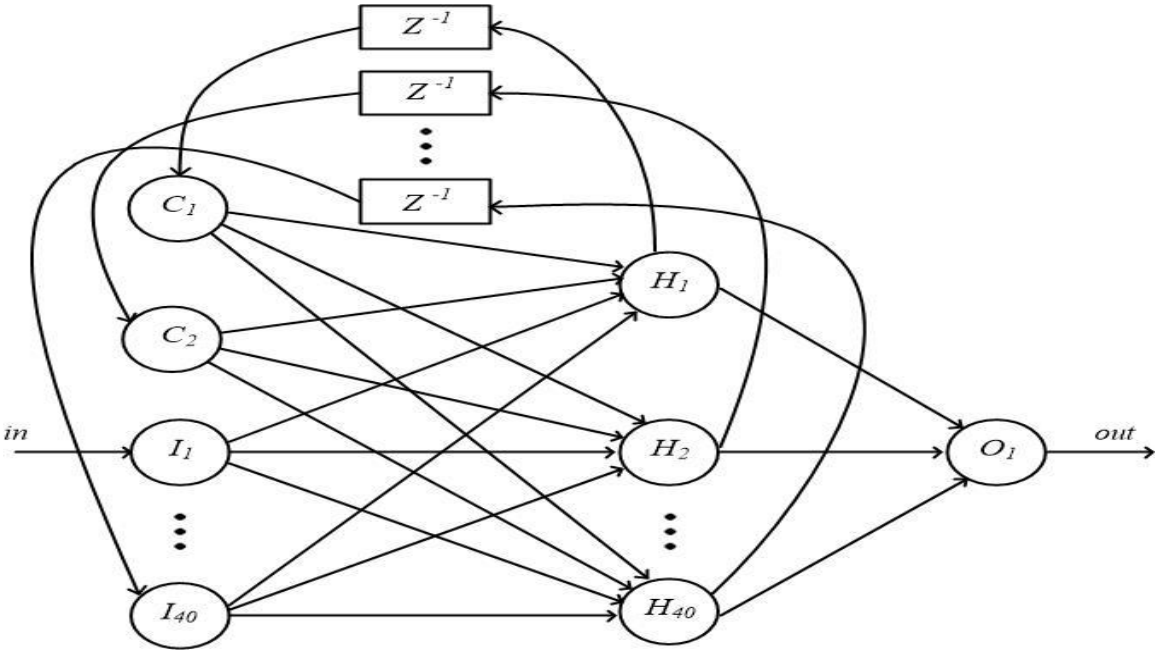

Figure 4.3: Recurrent network with hidden neurons.

4.1.2 Training Algorithms

One of the major properties of a neural network is the ability to learn from training data, thus improving the performance through learning. The learning paradigm can be divided into three different classes.

First, there is supervised learning, where network parameters are adjusted by the combined effect of training data and error signal. An error signal is defined as the difference between the actual response of the network and the designed network.

Examples of supervised learning paradigm include the back-propagation (BP) algorithm [30]. As the name implies, the error in this algorithm is back-propagated layer-by-layer through the network. Supervised learning can be performed off-line or on-line. The off-line learning mechanism is the static one, where the learning process freezes once the desired performance is reached. On the other hand, on-line training performs the adjustment of parameters dynamically and the learning process is accomplished in real-time.

Secondly, there is the reinforcement learning, which involves a guide that is developed by a trial-and-error method over the course of time. Contrary to supervised learning, this type of learning is carried out on the basis of reinforcement or feedback received from the environment. Unlike supervised learning, there is no instruction that can provide the gradient information. The information for learning is acquired by probing the environment

through the combined use of trial-and-error and delayed reward. This kind of learning is more appropriate as there is also the possibility of improvement in the performance of a plant by means of on-line reinforcement learning [31].

In the third category, which is the unsupervised learning, the network is neither instructed nor guided. Instead, it is a self-organized sort of learning. The quality of representation that the network needs is made for a task-independent measure. It is worth mentioning that during unsupervised learning, the network is able to develop a structure of the input data in an explicit manner. Examples of most important unsupervised learning networks are Kohonen's Self Organizing Map and Grossbeerg's ART networks [32].

4.1.3 Characteristics of ANNs

A neural network provides the solutions to many problems whose solutions are not possible through ordinary algorithms. Some potential characteristics of neural networks are briefly discussed below:

i. Nonlinearity: A single neuron is mainly a nonlinear element by its structure. Hence, the neural network whose building block is a neuron is nonlinear itself.
ii. Learning: A neural network can learn from the environment and examples, rather than from extensive explicit programming. It learns by examples through developing input-output mapping for the problem at hand.
iii. Complex Mapping: Very complex mapping can be synthesized, which may be very difficult or even impossible to put in a mathematical expression.
iv. Generalization: It is possible to generalize the training information, so that it can be applied to similar situations which have never been experienced before.
v. Speed: This is a very fast mapping technique in the sense that the ANN has to be trained only once then it can map the problems much faster than the other conventional and artificial methods.
vi. Robustness and Fault Tolerance: If the data is noisy, the ANNs can still provide reasonable results. It also has the capability of fault tolerance.

Despite certain unique characteristics, such as the learning ability, that cannot be found in other techniques, even in the fuzzy logic controllers, there are certain limitations of ANNs. These limitations are thoroughly described below:

i. Black Box: One of the major limitations of ANNs is their black-box characteristic. Information cannot be easily understood once stored in the ANN. Training sets do not contain the complete input-output relationship and once the learning process ceases, modification may be needed in the future. This modification will only be possible if the information is stored in a transparent fashion.
ii. Long Training Time: A long training time is needed to train the ANN. The required time to train the ANN depends upon the size and complexity of the neural network.
iii. Network Structure: The selection of the number of hidden layers and the number of neurons in a single layer is a rigorous task as it is a process of trial-and-error.

4.2 Artificial Neural Network-Based Power System Stabilizer

Approaches of artificial neural networks (ANN) have been developed to counteract the problems in the power systems, such as sensor validation, fault monitoring and diagnosis in power plants, tuning of controllers, process identification, load identification, load modeling and load forecasting in power systems; Table 4.1.

The PSS based on the ANN technique has various advantages, which include high reliability, good fault tolerance, and adaptive capabilities in a network learning process. It also provides better performance on non-linear power systems. Neural networks can be utilized to identify and control a wide range of non-linear systems since they can approximate any desired degree of accuracy with nonlinear models.

A variety of strategies of neural network training can help identify the right set of weights. Feed-forward, multi-layer, neural networks is mainly the most widespread neural network architecture used as an appropriate solution to the problem of control. Back-propagation algorithm is a broadly and commonly used training technique for feed-forward, multi-layer, neural networks. In addition, back-propagation is one of the most broadly practiced, and among the most extensively investigated techniques. As shown in Table 4.1, it is capable of handling a great number of problems, which cannot be fixed by other techniques.

Table 4.1: Application of ANN in Power Systems.

Nature of Problem	**ANN and Learning Algorithm**	**Use of the ANN**	**References**
Static and Dynamic Security Assessment	Feed forward and Back propagation	Estimation of post-fault parameter	51, 63
	Feed forward and Back propagation	Prediction of post contingency voltages	52
	Feed forward and Back propagation	Classification of states of power systems	61, 62
	Feed forward and Back propagation	Prediction and estimation of the state of the power system	64
Transient Stability Assessment	Decision Making System (comparable with a Feed forward and Back propagation)	Mapping transient stability assessment problem into the frequency domain	53
	Hybrid Perceptron and Kohonen's NN	Classification of power system conditions and prediction of voltage instability indices.	65
Identification, modeling and prediction	Feed forward and Back propagation	Modeling of dynamic load	54
	Feed forward and Back propagation	General treatment of modeling and identification in the electric power industry	55
Control	not explicitly specified	Control of load Shedding	56
Load Forecasting	Feed forward and Back propagation	Forecasting of one hour and day	57
	Feed forward and Back propagation with knowledge incorporated in its construction	Forecasting of short-term and long-term	58
	Recurrent multilayer perceptron and Back propagation	Prediction of long-term	59
Fault Diagnosis	Feed forward and Back propagation	Detection of incipient faults in power distribution feeders	60

4.2.1 Artificial Neural Network Description

An ideal method used in creating an ANN-based PSS is extensively discussed in this section. The chief advantage of this technique is the resistance to the changes of the system operation. In this research, we want to design a PSS-based on ANN, to regulate reactive power delivery and to demonstrate the effectiveness of the controller on the IEEE 9-bus system. In addition, we want to develop a better understanding of reactive power control with the help of the customized performance function of the artificial neural networks for the power stabilization system.

The ANN used in the training process encompasses the following characteristics. It is a feed-forward neural network that has four inputs, one hidden layer, and one output layer. The hidden layer has fifty neurons that are activated with sigmoid functions while the output layer has a linear activation function. The output layer has only one neuron, which is meant for the excitation voltage of the synchronous condenser. Several arrays of ANNs were proved to design the model. Even though some arrays present clear results when they are trained for a specific fault, they do not offer good performance when another fault different from the previous one is applied. Refer to Figure 4.4.

The ANN is trained with the Levenberg-Marquardt method. All the weights from input, hidden to output, are randomly initialized. Although the network is trained for 1000 epochs, most of the times, it converges instantly.

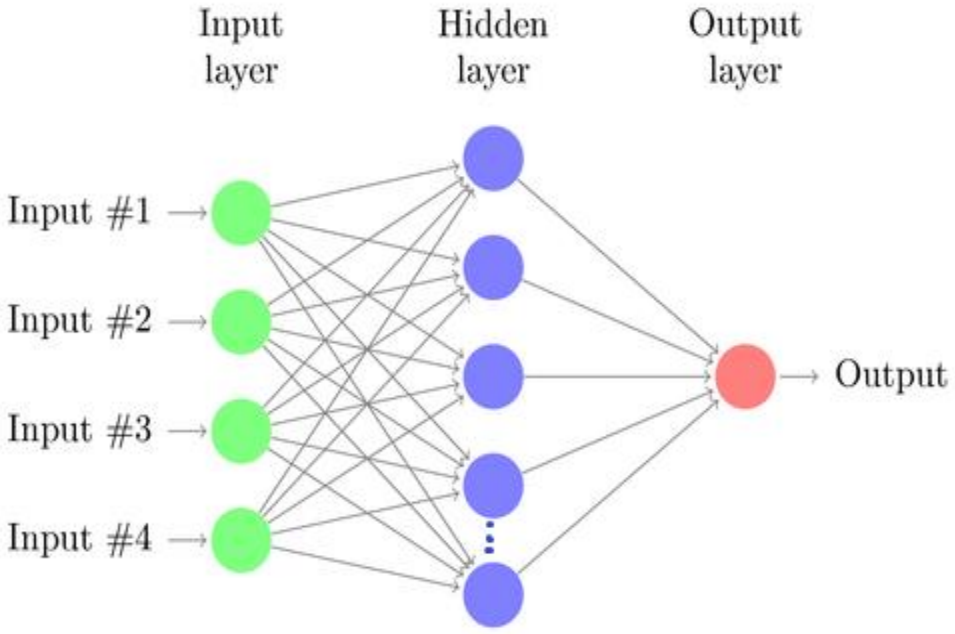

Figure 4.4: ANN model architectures.

4.2.2 ANN Training Process

The ANN is composed of processing networks that are arranged in a layer sequence. There are three layers, namely the input layer, the hidden layer and the output layer. In the present research work, learning network data are acquired with the help of the synchronous condenser. The voltage direct axis V_d, the voltage quadrature axis V_q, the rotor speed w, and the speed deviation dw of the synchronous condenser are taken as inputs. The first two inputs, V_d and V_q, will symbolize the machine while the rest will anticipate changes in the system's operation. Therefore, four neurons are required to be placed in the input layer. The network has previously been trained with the help of 14401 sample training data that were acquired from the operation of the synchronous condenser that is located on the IEEE 9-bus system. These are produced with an awareness of the various operating conditions such as different types of fault and different fault locations.

The common practice is to divide the sample training data into three subsets: the training set, that is used for updating the weights and biases of the network, the validation set, which is monitored during the learning process, and the test set, which is used to compare different models. Out of the three subsets: 70% of the data set is allocated for training, 15% is allocated for validation, and 15% is allocated for test.

As shown in Figure 4.5, the fluctuation in the graph indicates the reaction of the synchronous condenser through V_d and V_q toward different kinds of operation at various periods of time. On the other side, the speed deviation is kept at around zero.

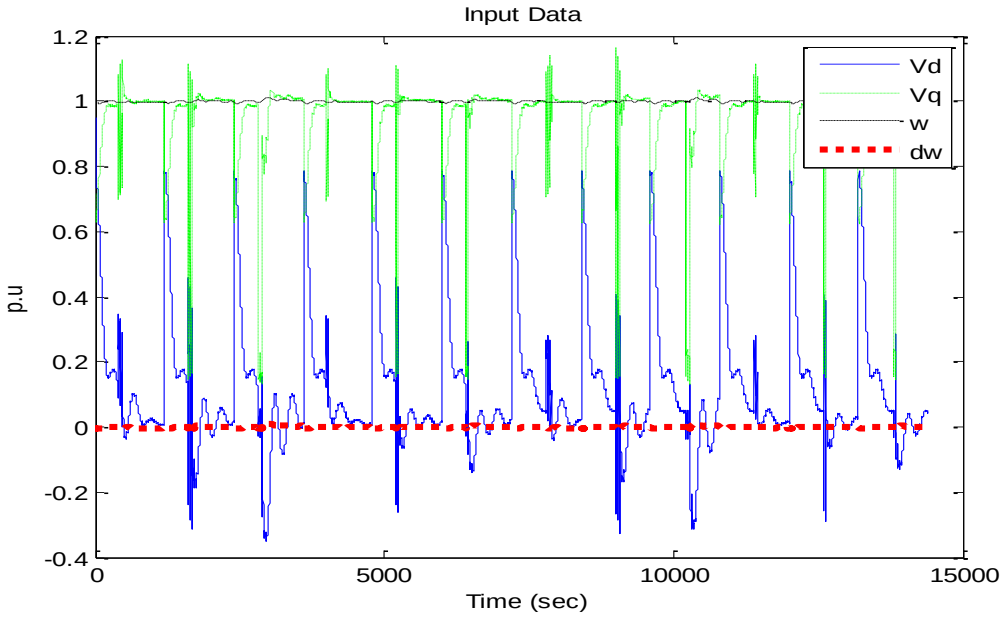

Figure 4.5: Input data of training process.

Several technical papers have revealed that one or two hidden layers, with an appropriate number of neurons, are sufficient for the modeling of any solution surface of practical interest. The general trend is that the greater the number of hidden layers, the smaller the approximation error. However, so many hidden layers also demand more memory storage [21][22][24]. Hence, there is not an exact method with which the appropriate number of hidden layers, along with the number of neurons in each hidden layer, can be determined. In the present study, one hidden layer is placed between the input and output layer and fifty neurons are used in the hidden layer. The number of hidden layer neurons has been adjusted by the trial and error method and some other heuristic methods [72].

On the other side, any continuous function can be approximated by the feed-forward neural network power system stabilizer (FNNPSS). In fact, the FNNPSS is a static mapping technique. For dynamic problems, a great number of neurons are needed for the dynamical responses in the time domain. The neural network, back-propagation algorithm is used for the purpose of training. When the neural networks are properly trained, they give satisfactory answers when exposed to unseen inputs. Generally, a new input gives an output similar to the accurate output for the similar input vectors used in the process of training. Hence, this general property makes it possible to train the network for the few inputs, but not all the unexpected inputs are needed during the training process. The ideal results can be acquired without training the network for all the possible input/output pairs. The state of the system does not need to be determined for the training purpose and the NN can be directly trained. Besides, the error is calculated by the error function.

The sampled values of machine parameters are used by the NN to generate the inputs for the error function for the purpose of calculating the error. The sigmoid function is utilized for activating the neurons in the hidden layer. However, the linear function has been used for the output layer since the output was not limited to 0 and 1 values. The numerical representation of *tansig* function and its derivative are expressed as follows:

$$\phi(v) = \frac{1}{1+e^{-g_a v}} - 1 \qquad (4.6)$$

$$\phi'(v) = g_a \frac{4\, e^{-2g_a v}}{(1+e^{-2g_a v})^2} = g_a(1 - \phi^2) \qquad (4.7)$$

In equations (4.6) and (4.7),$\phi\ (v)$ is the nonlinear activation function and g_a is a constant. Refer to Figure 4.6.

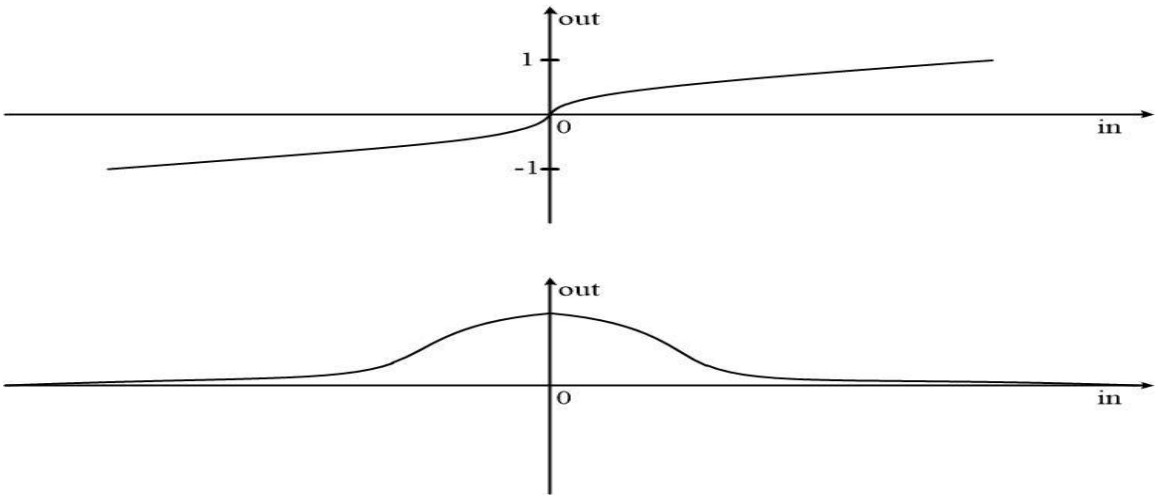

Figure 4.6: Tansig activation function and its derivative.

The neuron inputs and outputs can be determined as follows:

$$y_{ki} = \phi\left(\sum_k w_{kij}\, x_{kj} + b_1\right) \tag{4.8}$$

Where y_{ki} is the output of the neuron *i* presented in the layer *k*, ϕ is the nonlinear activation function of *i*, *w* is the neuron weight, *x* is the input signal, and *b* is the bias.

The back-propagation algorithm is an iterative technique that aims to minimize the mean square error between the NN desired output and the actual output. It is a recursive algorithm, that starts at the output and works back on the hidden layer by adjusting the weights according to the following relation:

$$w_{kij}(t+1) = w_{kij}(t) + \Delta w_{kij}(t) \tag{4.9}$$

$$\Delta w_{ji} = \eta\, \delta_j(n)\, y_i(n) \tag{4.10}$$

$$\delta_j(n) = e_j(n)\, \phi_j'(v_j(n)) \tag{4.11}$$

Where w_{kij} is the weight of neuron *i* in the layer *k* of the previous neuron *j*, η is the learning rate, δ is the local gradient, *e* is the output from the error function and ϕ_j' is the derivative of the activation function.

By using gauss newton algorithm (GS), the slow convergence problem of steepest descent method can be greatly improved. The curvature of the error surface can be normally evaluated by the use of second order derivatives of the error function. Gauss newton algorithm can counteract the problem even in the first iteration if the error function has a quadratic function. GS algorithm can find the appropriate step size for each direction. Thus, it is able to converge very fast. Furthermore, Levenberg-Marquardt (LM) is a mix of gauss newton algorithm and steepest descent method. Hence, LM possesses the converging speed of gauss newton algorithm and the stability of steepest descent method.

The core theme behind LM is that it combines the properties during the training process. LM switches to the steepest descent algorithm near the complex curvature area. It remains in this mode until the curvature is appropriate to make the quadratic approximations. During such curvature, LM shifts to gauss newton algorithm and speeds up the process of convergence. LM can train any sort of network as long as its weight, net input and the transfer function have their existing derivative. LM is a highly recommended training algorithm for training purposes, regardless of its large memory storage demand. It has been formulated to approach the second order training speed without the solution of hessian matrix.

LM introduces an approximation to hessian matrix for the purpose of ensuring that the approximated hessian matrix $J^T J$ is not singular i.e.; invertible.

$$H = J^T J + \mu I \tag{4.12}$$

$$\Delta W = (J^T J + \mu I)^{-1} J^T e \tag{4.13}$$

Where the value of μ is always positive, which is known as the combination coefficient that controls the size of the trust region and *I* is the identity matrix.

When the value of μ is 0, formulation ΔW is gauss newton's algorithm approach. On the other hand, when the value of μ is big enough, the formulation ΔW is a gradient descent algorithm with a smaller step size. The Jacobian matrix is easy to solve with the help of a standard back-propagation (BP) technique, which is much simpler than the hessian matrix.

This equation verifies that the elements on the main diagonal of the approximated hessian matrix will be larger than zero. Thus, it ensures that the hessian matrix is invertible.

$$w_{k+1} = w_k - (J_k^T + \mu I)^{-1} J_k e_k \tag{4.14}$$

Table 4.2: Different Types of Algorithms.

Algorithm	**Update Rule**	**Convergence**	**Computation Complexity**
EBP algorithm	$w_{k+1} = w_k - a\, g_k$	Stable, Slow	Gradient
Gauss-Newton	$w_{k+1} = w_k - (J_k^T J_k)^{-1} J_k e_k$	Unstable, Fast	Jacobian
Levenberg-Marquardt	$w_{k+1} = w_k - (J_k^T + \mu\, I)^{-1} J_k e_k$	Stable, Fast	Jacobian

The performance of ANN is evaluated for 30, 50 and 100 neurons. When the neurons are 30, the target is reached for 673 iterations. The performance goal is reached for 112 iterations in 0.48 min only for 50 neurons. Also, the goal is reached for 212 iterations in 2 min for 100 neurons. However, for 100 neurons, huge memory is required. Thus, a suitable value is chosen, such as 50 neurons, in the above experiment. As shown in Figure 4.7, the training is done for 1000 epochs, but it always converges before the epoch number is reached. Notice that we have more than 14000 data points.

Different types of ANN training with different parameters.

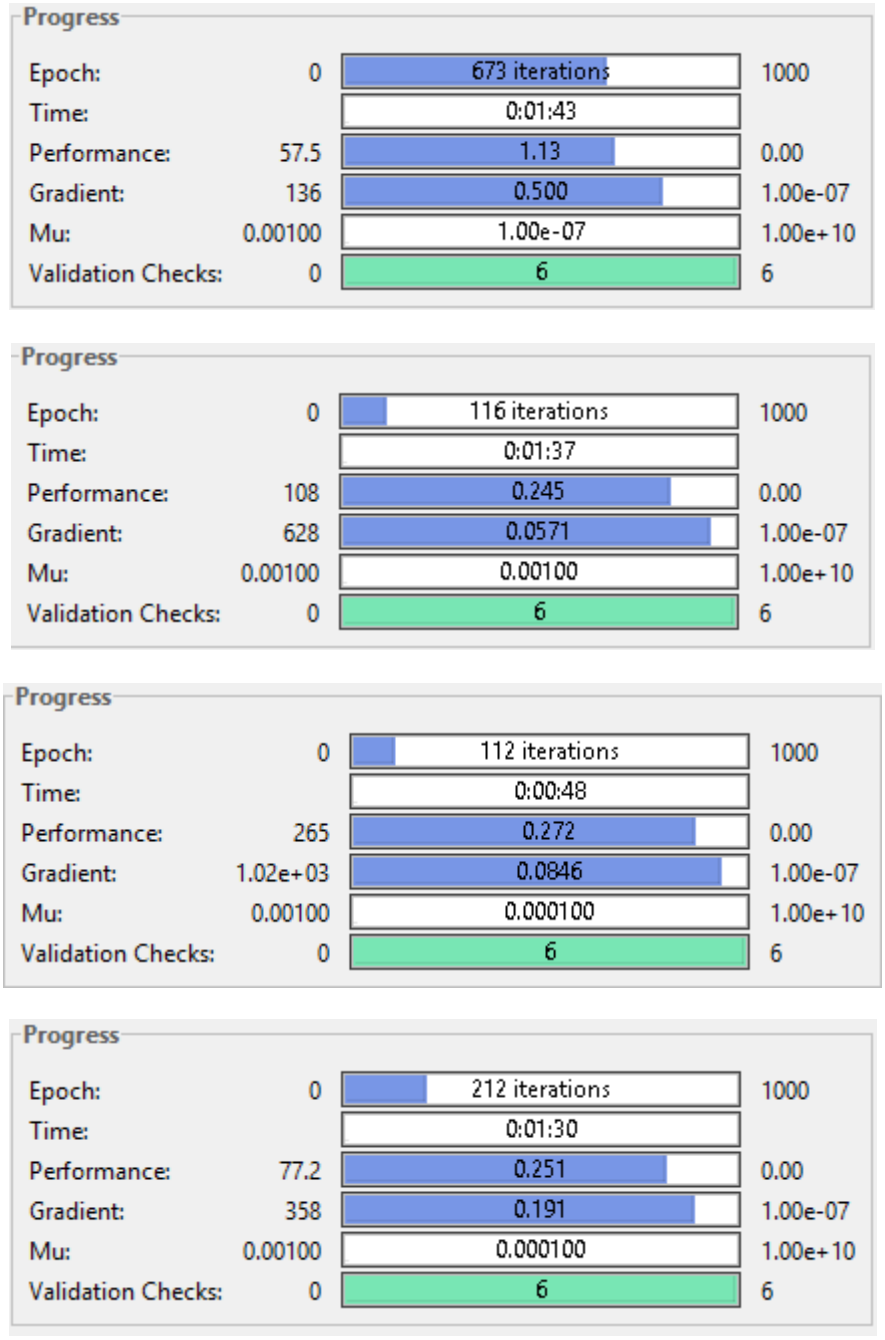

Figure 4.7: ANN scheme's training.

4.2.3 ANN Performance

The Back-propagation algorithm looks like a fully integrated algorithm. However, it still has some disadvantages in regard to slow convergence and over fitting problems. In some cases, the error is minimized, but when new data is shown to the network, the error becomes more serious, which means the network has not learned to be generalized to the new operation point.

In the previous section, the slow convergence rate has been addressed by using an optimizing technique LM to make the training process much swifter. In this section, the way a change in the ANN traditional structure can improve the performance of the ANN is described. As mentioned in section 1.2, there are several methods that can improve the generalization ability of the ANN [66][67][79][80][81]. One method is multi-object optimization. In this approach, several cost functions can be used instead of just using the mean square error of the training data [68][83][84].

For the training process of ANN, the typical performance function is the sum of the mean square error of the network (mse), and it is given as follows:

$$mse = \sum_{i=1}^{N} \sum_{j=1}^{n} (e_i^2) = \sum_{i=1}^{N} \sum_{i=1}^{N} (t_i - a_i)^2 \qquad (4.15)$$

Where N is number of samples; t_i is the target based on the ANN model; a_i is the output value of the j-th sample.

The main contribution of the proposed method is that it can improve the learning process by using the generalization property of the ANN. This can be done by modifying the performance function by adding another term, which is the sum of the mean squares of the network weights and biases (msw), to represent the weights of the system. This method restricts the magnitude of the weight. (4.16).

$$msw = \sum_{j=i}^{n} w_j^2 = \sum_{j=\mathrm{i}}^{n} (\hat{\mu}_j - \mu_j)^2 \qquad (4.16)$$

Where n is number of output parameters; $\hat{\mu}_j$ is the target mean value of the ANN; μ_j is the mean output of the J-th sample.

The key to obtain good generalization is to find the simplest model that can clearly explain the data. This is a variation of the principle called *Occam's razor*. The idea is that the more complex model will lead to a high probability of error. In this study, the simplest model is the model that has the smallest number of weights and biases. Thus, we give more weight to error than the second term to keep the error as small as possible.

A large weight on the bias term would mean that variability of the output would not be preserved. Moreover, when the weights are large, the function produced by the network can have large slopes, which is more likely to over-fit the training data. Over-fitting occurs, rather than generalizing, when a model captures the internal patterns of the input data. We used weighting coefficients $\gamma = 0.9$ in (4.17) for all analyses [75]. Optimization methods are not necessary as the value of γ can easily converge by simplified trial and update procedures [76].

The neural activity of the brain includes the principle of reducing minimized energy and maximizing signal transmission efficiency. This is logical because the brain weighs only 3% of the body mass, but it consumes up to 60% of the entire body's energy [2][74].

$$F = \gamma\, mse + (1 - \gamma\,)msw \tag{4.17}$$

Where: γ is the performance ratio that shows the importance of each term.

For simplicity assume that $\gamma = \beta$ and $(1 - \gamma\,) = \alpha$

$$F = \beta[\sum_{i=1}^{N} e_i{}^2] + \alpha[\sum_{j=1}^{n} w_j{}^2] \tag{4.18}$$

$$F = \beta[\sum_{i=1}^{N} (t_i - a_i)^2] + \alpha[\sum_{j=1}^{n} (\hat{\mu}_j - \mu_j)^2\,] \tag{4.19}$$

Where: α/β is the control ratio of the complexity of the network solution.

With the use of this modified performance function, the network weights and biases can be minimized, thus forcing the network response to be smoother and unlikely to over fit [69]. This type of modification expedites the BP algorithm, thus providing fast convergence.

The performance function of equation (4.15) can be modified to improve the generalization ability of the network by using an additional term that relates to the derivatives of the traditional performance function. As discussed, a modified performance function can be more valuable than the standard mean square error (mse), particularly in practical applications where bias of data may occur, when the operation parameters were sampled in only part of the operating conditions. The performance based on mse will introduce bias of variables. The modified function penalizes differences between the network output mean and the target mean value.

This can be done by redefining (4.19), by using derivative-based error minimization to get the derivative of (4.19) with respect to excitation output (4.20) - (4.31).

Differentiating the first part of (4.18) with respect to the output excitation parameter:

$$\frac{\partial}{\partial t_{kl}} \sum_{i=1}^{N} \sum_{j=1}^{n} \beta_{ij} \, (t_{ij} - a_{ij})^2 \tag{4.20}$$

$$= \sum_{i=1}^{N} \sum_{j=1}^{n} \frac{\partial}{\partial t_{kl}} \{\beta_{ij} \left(t_{ij} - a_{ij}\right)^2 \} \tag{4.21}$$

$$= \sum_{i=1}^{N} \sum_{j=1}^{n} 2 \, \beta_{ij} \left(t_{ij} - a_{ij}\right) \left(\frac{\partial \, t_{ij}}{\partial t_{kl}}\right) \tag{4.22}$$

$$= \sum_{i=1}^{N} \sum_{j=1}^{n} 2 \, \beta_{ij} \left(t_{ij} - a_{ij}\right) \delta_{ij} \, \delta_{jl} \tag{4.23}$$

$$= 2 \, \beta_{kl} \, (t_{kl} - a_{kl}) \tag{4.24}$$

Differentiating the second part of (4.19) with respect to the output excitation parameter:

$$\frac{\partial}{\partial t_{kl}} \sum_{j=1}^{n} \alpha_j \, (\hat{\mu}_j - \mu_j)^2 \tag{4.25}$$

$$= \sum_{j=1}^{n} \frac{\partial}{\partial t_{kl}} \{\alpha_j \, (\hat{\mu}_j - \mu_j)^2\} \tag{4.26}$$

$$= \sum_{j=1}^{n} 2 \, \alpha_j \, (\hat{\mu}_j - \mu_j) \left(\frac{\partial \, \hat{\mu}_j}{\partial t_{kl}}\right) \tag{4.27}$$

$$= \sum_{j=1}^{n} 2 \, \alpha_j \, (\hat{\mu}_j - \mu_j) \frac{\partial \, \hat{\mu}_j}{\partial t_{kl}} \left(\frac{1}{N} \sum_{m=1}^{N} t_{jm} \right) \tag{4.28}$$

$$= \sum_{j=1}^{n} 2 \, \alpha_j \, (\hat{\mu}_j - \mu_j) \frac{1}{N} \, \frac{\partial \, \hat{\mu}_j}{\partial t_{kl}} \left(\sum_{m=1}^{N} t_{jm} \right) \tag{4.29}$$

$$= \sum_{j=1}^{n} 2\,\alpha_j\,(\hat{\mu}_j - \mu_j)\frac{1}{N}\;\;\delta_{jk} \tag{4.30}$$

$$= \frac{2}{N}\,\alpha_k\,(\hat{\mu}_j - \mu_j) \tag{4.31}$$

Where δ_{ij} δ_{jl} are the Kronecker deltas, with properties δ_{ij} = 1 for $i = k$ and δ_{jl} = 1 for $j = l$ and zero elsewhere.

The regularization method makes the neural network converge to a set of weights and biases having smaller values [19-20]. This makes the network response smoother and less likely to over-fit training data. As shown in Figure 4.10, the ratio α/β = 0. 1/0.9 = 0.11 produces the best fit to the true function. For a ratio larger than this, the network response has more error.

It should be mentioned that the proposed neural network algorithm needs the same input and output variables as the conventional one, but uses a modified performance function (objective function) that includes a penalty or regularization term in addition to the mean square error.

Table 4.3 shows the result of the experiment for the function approximation.

Table 4.3: Improvement of the Generalization Ability.

	Average Performance Function for 50 iterations		
Traditional ANN (mse) (4.15)	F= 0.28		
Modified ANN (F) (4.17), (4.18), (4.19)	$\gamma = 0.2$ F= 1.19	$\gamma = 0.5$ F= 0.39	$\gamma = 0.9$ F= 0.17

Also, the performance can be improved by specifying the way with which the speed and the efficient use of memory can be enhanced for the calculation of Jacobian *jX*. If the value of memory reduction is 1, the training process goes faster but demands a larger memory. By increasing the value of memory reduction to 2, the memory requirement decreases to one half, but it slows the training process. In the same way, the increment in the memory reduction value decreases the memory requirement and increases the training time.

Figure 4.8 shows the iteration at which the validation performance reached a minimum. The training process continued for six more iterations before it completely stopped. The validation and test curves look similar. Generally, the figure does not show any major problem with the training process. However, the difference can be noticed in the sense of performance function and the epoch number, as well.

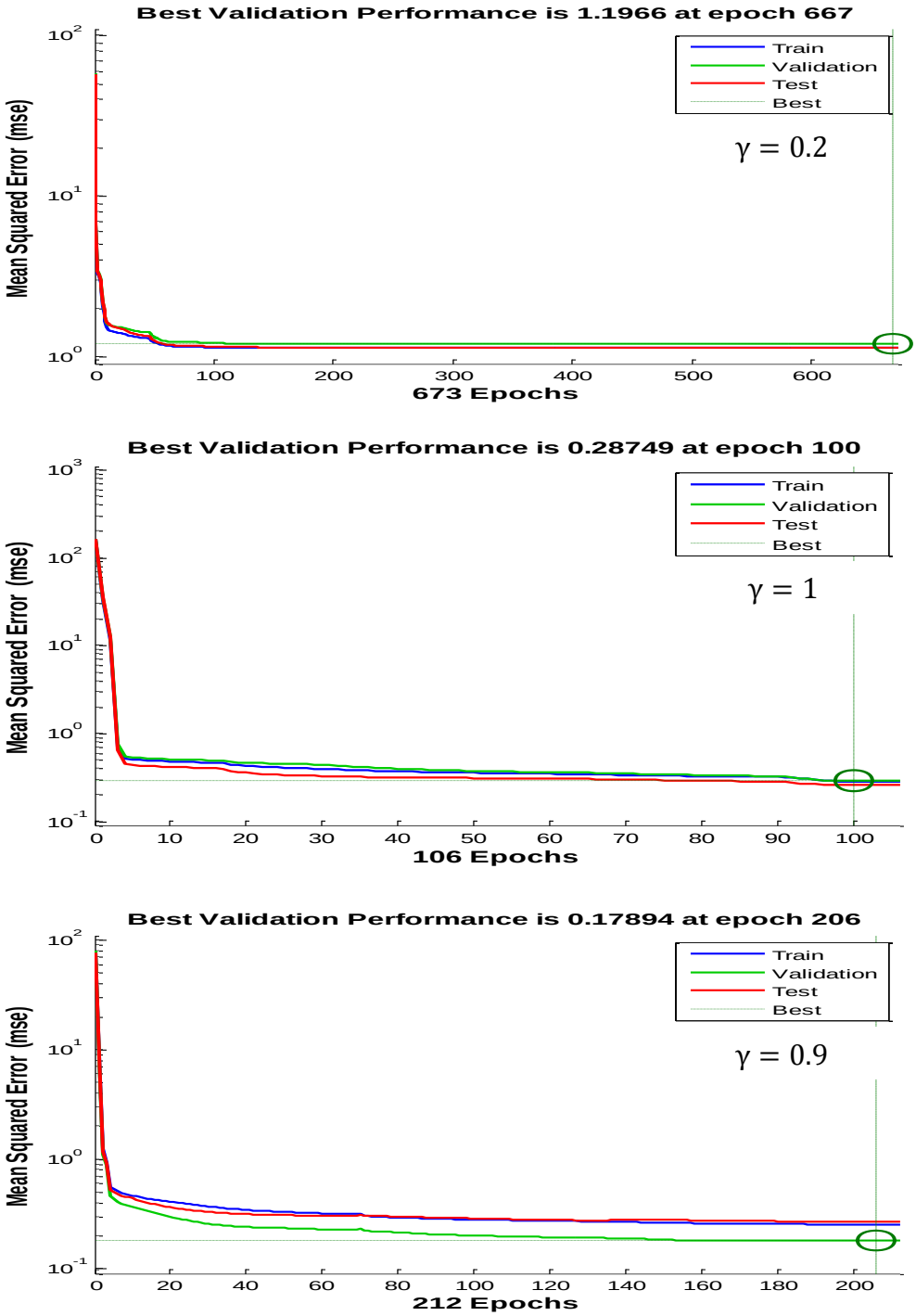

Figure 4.8: Performance of ANN scheme.

Figure 4.9 gives an indication of outliers. In other words, this plot shows the data points where the fit is worse than the majority of data. Most errors in the first plot are located between - 3.08 and 4.09. In addition, there certain errors that show on each side beyond this range; a fact that indicates a noise data or a fitting problem. On the other hand, in the second plot, most errors fall between - 1.3 and 1.1 then there is a good fit relationship between the outputs of the network and the target.

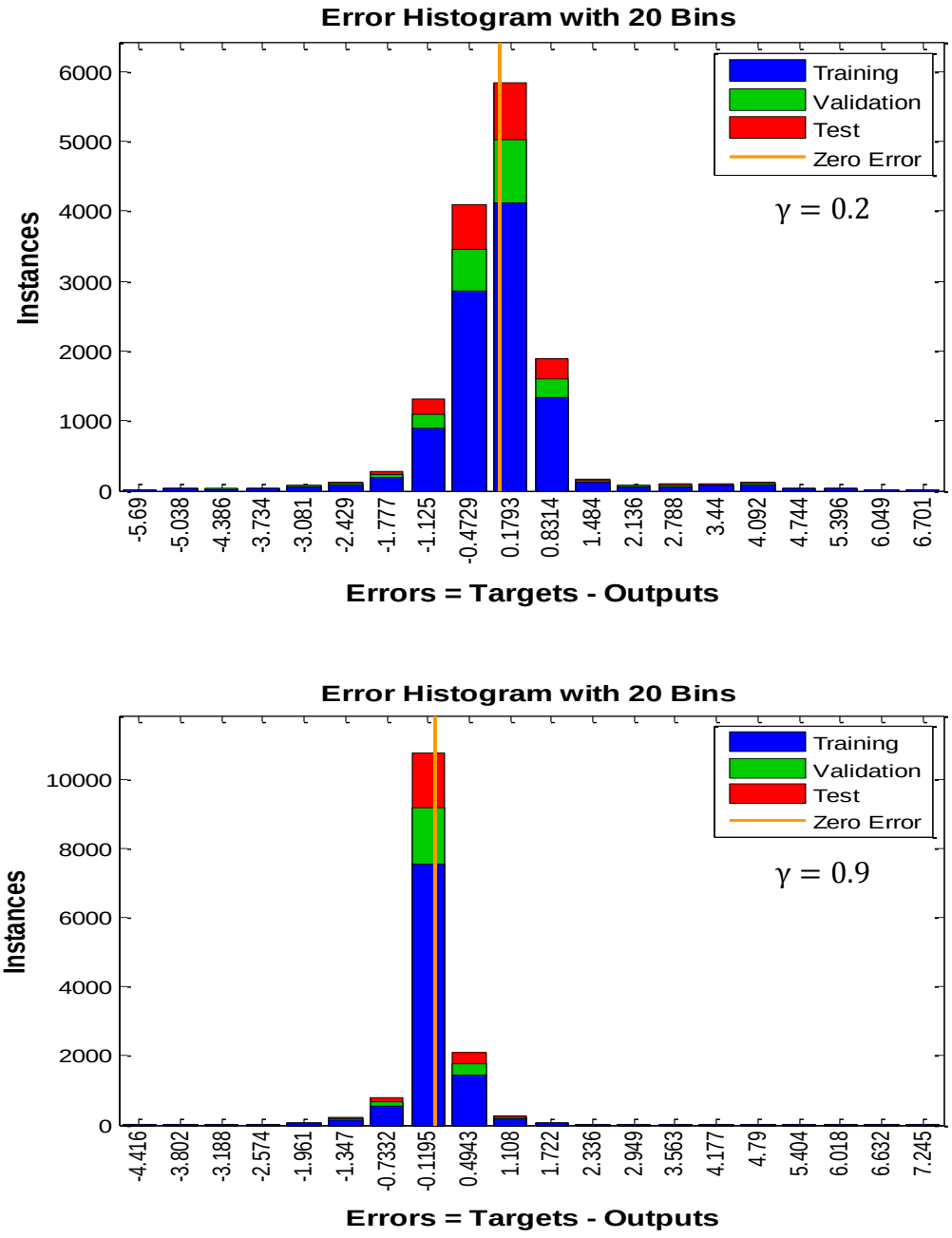

Figure 4.9: Error histogram of ANN scheme.

In Figure 4.10, a regression plot shows the relationship between the outputs and targets. The dashed line represents the perfect relationship where outputs = target. The solid line represents the best fit linear regression line between the outputs of the network and the targets. This relationship can be indicated by R value. When R=1, there is an exact relationship between outputs and targets. However, if R=0, there is no linear relationship. In this figure, the results show that the training data indicate a good fit.

$\gamma = 0.2$

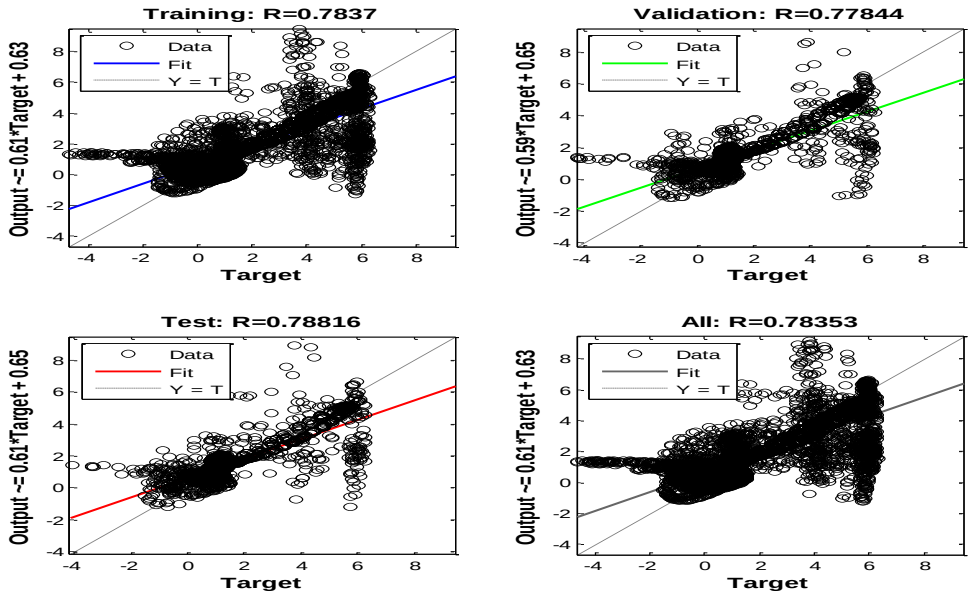

.....

$\gamma = 0.9$

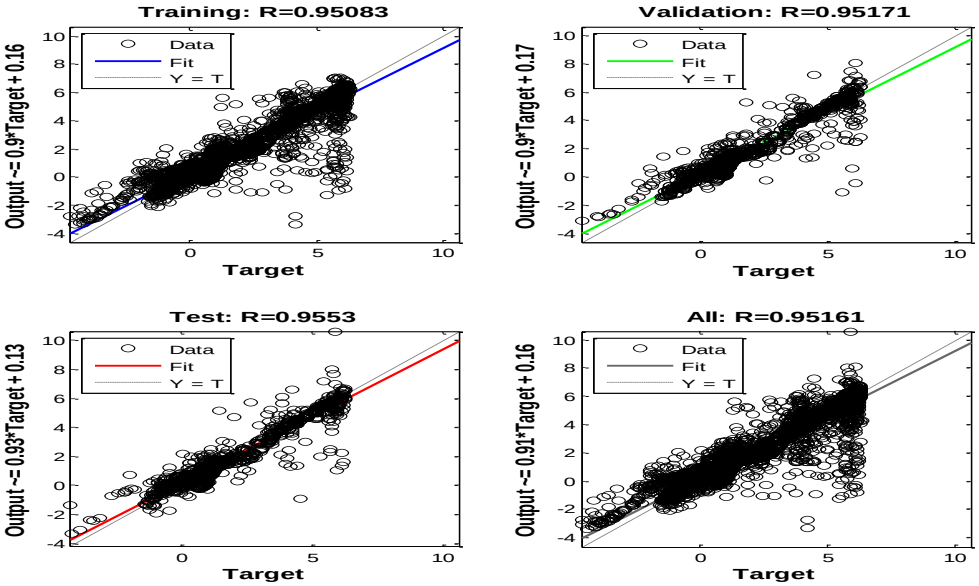

Figure 4.10: Regression of ANN scheme that shows the development.

As mentioned, the linear function was used for activating the neuron in the output layer since the output was not limited to 0 and 1 values as shown in Figure 4.12.

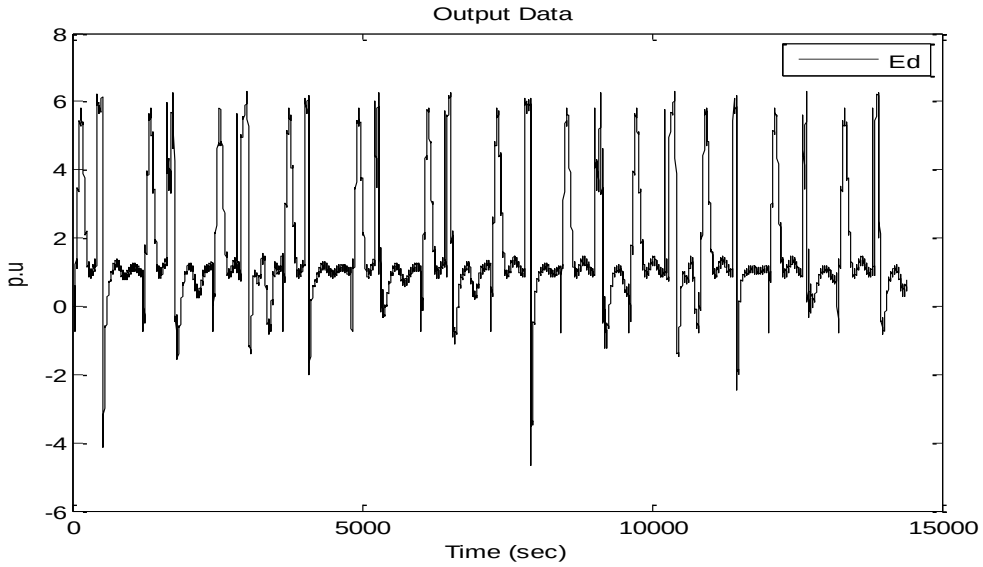

Figure 4.12: Output data of training process.

The property of learning is the most critically important advantage associated with the ANN. It can be carried out with a large amount of data.

Chapter 5:

Results and Discussion

A grid setup comparison between the conventional excitation and the ANN-Based PSS is discussed here. Figure 5.1 shows the IEEE 9-bus system that was used to make this comparison. The system shown in the figure used a 100 MVA synchronous condenser that was connected to bus no. 5 to provide reactive power compensation for faults during the operation. Figure 5.2 shows the IEEE 9-bus system with the synchronous condenser connected to bus no. 5 in the SIMULINK environment. Figure 5.3 magnifies the control scheme (ANN-based PSS).

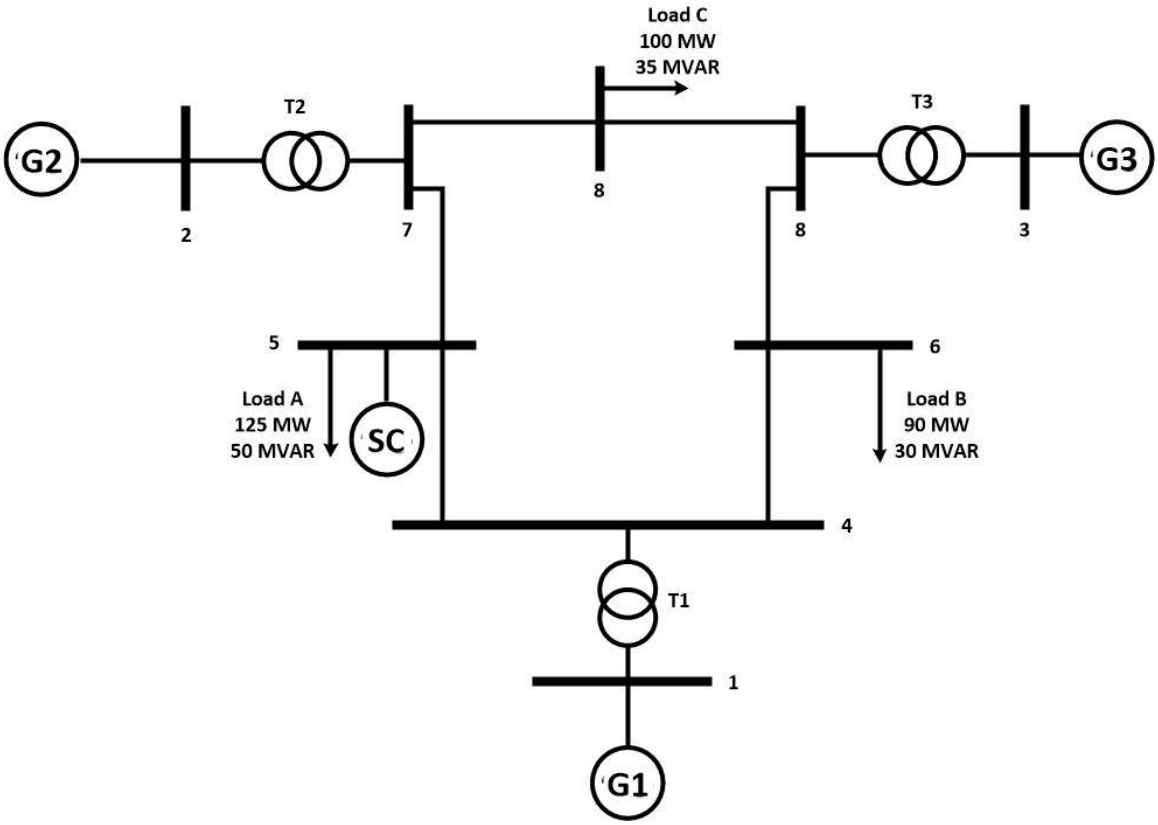

Figure 5.1: IEEE 9 bus power system [9].

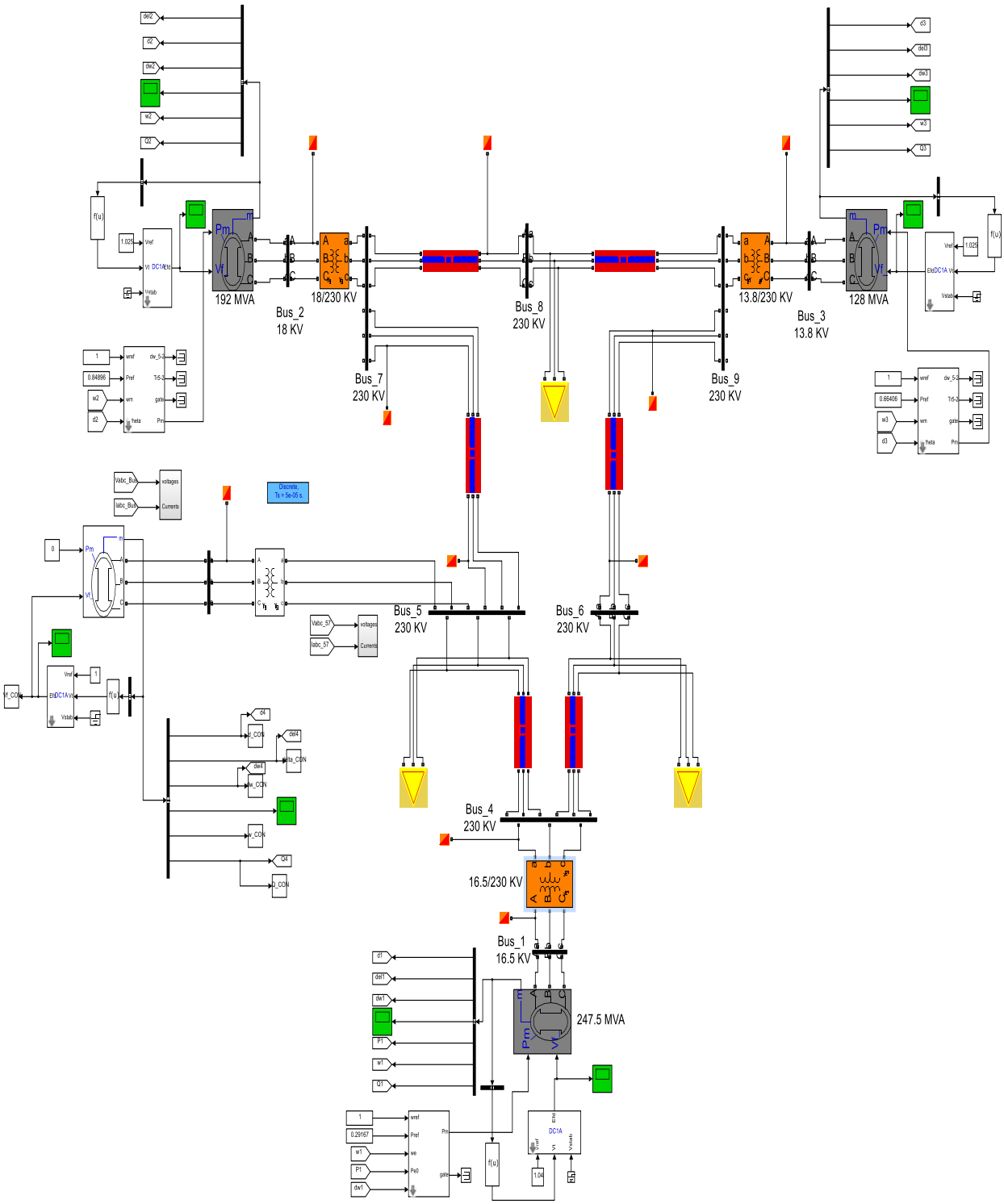

Figure 5.2: IEEE 9 bus including synchronous condenser connected to Bus #5.

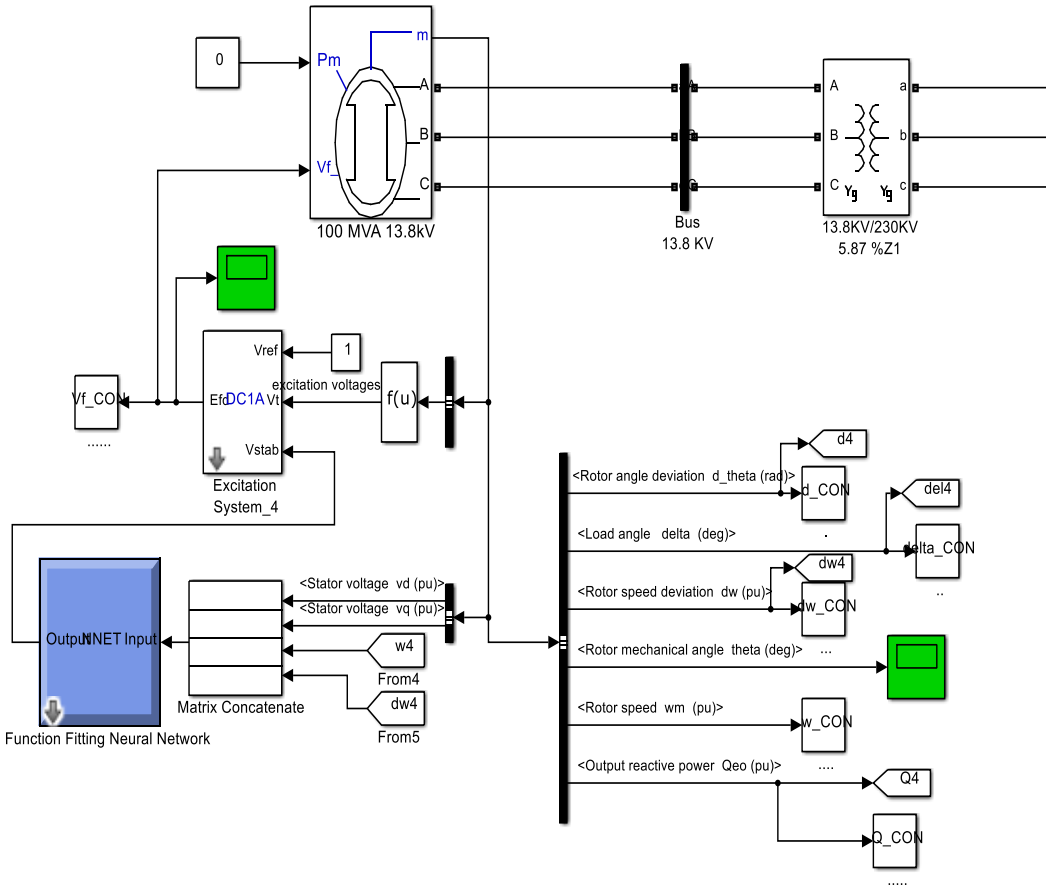

Figure 5.3: Synchronous condenser with ANN-Based PSS connected to Bus #5.

In order to compare the ANN-based PSS with a conventional excitation system, different cases were studied by changing parameters in the test system. The comparison of simulation results for the three cases are shown in Figures 5.4 through 5.13. These figures represent the simulation results without stabilizing control and with stabilizing control (ANN-based PSS).

In the following section, the conventional synchronous condenser was compared with the ANN-based PSS under three different cases.

Case 1: A 100ms 1-phase short circuit fault at bus no.5 happens at 1s and is cleared at 1.1s.

Case 2: An 80ms 3-phase short circuit fault at bus no.5 happens at 1s and is cleared at 1.08s. Then, a 50ms 1-phase short circuit fault at line 5-4 happens at 5s and is cleared at 5.05s.

Case 3: The impedance of the line between bus no. 7 and bus no. 5 changes from R_e= 0.169 and X_e = 2.259 x 10^{-3} to R_e= 0.338 and X_e = 4.518 x 10^{-3}.

For cases 4 and 5, we replace the ANN-based PSS with the SVC to determine which equipment responds more quickly. The comparison of simulation results for the two cases are shown in Figures 5.14 through 5.15. These figures represent the simulation results of the SVC, and the ANN-based PSS.

Case 4: A 100ms 1-phase short circuit fault at bus no.5 happens at 1s and is cleared at 1.1s.

Case 5: A 80ms 3-phase short circuit fault at bus no.5 happens at 1s and is cleared at 1.1s. Then, a 50ms 1-phase short circuit fault at line 5-4 happens at 5s and is cleared at 5.05s.

Table 5.1 lists the figures result.

Table 5.1: Results Direction

Figure No.	**Title**
Figure 5.4	Phase voltage of bus no. 5 (case 1)
Figure 5.5	Positive sequence voltage of synchronous condenser (case 1)
Figure 5.6	Reactive power injected (case 1)
Figure 5.7	Rotor speed deviation of the synchronous condenser (case 1)
Figure 5.8	Phase voltages of bus no. 5 (case 2)
Figure 5.9	Positive sequence voltage of synchronous condenser (case 2)
Figure 5.10	Reactive power injected (case 2)
Figure 5.11	Rotor speed deviation of the synchronous condenser (case 2)
Figure 5.12	Phase voltages of bus no. 5 (case 3)
Figure 5.13	Rotor speed deviation of the synchronous condenser (case 3)
Figure 5.14	Phase voltages of bus no. 5 (case 4)
Figure 5.15	Phase voltages of bus no. 5 (case 5)
Figure 5.16	Phase voltages of bus no. 5

5.1 Comparison of ANN-based PSS and Conventional Synchronous Condenser

The 100 MVA synchronous condenser is connected to bus no. 5 (230 kV) to provide reactive power compensation especially in the case of faults that can occur in the lines that provide power to the load. During the simulations, DC1A exciter is used for the conventional synchronous condenser. In the connection of the SC to the network, a Y_g/ Y_g coupling transformer with the same rated reactive power is used.

The parameters of the SC device is shown in Table 5.2:

Table 5.2: The SC Parameters

Reactances (pu)	
X_d	1.68
X'_d	0.23
X''_d	0.19
X_q	1.61
X'_q	0.23
X''_q	0.19
Xl	0.314
Time constants (s)	
T'_{do}	5.89
X''_{do}	0.001
X'_{qo}	0.6
X''_{qo}	0.001
Coupling Transformer	
Type	Y_g/ Y_g
V	13.8/ 230 Kv
X	j 0.0586 Ω

Case 1: A 100ms 1-phase short circuit fault at bus no.5 happens at 1s and cleared at 1.1s.

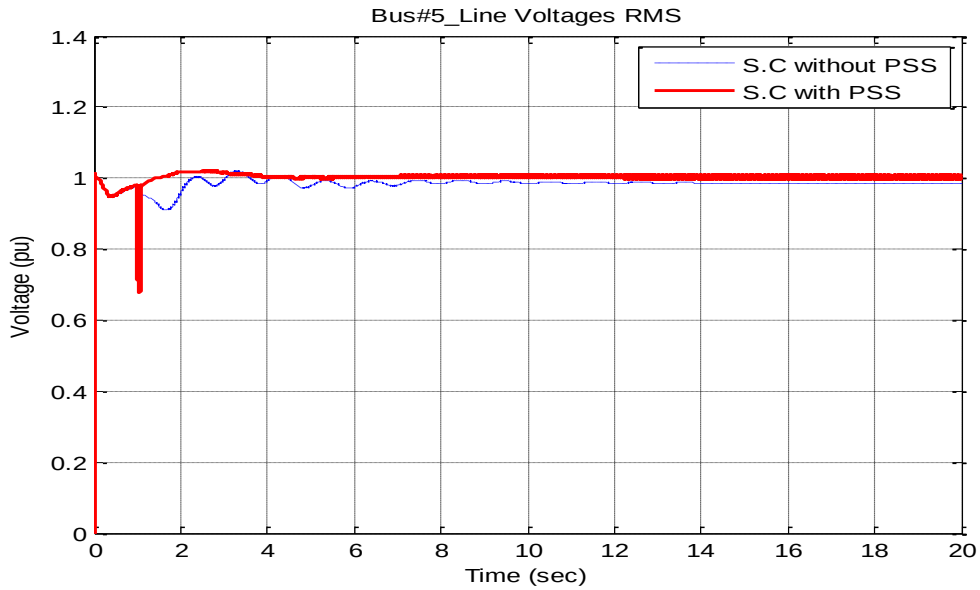

Figure 5.4: Phase voltage of bus no. 5 (case 1).

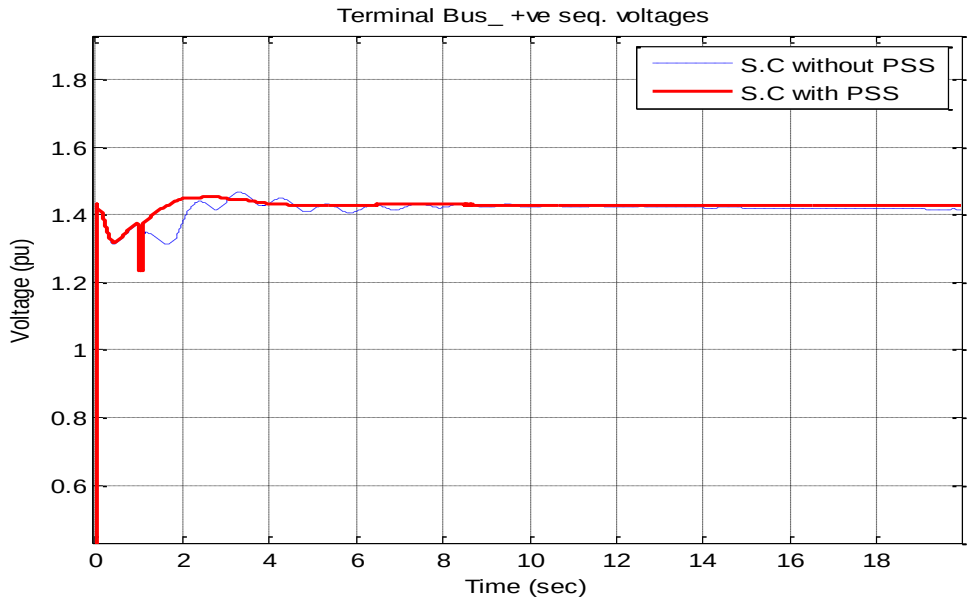

Figure 5.5: Positive sequence voltage of synchronous condenser (case 1).

The minimum voltage during the fault at bus no.5 for the SC without PSS is 0.71 p.u and 0.7 p.u for the SC with PSS. The SC with PSS brings the voltage back to nominal in less than 0.1 sec. However, it takes about 6 sec from SC without PSS to achieve that.

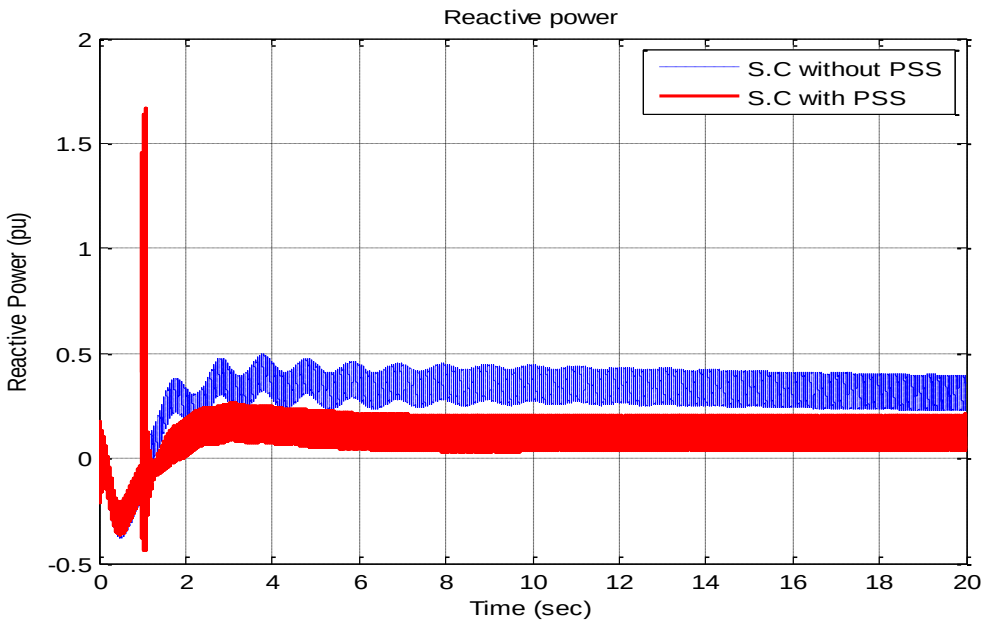

Figure 5.6: Reactive power injected (case 1).

It can be seen in Figure 5.6 that the reactive power injected by the ANN-based PSS is 1.7 p.u, whereas the reactive power injected by the conventional synchronous condenser is 0.38 p.u.

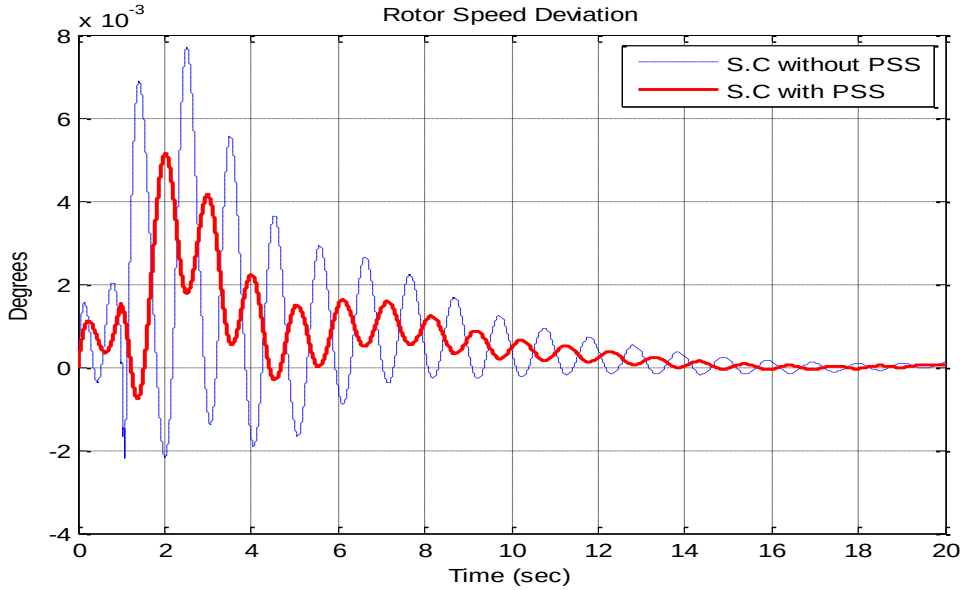

Figure 5.7: Rotor speed deviation of the synchronous condenser (case 1).

We can see from Figure 5.7 that not only does the conventional synchronous condenser deviate more than the ANN-based PSS, the settling time for SC without PSS is 19.5 sec, whereas the settling time for SC with PSS is around 16.2 sec. Additionally, the overshoot reduced from 7.7×10^{-3} degree to 5×10^{-3} degree.

Case 2: An 80ms 3-phase short circuit fault at bus no.5 occurs at 1s and cleared at 1.1s. Then, a 50ms 1-phase short circuit at line 5-4 occurs at 5s and cleared at 5.05s.

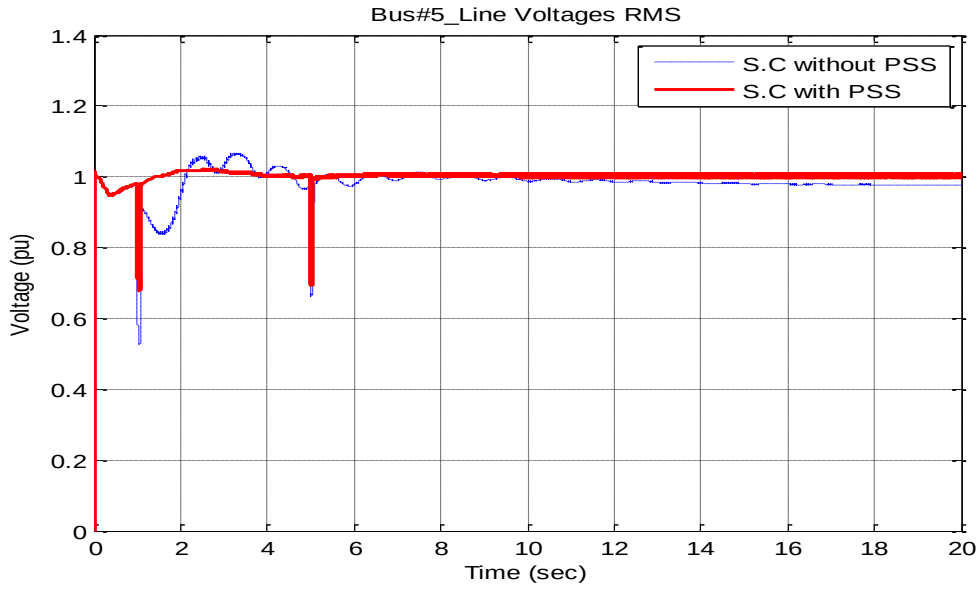

Figure 5.8: Phase voltages of bus no. 5 (case 2).

It can be seen that the ANN-based PSS synchronous condenser keeps the voltage level higher than the conventional excitation due to more reactive power injected by the ANN-based PSS synchronous condenser. The minimum voltage for the SC without PSS is 0.52 p.u and 0.66 p.u for the SC with PSS. So, the voltage dip is smaller when the SC with PSS is used.

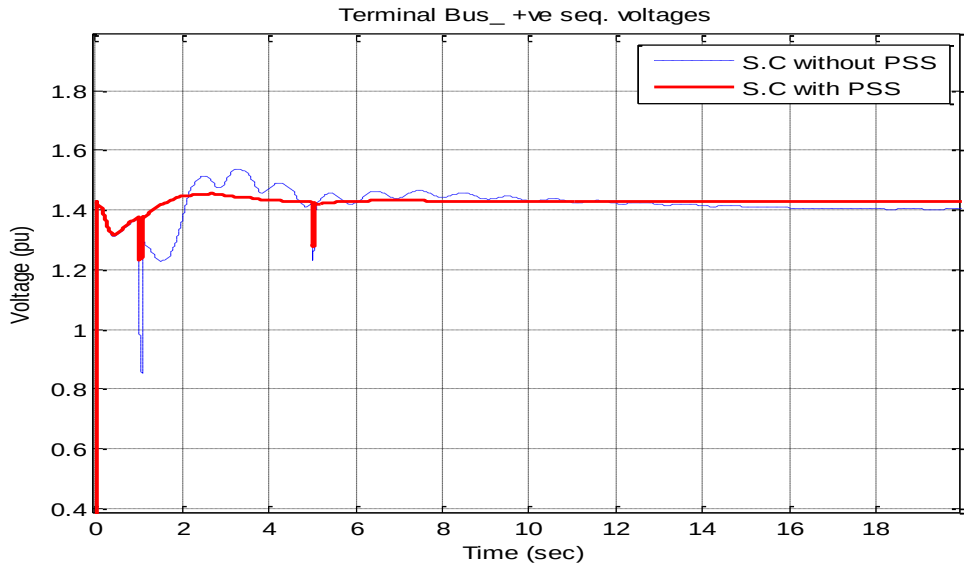

Figure 5.9: Positive sequence voltage of synchronous condenser (case 2).

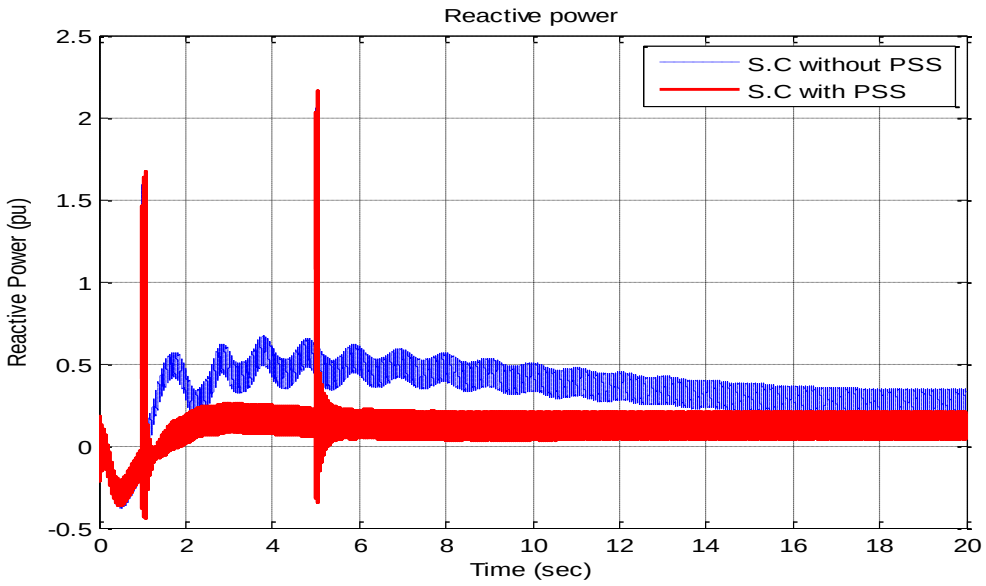

Figure 5.10: Reactive power injected (case 2).

Figure 5.10 shows that the reactive power injected by the ANN-based PSS is 2.2 p.u, whereas the reactive power injected by the conventional synchronous condenser is 1.6 p.u.

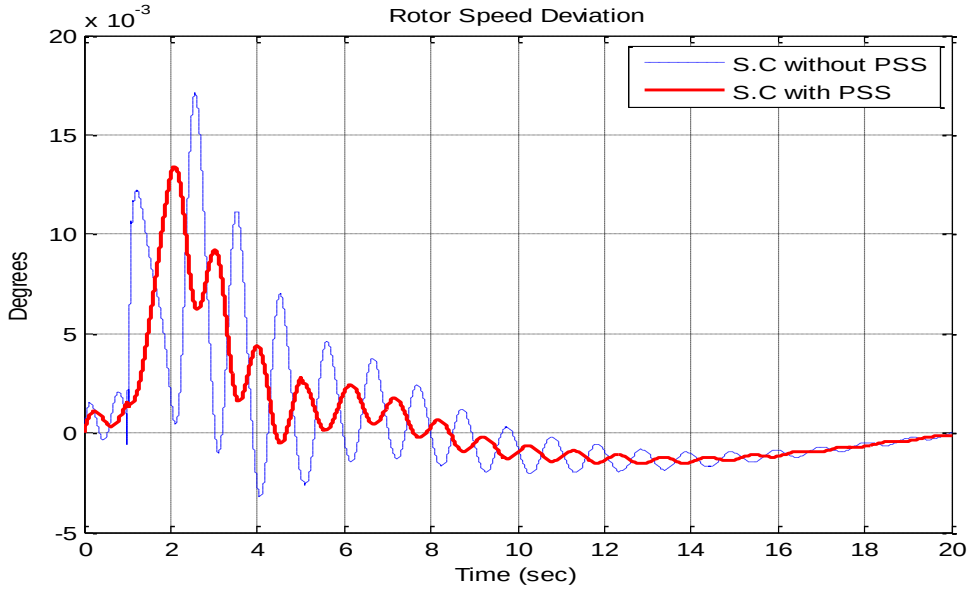

Figure 5.11: Rotor speed deviation of the synchronous condenser (case 2).

It can be seen that the speed deviates more with the conventional excitation due to greater voltage drop during the fault. In addition, the overshoot of the SC without PSS reaches 17×10^{-3} degree compared to 13×10^{-3} degree with PSS.

Case 3: The impedance of the line between bus no. 7 and bus no. 5 changes from R_e= 0.169 and X_e = 2.259 x 10^{-3} to R_e= 0.338 and X_e = 4.518 x 10^{-3}.

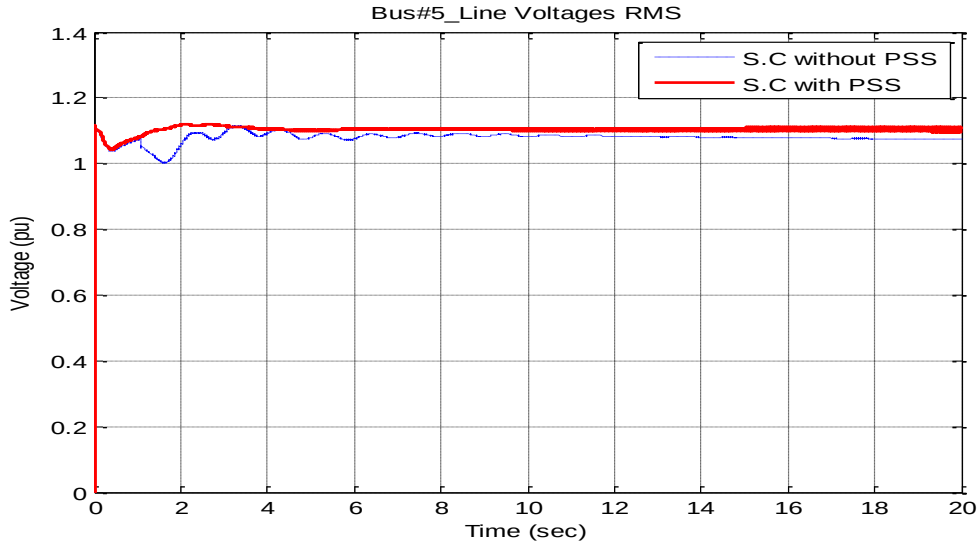

Figure 5.12: Phase voltages of bus no. 5 (case 3).

Since the impedance has changed, we expect to have a higher level of voltage compared to previous cases which had 1 p.u voltage. Now, we can see the voltage is about 1.1 p.u. The voltage appears to have oscillations which is likely caused by the swing of the SC's rotor.

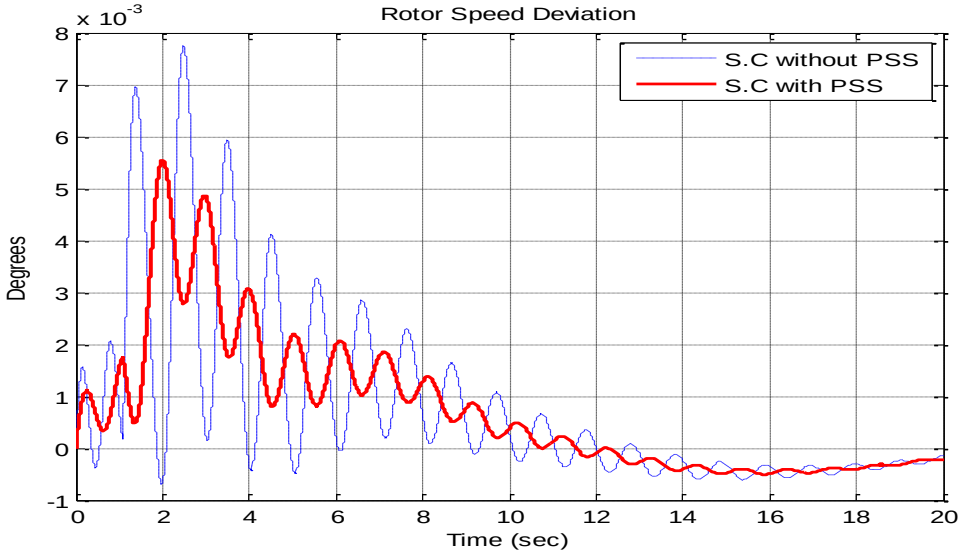

Figure 5.13: Rotor speed deviation of the synchronous condenser (case 3).

5.2 Comparison of ANN-based PSS and SVC

The inductance values have been adjusted in order to get a 100 MVA SVC model. In the connection of the SVC to the IEEE 9-bus system, a Δ/Y_g coupling transformer with the same rated power is used.

The parameters of the SVC device are shown in Table 5.3:

Table 5.3: The SVC Parameters

SVC device	
S	100 MVA
X	5.1 Ω
V	13.8 Kv
Coupling Transformer	
Type	Δ/Y_g
V	13.8/ 230 Kv
X	j 0.0586 Ω

Case 4: A 100ms 1-phase short circuit fault at bus no.5 happens at 1s and cleared at 1.1s (SVC and ANN-based PSS).

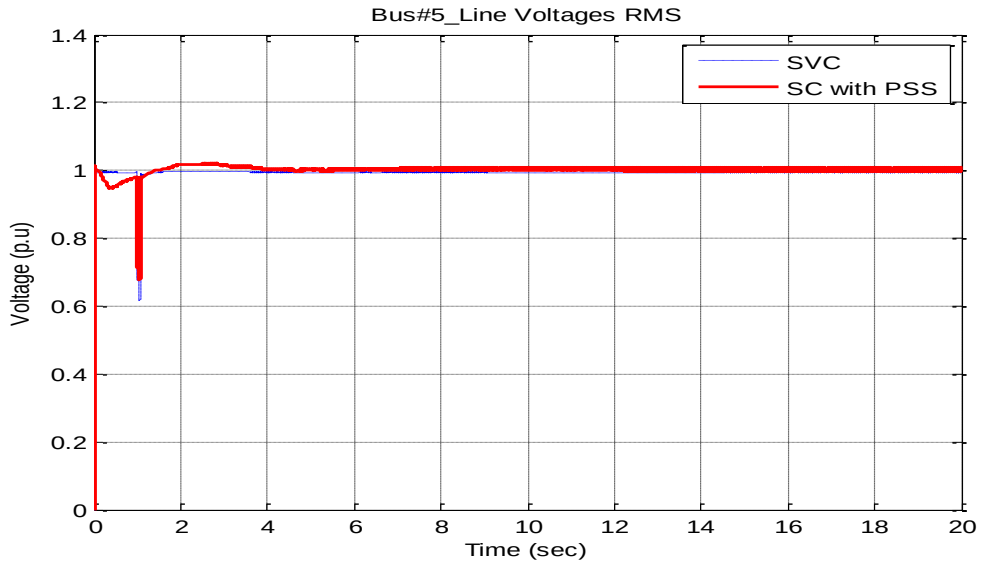

Figure 5.14: Phase voltages of bus no. 5. (case 4)

The SVC has fast response speed. Figure 5.14 shows SVC brings the voltage to nominal in 1.2 sec. However, it takes about 2.8 sec from the SC with PSS to do the same.

Case 5: An 80ms 3-phase short circuit fault at bus no.5 happens at 1s and cleared at 1.08s. Then, a 50ms 1-phase short circuit at line 5-4 happens at 5s and cleared at 5.05s (SVC and ANN-based PSS).

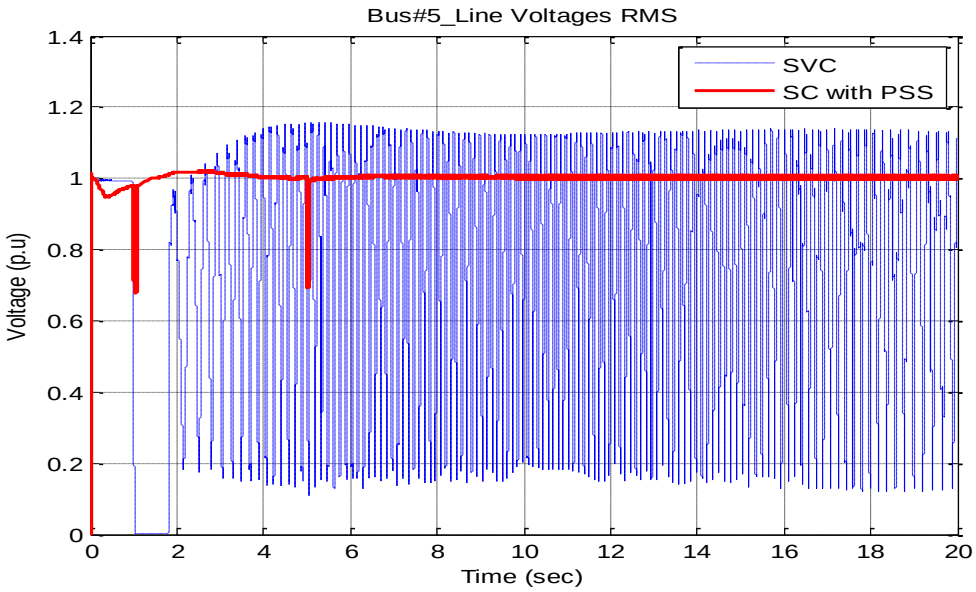

Figure 5.15: Phase voltages of bus no. 5. (case 5)

During faults that cause less voltage drop, such as Figure 5.14, SVC shows a better performance, whereas, during severe faults, such as Figure 5.15, synchronous condensers bring the voltage to nominal value in less than 1 sec.

Finally, we use the SVC and the synchronous condenser on the same bus. Then we apply case 5. Figure 5.16 shows that the SC helps the SVC to bring the voltage back to nominal voltage.

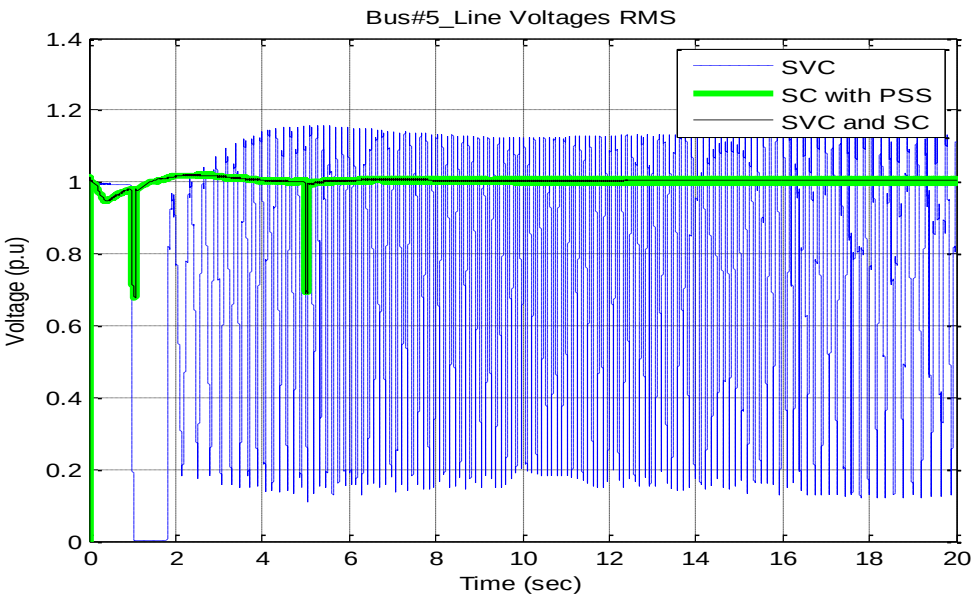

Figure 5.16: Phase voltages of bus no. 5.

Chapter 6

Conclusion and Suggestions for Future Work

In this thesis, the IEEE 9-bus system is implemented in MATLAB/SIMULINK and verified with another case simulated in the Powerworld environment. After verifying the model, a comparison between a conventional synchronous condenser and a synchronous condenser with ANN-based PSS was made by simulating different cases on the IEEE 9-bus system.

6.1 Conclusions:

i. The effectiveness of the power system stabilizer in achieving damping network oscillations was reviewed. Then the ANN-based PSS was introduced by taking the V_d, V_q, w, and dw of the synchronous condenser as the input signals to the ANN, and the excitation voltage as the output signal. The analysis shows that the ANN-based PSS shows better control performance in terms of settling time and damping effect.

ii. The general trend in ANN training is that the greater the number of hidden layers, the smaller the approximation error. However, so many hidden layers also demand more memory storage. In addition, more neurons mean more training time and hence, more memory consumption.

iii. Over-fitting may occur, rather than generalization, when a model captures the internal patterns of the input data.

iv. During the faults, the synchronous condenser with the ANN-based PSS injects more reactive power than the conventional synchronous condenser due to its higher level of robustness. Hence, the ANN-based PSS keeps the load voltage more stable.

v. The performance of reactive power compensation units depends on several factors such as fault type and fault location.

vi. During faults that cause less voltage drop on terminal bus, such as single phase to ground faults, the SVC shows a better performance since the SVC injects reactive power proportional to the square of its terminal voltage. On the other hand, during severe faults, such as three phase to ground faults, the ANN-based PSS synchronous condensers bring the voltage to the nominal voltage quicker. In addition, we notice that the SVC would need another compensator to survive and maintain the voltage of the system.

6.2 Suggestions for Future Work:

i. In general, a neural network can be used as a multi-input multi-output controller. In this work, four inputs and one output are considered for the ANN-based PSS. Increasing the number of inputs and outputs could enhance the learning process. In the case of a generator, the combination of AVR Ioop and Governor loop could be achieved. Both power oscillations and terminal voltage deviation could be controlled at the same time and in one control loop.

ii. This thesis mainly investigates the performance of a synchronous condenser as a reactive power compensation device in the IEEE 9-bus system. Further research could be done with similar methods to examine the performance of different combinations of reactive power compensation devices, such as synchronous condenser and SVC. An optimal solution might be found with the proper combination of various compensators to achieve optimal performance with minimum cost.

APPENDEX A

A.1

IEEE 9-Bus System Data

S_{base}= 100 MVA V_{base}= 230 KV Z_{base}= 529 Ohms

Transformer (T.F):

T.F number	T.F Voltage		Bus		Impedance		
			From	To	R(p.u)	X(p.u)	Y/2(p.u)
1	16.5 / 230 Kv	Delta/Way-g	1	4	0	0.0576	0
2	18 / 230 Kv	Delta/Way-g	2	7	0	0.0625	0
3	13.8 / 230 Kv	Delta/Way-g	3	9	0	0.0586	0

- Note: Values for the generator's transient reactance $X'_d(pu)$ are added to the reactance of the generator transformers.

Transmission Lines:

Line number	Bus		Impedance (p.u)		
	From	To	R(p.u)	X(p.u)	Y/2(p.u)
4	4	6	0.0170	0.0920	0.0790
5	4	5	0.0100	0.0850	0.0880
6	5	7	0.0320	0.1610	0.1530
7	6	9	0.0390	0.1700	0.1790
8	9	8	0.0119	0.1008	0.1045
9	8	7	0.0085	0.0720	0.0745

Bus		Impedance (Actual)					
From	**To**	**R (+ve seq.)**	**R (zero seq.)**	**L (+ve seq.)**	**L(zero seq.)**	**C (+ve seq.)**	**C(zero seq.)**
4	6	0.08993	0224	$1.29 * 10^{-3}$	$3.22 * 10^{-3}$	$7.92 * 10^{-9}$	$4.7 * 10^{-9}$
4	5	0.052	0.132	$1.19 * 10^{-3}$	$2.38 * 10^{-3}$	$8.8 * 10^{-9}$	$5.18 * 10^{-9}$
5	7	0.169	0.423	$2.25 * 10^{-3}$	$5.64 * 10^{-3}$	$15.3 * 10^{-9}$	$9.02 * 10^{-9}$
6	9	0.206	0.515	$2.38 * 10^{-3}$	$6.09 * 10^{-3}$	$17.9 * 10^{-9}$	$10.5 * 10^{-9}$
9	8	0.0629	0.157	$1.4 * 10^{-3}$	$3.53 * 10^{-3}$	$10.4 * 10^{-9}$	$6.15 * 10^{-9}$
8	7	0.0449	0.112	$1.01 * 10^{-3}$	$2.02 * 10^{-3}$	$7.47 * 10^{-9}$	$7.39 * 10^{-9}$

Values for the generator's transient reactance $X'_d(pu)$ are added to the reactance of the generator transformers. For example: for generator 2, bus 2 will be the internal bus for the voltage behind transient reactance; the reactance between bus 2 and bus 7 is the sum of the generator and transformer reactance (0.1198 + 0.0625)

Generator number	Bus		Impedance		
	From	**To**	**R(pu)**	**X(pu)**	**Y/2(pu)**
1	1	4	0	0.1184	0
2	2	7	0	0.1823	0
3	3	9	0	0.2399	0

Machine Data: All Data are in p.u on a 100 MVA base. All time constants are in sec.

Parameters	**M/C1**	**M/C2**	**M/C3**
Rated MVA	247.5	192	128
Power factor	1.0	0.85	0.85
Type	Hydro Salient-pole	Steam round	Steam round
Speed	180 r/min	3600 r/min	3600 r/min
Reactance (pu)			
$Xd\ (pu)$	0.361	1.72	1.68
$Xd'\ (pu)$	0.1504	0.23	0.23206
$Xd''\ (pu)$	0.099	0.1728	0.19
$Xq\ (pu)$	0.2398	1.65	1.61
$Xq'\ (pu)$	-	0.23	0.23206
$Xq''\ (pu)$	0.099	0.1728	0.19
X (leakage)	0.062	0.4224	0.314
Time Constants (sec)			
$Tdo'\ (sec)$	8.96	6	5.89
$Tdo''\ (sec)$	0.001	0.001	0.001
$Tqo'\ (sec)$	-	0.53	0.6
$Tqo''\ (sec)$	0.001	0.001	0.001
Inertia Coefficient			
H (sec)	9.55	3.33	2.35

Exciter Data:

Parameters	**M/C1**	**M/C2**	**M/C3**
TR (sec)	$20 * 10^{-3}$	$20 * 10^{-3}$	$20 * 10^{-3}$
KA	20.0	20.0	20.0
TA (sec)	0.20	0.20	0.20
Kf	0.063	0.063	0.063
Tf (sec)	0.35	0.35	0.35
Ke	1	1	1
Te (sec)	0.314	0.314	0.314
Vf	1.0818	1.7895	1.4036
R_s	0	0	0
A_{ex}	0.0039	0.0039	0.0039
B_{ex}	1.555	1.555	1.555

A.2

IEEE 9-Bus System Load Flow Report

Table 1 shows the load flow of IEEE 9-bus system which is obtained from the developed SIMULINK model compared with the load flow of the IEEE 9-bus model which is simulated in PowerWorld environment. It is evident that load flow obtained from developed SIMULINK model correlate very well with those reported in [2] as well. This validates the developed SIMULINK model.

Bus	**Type**	**Angles**	**Voltages SIMULINK**	**Voltages PowerWorld**	**PL**	**QL**	**PG**	**QG**
1	SL	0	1.0400	1.040	0	0	0.7164	27.05
2	PV	9.2800	1.0250	1.025	0	0	1.6300	6.65
3	PV	4.6648	1.0250	1.025	0	0	0.8500	-10.8
4	PQ	-2.217	1.0258	1.025	0	0	0	0
5	PQ	-3.988	0.9756	0.985	125.00	50.00	0	0
6	PQ	-3.687	1.0127	1.012	90.00	30.00	0	0
7	PQ	3.7197	1.0258	1.027	0	0	0	0
8	PQ	0.7275	1.0159	1.017	100.00	35.00	0	0
9	PQ	1.9667	1.0324	1.033	0	0	0	0

A.3

Excitation System of Synchronous Condenser

```
clear all;
clc;
close all;
%Open loot transfer function

num = 2.86;
den= [1 12.04 50.5 84.5 45.5];
rlocus(num,den)

%rlocus function to obtain the root locus plot
figure(1);
rlocus(num,den),ylabel('Imaginary Axis'),xlabel('Real Axis');

%Amplifier gain of 10 is taken
ka=20;

%The closed loop transfer function is given by
num1 = ka*[15.9 45.5];
den1 = [ 1 12.04 50.5 84.5 45.5+2.86*ka];

%function step is used to obtain the step response of the transfer
function
t = 0:0.05:20;
p=step(num1,den1,t);
figure(2);
plot(t,p),ylabel('Volatge'),xlabel('Time')

%sisotool is used to determine the time response characteristics
q=tf(num1,den);
sisotool('rlocus',q)
```

APPENDEX B

B.1

ANN Training Program

Data Collection:

Save ('PSS01.mat', 'Vd','Vq','W','dW','Vf','Vt_A','Vt_B','Vt_C');

SCR= 0.001
[1 1.2]
001 A,G,0.2sec
002 AB,G,0.2sec
003 ABC,G,0.2sec
[1 1.1]
004 A,G,0.1sec
005 AB,G,0.1sec
006 ABC,G,0.1sec

SCR= 0.001
[1.5 1.7]
007 A,G,0.2sec
008 AB,G,0.2sec
009 ABC,G,0.2sec
[1.5 1.6]
010 A,G,0.1sec
011 AB,G,0.1sec
012 ABC,G,0.1sec

Data concatenation:

```
clc
clear all

Vd1= [Vd.data];
Vq1= [Vq.data];
W1 = [W.data]
dW1= [dW.data];
Vf1= [Vf.data];

clear Vd Vq W dW Vf

%%%%%%%%%%%%%%%%%%%%%%%%%%
```

```
Vd1= [Vd1 Vd.data];
Vq1= [Vq1 Vq.data];
W1= [W1 W.data];
dW1= [dW1 dW.data];
Vf1= [Vf1 Vf.data];

clear Vd Vq W dW Vf

%%%%%%%%%%%%%%%%%%%%%%%%

Vd=Vd1(:);
Vq=Vq1(:);
W=W1(:);
dW=dW1(:);
Vf=Vf1(:);

clear Vd1 Vq1 W1 dW1 Vf1

%%%%%%%%%%%%%%%%%%%%%%%%%%
%
Input= [Vd, Vq, W, dW];
Output= Vf;
clear Vd Vq W dW Vf

%%%%%%%%%%%%%%%%%%%%%%%%%
load('traning_data_full.mat');

Input1=downsample(Input,500);
Output1=downsample(Output,500);

clear Input Output
%%%%%%%%%%%%%%%%%%%%%%

t=0:50e-6:60;
```

Training Process:

```
% This script assumes these variables are defined:
%   Input1 - input data.
%   Output1 - target data.
 load('traningdatadownsample.mat');

inputs = Input1';
targets = Output1';

% Create a Fitting Network
hiddenLayerSize = 50;
net = fitnet(hiddenLayerSize);
```

```
% Choose Input and Output Pre/Post-Processing Functions
% For a list of all processing functions type: help nnprocess
net.inputs{1}.processFcns = {'removeconstantrows','mapminmax'};
net.outputs{2}.processFcns = {'removeconstantrows','mapminmax'};


% Setup Division of Data for Training, Validation, Testing
% For a list of all data division functions type: help nndivide
net.divideFcn = 'dividerand';  % Divide data randomly
net.divideMode = 'sample';  % Divide up every sample
net.divideParam.trainRatio = 70/100;
net.divideParam.valRatio = 15/100;
net.divideParam.testRatio = 15/100;

% For help on training function 'trainlm' type: help trainlm
% For a list of all training functions type: help nntrain
net.trainFcn = 'trainlm';  % Levenberg-Marquardt

% Choose a Performance Function
% For a list of all performance functions type: help nnperformance
net.performFcn = 'msereg';  % Mean squared error + Mean square weight


net.trainParam.regularization = 0.98;

net.trainParam.mem_reduc = 1;

% Choose Plot Functions
% For a list of all plot functions type: help nnplot
net.plotFcns = {'plotperform','plottrainstate','ploterrhist', ...
  'plotregression', 'plotfit'};


% Train the Network
[net,tr] = train(net,inputs,targets);

% Test the Network
outputs = net(inputs);
errors = gsubtract(targets,outputs);
performance = perform(net,targets,outputs)

% Recalculate Training, Validation and Test Performance
trainTargets = targets .* tr.trainMask{1};
valTargets = targets  .* tr.valMask{1};
testTargets = targets  .* tr.testMask{1};
```

```
trainPerformance = perform(net,trainTargets,outputs)
valPerformance = perform(net,valTargets,outputs)
testPerformance = perform(net,testTargets,outputs)

% View the Network
view(net)

% Plots
% Uncomment these lines to enable various plots.
%figure, plotperform(tr)
%figure, plottrainstate(tr)
%figure, plotfit(net,inputs,targets)
%figure, plotregression(targets,outputs)
%figure, ploterrhist(errors)
gensim(net,50e-6);
```

Generate Plotting

```
set(0,'ShowHiddenHandles','On')   % This command used for menu bar.
set(gcf,'menubar','figure')

close all

load ('traningdatadownsample_plot');

figure(1);
plot (Vd,'-b');
hold on
plot (Vq,':g');
hold on
plot (w,'--k','LineWidth',1);
hold on
plot (dw,':r','LineWidth',3);
title('Input Data ');
xlabel('Time (sec)');
ylabel('p.u');
legend('Vd','Vq','w','dw');

figure(2);
plot (Output1,'-k');
title('Output Data ');
xlabel('Time (sec)');
ylabel('p.u');
legend('Ed');
```

```
close all

load('Case.mat');

figure(1);
plot(V_A5,'-k','LineWidth',2); grid on
hold on
plot(V_A5_CON,'-b','LineWidth',2);
hold on
plot(V_A5_NN,'-r','LineWidth',2);
title('Bus#5_Line Voltages Phase A');
xlabel('Time');
ylabel('Volts');
legend('Base Case', 'without PSS','ANN based-PSS');

figure(2);
plot(V_B5,'-k','LineWidth',2); grid on
hold on
plot(V_B5_CON,'-b','LineWidth',2);
hold on
plot(V_B5_NN,'-r','LineWidth',2);
title('Bus#5_Line Voltages Phase B');
xlabel('Time');
ylabel('Volts');
legend('Base Case', 'without PSS','ANN based-PSS');

figure(3);
plot(V_C5,'-k','LineWidth',2); grid on
hold on
plot(V_C5_CON,'-b','LineWidth',2);
hold on
plot(V_C5_NN,'-r','LineWidth',2);
title('Bus#5_Line Voltages Phase C');
xlabel('Time');
ylabel('Volts');
legend('Base Case', 'without PSS','ANN based-PSS');

figure(4);
plot(Vt_CON,'-b','LineWidth',2); grid on
hold on
plot(Vt_NN,'-r','LineWidth',2);
title('Terminal Bus of SC_ +ve seq. voltages');
xlabel('Time');
ylabel('Volts');
legend('Base Case', 'without PSS','ANN based-PSS');

figure(5);
plot(Q_CON,'-b','LineWidth',2); grid on
hold on
plot(Q_NN,'-r','LineWidth',2);
title('Reactive power');
xlabel('Time');
ylabel('Reactive Power PU');
```

```
legend('without PSS','ANN based-PSS');

figure(6);
plot(Vf_CON,'-b','LineWidth',2); grid on
hold on
plot(Vf_NN,'-r','LineWidth',2);
title('Excitation Voltages');
xlabel('Time');
ylabel('Volts');
legend('without PSS','ANN based-PSS');

figure(7);
plot(delta_CON,'-b','LineWidth',2); grid on
hold on
plot(delta_NN,'-r','LineWidth',2);
title('load angle');
xlabel('Time');
ylabel('Degree');
legend('without PSS','ANN based-PSS');

figure(8);
plot(dw_CON,'-b','LineWidth',2);
hold on
plot(dw_NN,'-r','LineWidth',2);
title('Rotor Speed Deviation');
xlabel('Time');
ylabel('Degrees');
legend('without PSS','ANN based-PSS');
```

BIBLIOGRAPHY

[1] J. Duncan Glover, Mulukutla S. Sarma, and Thomas J. "Overbye, Power System Analysis and Design," Cengage Learning, 2012.

[2] A.E. Fitzgerald, Charles Kingsley Jr. and Stephen Umans, "Electric Machinery," McGraw-Hill, 2003.

[3] T. J. E. Miller, "Reactive Power Control in Electric Power Systems," New York: Wiley, 1982.

[4] Sercan Teleke, Tarik Abdulahovic, Torbjörn Thiringer, and Jan Svensson. "Dynamic Performance Comparison of Synchronous Condenser and SVC," IEEE Transactions on Power Delivery, Vol. 23, no. 3, July 2008.

[5] Paul E. Marken, Arthur C. Depoian, John Skliutas, and Michael Verrier. "Modern Synchronous Condenser Performance Considerations," IEEE Power and Energy Society General Meeting, p 5 pp, 2011.

[6] Paul E. Marken, Mike Henderson, Dean LaForest, John Skliutas, Jim Roedel, and Todd Campbell. "Selection of Synchronous Condenser Technology for the Granite Substation," IEEE/PES Transmission & Distribution Conference & Exposition (T&D), p 6 pp., April 2010.

[7] P. Marken, D. LaForest, R. D'Aquila, D. Wallace, E. Kronbeck, and J. Skliutas. "Dynamic Performance of the Next Generation Synchronous Condenser at VELCO,"presented at IEEE PES Power Systems Conference and Exposition, Seattle, WA, March 2009.

[8] P. E. Marken, J. P. Skliutas, P.Y. Sung, K.S. Kim, H.M. Kim, L.H. Sailer, and R.R. Young. "New Synchronous Condensers for Jeju Island," presented at IEEE Power & Energy Society General Meeting. New Energy Horizons - Opportunities and Challenges, p 6 pp., 2012.

[9] P.M. Anderon, A.A Fouad, "Power System Control and Stability," Wiley, 2003.

[10] S. Kalsi, D. Madura, R. Howard, G. Snitchler, T. MacDonald, D. Bradshaw, I. Grant, and M. Ingram, "Superconducting Dynamic Synchronous Condenser for Improved Grid Voltage Support," presented at the IEEE Transm. Distrib. Conf., Dallas, TX, Sep. 2003.

[11] A. Hammad and B. Roesle, "New Roles for Static Var Compensators in Transmission Systems," Brown Boveri Rev., vol. 73, pp. 314–320, Jun. 1986.

[12] Yi Zhang, Aniruddha M. Gole, "Consideration of Inertia for Design of Reactive Power Compensation Devices for HVDC Transmission Systems," 10th IET International Conference on AC and DC Power Transmission (ACDC 2012), p 6 pp., 2012.

[13] O.B. Nayak, A.M. Gole, et al, "Dynamic Performance of Static and Synchronous Compensators at an HVDC Inverter Bus in A Very Weak AC System," IEEE Transactions on Power Delivery, vol. 9, no. 3, pp 1350-1358, April 1994.

[14] Swarn Kalsi, David Madura, Tim MacDonald, Mike Ingram, and Ian Grant, "Operating Experience of a Superconductor Dynamic Synchronous Condenser," IEEE/PES Transmission and Distribution Conference and Exhibition, p 4 pp., 2005-2006.

[15] K.K. Yagnik, V. Ajjarapu, "Consideration of the Wind and Solar Generation Reactive Power Capability on Grid Voltage Performance," 2012 IEEE Power & Energy Society General Meeting. New Energy Horizons - Opportunities and Challenges, p 7 pp., 2012

[16] P. Kundur, D. C. k,and H. M. Zein El-Din, "Power System Stabilizers for Thermal Units: Analytical Techniques and On-Site Validation," IEEE Trans.. Power Apparatus and System, vol. PAS-100, pp. 81-95, Jan. 1981.

[17] J. P. Bayne, D. C. Lee, and W. Watson, "A Power System Stabilizer for Thermal Units Based on Deviation of Accelerating Power," IEEE Trans. Power Apparatus and Systems, vol. PAS-96, pp. 1777-1783, 1977.

[18] R. G. Faxmer, "State-of-the-Art Technique for System Stabilizer Tuning," IEEE Trans. Power Apparatus and System, vol. PAS-102, pp. 699-709, 1983.

[19] A. Doi and S. Abe, "Coordination Synthesis of Power System Stabilizer in Multimachine Power System," IEEE Trans. Power Apparatus and Systems, vol. PAS-103, pp. 14734479, June 1984.

[20] W. C. Chan and Y. Y. Hsu, "An Optimal Variable Structure Stabilizer for Power System Stabilizer," IEEE Trans. Power Apparatus and Systems, vol. PAS-102, pp. 1738-1746, 1983.

[21] D.E. Rumelhart, G.E. Hinton, and R.J. Williams, "Learning Internal Representation by Error Propagation," Parallel Distributed Processing: Explorations in the Microstructure of Cognition, ml. 1, pp. 318-362, 1986.

[22] S. Haykin, "Neural Network, A Comprehensive Foundation, Multi-Layer Perception," pp. 138-229, 1994, IEEE Press.

[23] Y. Zhaag, G.P. Chen, O.P. Malik, and G.S. Hope, "An Artificial Neural Network Based Adaptive Power System Stabilizer," IEEE Trans. on Energy Conversion, vol. 8, no. 1, pp. 71-77, 1993.

[24] Y. Zhang, O.P. Malik, G.S. Hope, and G.P. Chen, "Application of an Inverse Input-Output Mapped as a Power System Stabilizer," IEEE Trans. on Energy Conversion, vol. 9, no. 3, pp. 433-441, 1999.

[25] P. Kundur, "Power System Control and Stability," New York: McGraw-Hill, vol. PAS-88, pp. 1103–1166, 1994.

[26] N.G. Hingorani, L. Gyugyi, Understanding FACTS, "Concepts and Technology of Flexible AC Transmission Systems," IEEE Press, 2000.

[27] N.G. Hingorani, "High Power Electronics and Flexible Ac Transmission System," IEEE Power Engineering Review, vol.8, no.7, pp.3-4, July 1988.

[28] IEEE FACTS Terms & Definitions Task Force of the FACTS Working Group of the DC and FACTS subcommittee, "Proposed Terms and Definitions for Flexible AC Transmission System (FACTS)," IEEE Trans. on Power Delivery, vol. 12, no. 4, pp. 1848-1853, Oct. 1997.

[29] L. Gyugyi, "Application Characteristics of Converter-based FACTS controllers," IEEE Conference on Power System Technology, vol. 1, pp. 391 - 396, Dec. 2000.

[30] P. J. Werbos, “Back propagation and neurocontrol: A Review and Prospectus, International Joint Conference on Neural Networks,” Washington, DC, vol. 1,pp. 209-216, 1989.

[31] J. M. Mendel and R. W. McLaren, “Reinforcement Learning Control and Pattern Recognition Systems, in Adaptive, learning and Pattern Recognition System Theory and Application,” New York, Academic Press, pp. 287-318, 1970.

[32] T. Kohonen, “Self-organization and Associative Memory,” Berlin: Springer - Verlag, 1989.

[33] I. D. Landau, “A Survey of Model Reference Adaptive Techniques: Theory and Application,” Automatica, vol. 10, pp. 353-379, 1974.

[34] A. Gosh, G. Ledwich, O.P. Malik, and G.S. Hope, “Power System Stabilizer based on Adaptive Control Techniques,” IEEE Trans. on Power Apparatus and Systems, vol. PAS-103, pp. 1983-1986, 1984.

[35] S.J. Cheng, O.P. Malik, and G.S. Hope, “Damping Of Multi-Mode Oscillations in Power System Using a Dual-Rate Adaptive Stabilizer,” IEEE Trans. on Power Systems, vol. PWRS-3, no. 1, pp. 101-108, 1988.

[36] T. Thgi and M. Sugaio, “Derivation of Fuzzy Control Rules From Human Operator's Control Action,” Proc. IFAC Symp. Fuzzy Inform Knowledge Representation and Decision Analysis, pp. 55-60, July 1983.

[37] P.J. King and E.H. Mamdani, “The Application of Fuzzy Control Systems to Industrial Processes,” Automatica, vol. 13, no. 3, pp. 235-242, 1977.

[38] C.C. Lee, “Fuzzy Logic in Control System: Fuzzy Logic Controller Part I and II,” IEEE Trans. on Computers, vol. 20, no. 2, pp. 404-435, 1990

[39] T. Hiyama and T. Sameshima, “Fuzzy Logic Control Scheme for On-Line Stabilization of Multi-Machine Power System,” Fuzzy Sets and Systems, vol 39, pp. 181494, 1991.

[40] M.A.M Hassan, O.P. Malik, and G.S. Hope, “A Fuzzy Logic Based Stabilizer for a Synchronous Machine,” IEEE Trans. on Energy Conversion, vol. 6, no. 3, pp. 407-413, 1991

[41] Canada-U.S. Power System Outage Task Force. "<http://www.knowledgerush.com/kr/encyclopedia/Canada-U.S_Power_System_Outage_Task_Force/>," Nov. 2003. Web. Aug. 2010.

[42] A. Glaninger-Katschnig. "Contribution of Synchronous Condensers for the Energy Transition," Elektrotechnik & Informationstechnik, , vol. 130, no. 1, pp. 28-32, February 2013.

[43] B. Gao, G. Morison, and P. Kundur, "Voltage Stability Evaluation Using Modal Analysis," IEEE Trans. on Power Systems, vol. 7, no. 4, pp. 1423-1543, Nov 1992.

[44] G. Morison, B. Gao and P. Kundur, "Voltage Stability Analysis Using Static and Dynamic Approaches," IEEE Trans. on Power Systems, vol. 8, no. 3, pp. 1159-1171, Aug. 1993.

[45] A. Ah-Hindi, and Muhammad Choudhry, "Voltage Collapse Prediction for Interconnected Power System," 33rd North American Power Symposium, Oct. 2001.

[46] J. Dixon, L. Moran, E. Rodriguez, R. Domke, "Reactive Power Compensation Technologies: State-of-the-Art Review," IEEE Trans. Ind. Appl., vol. 93, no. 12, pp. 2144-2164,Dec. 2005.

[47] S. Kalsi, "Development Status of Superconducting Rotating Machines," IEEE PES Meeting, New York, 27-31 January 2002

[48] S. Kalsi et al., "Development Status of Rotating Machines Employing Superconducting Field Windings," Proc. IEEE, vol. 92, no. 10, pp. 1688-1704, Oct. 2004.

[49] P. Kundur, "Power System Stability and Control," McGraw-Hill, Inc. 1994

[50] IEEE Power Engineering Society, "IEEE Recommended Practice for Excitation System Models for Power System Stability Studies," IEEE Std. 421.5-2005.

[51] Sobajic, D.J. and Yoh-Han Pao, "Neural Net Synthesis of Tangent Hypersurfaces for Transient Security Assessment of Electric Power Systems," same source as [5], pp. 87-92.

[52] Avramovic, B., "On Neural Network Voltage Assessment," Neural Network Computing for the Electric Power Industry: Proceedings Of The 1992 INNS Summer Workshop, Editor Dejan J. Sobajic, Lawrance Erlbaum Associates, Publishers, Hillsdale, pp. 81-85, N.J., 1993.

[53] Ostojic, D.R. and G.T. Heydt, "Transient Stability Assessment by Pattern Recognition in The Frequency Domain," IEEE Transactions on Power Systems, vol.6, no.1, pp. 231- 237, February 1991.

[54] Ren-mu, H. and A.J. Germond, "Comparison of Dynamic Load Models Extrapolation Using Neural Networks and Traditional Methods," same source as [5], pp. 77-80.

[55] Samad, T., "Modeling and Identification with Neural Networks," Neural Network Computing for the Electric Power Industry: Proceedings of the 1992 INNS Summer Workshop, Editor Dejan J. Sobajic, Lawrance Erlbaum Associates, Publishers, Hillsdale, N.J., pp. 129-134, 1993.

[56] Novosel, D. and R.L. King, "Intelligent Load Shedding," Neural Network Computing For the Electric Power Industry: Proceedings Of The 1992 INNS Summer Workshop, Editor Dejan J. Sobajic, Lawrance Erlbaum Associates, Publishers, Hillsdale, N.J., pp. 107-110, 1993.

[57] Park, D.C., M.A. El-Sharkawi, and R.J. Marks II, L.E. Atlas and M.J. Damborg, " Electric Load Forecasting Using an Artificial Neural Network," IEEE Transactions on Power Systems, vol. 6, no. 2, pp. 442-449, May 1991.

[58] Cheung, J.Y., D.C. Chance, and J. Fogan, "Load Forecasting By Hierarchical Neural Networks That Incorporate Known Load Characteristics," Neural Network Computing For the Electric Power Industry: Proceedings Of The 1992 INNS Summer Workshop, Editor Dejan J. Sobajic, Lawrance Erlbaum Associates, Publishers, Hillsdale, N.J., pp. 179-182, 1993.

[59] Parlos, A.G. and A.D. Patton, "Empirical Modeling in Power Engineering Using The Recurrent Multilayer Perceptron Network," Neural Network Computing For the Electric Power Industry: Proceedings Of The 1992 INNS Summer Workshop, Editor Dejan J. Sobajic, Lawrance Erlbaum Associates, Publishers, Hillsdale, N.J., pp. 123-128, 1993.

[60] Ebron, S., D. Lubkerman, and M. White, "A Neural Network Approach to the Detection of Incipient Faults on Power Distribution Feeders," IEEE Transactions on Power Delivery, vol.5, no.2, pp. 905-914, April 1990.

[61] Aggoune, M., M.A. El-Sharkawi, D.C. Park, M.J. Damborg and R.J. Marks II, "Preliminary Results on Using Artificial Neural Networks for Security Assessment," IEEE Transactions on Power Systems, Vol.6, No.2, pp. 890-896, May 1991.

[62] Chen, C-R. and Y-Y Hsu, "Synchronous Machine Steady-State Stability Analysis Using An Artificial Neural Network," IEEE Transactions on Energy Conversion, vol.6, no.1, pp. 12-20, March 1991.

[63] Santoso, N.I. and O.T. Tan, "Neural-Net Based Real-time Control Capacitors Installed on Distribution Systems," IEEE Transaction on Power Delivery, vol.5, no.1, pp. 266- 272, January 1990.

[64] Avramovic, B., "On Neural Network Voltage Assessment," Neural Network Computing For the Electric Power Industry: Proceedings Of The 1992 INNS Summer Workshop, Editor Dejan J. Sobajic, Lawrance Erlbaum Associates, Publishers, Hillsdale, N.J.,pp. 81-85,1993.

[65] Mori, H., "Voltage Stability Monitoring with Artificial Neural Networks," Neural Network Computing For the Electric Power Industry: Proceedings Of The 1992 INNS Summer Workshop, Editor Dejan J. Sobajic, Lawrance Erlbaum Associates, Publishers, Hillsdale, N.J., pp. 101-106, 1993.

[66] Lawrence S., Giles C.L., Tsoi A.C., "What Size Neural Network Gives Optimal Generalization?," Technical Report, Institute for Advanced Computer Studies, University of Maryland, 1996.

[67] Prechelt L., "Automatic Early Stopping using Cross Validation: Quantifying the Criteria," Neural Networks, vol. 11, no. 4, pp. 761-767, 1998.

[68] Teixeira R.A., Braga A.P., Takahashi R.H.C., Saldanha R.R., "Improving Generalization of MLPs with Multi-objective Optimization," Neurocomputing, vol. 35, no. (1-4), pp.189-194, 2000.

[69] Demuth H., Beale M., "Neural Network Toolbox for Use with MATLAB," user's guide version 4, 2000

[70] G. Verghes, I. Perez-Arriaga and F. Schewwppe, "Selective Modal Analysis with Application to Electric Power Systems," Part II IEEE trans, I. On Power APP. And System, vol. PAS 101, no. 9, pp. 3117-3134, 1982.

[71] Chun-Jung Chen and Tien-Chi Chen, "Design of a Power System Stabilizer Using a New Recurrent Neural Network," IEEE proceedings, First International Conference on Innovative Computing, Information and Control, vol. I, pp. 39-42, 2006.

[72] Holger R. Maier and Graeme C. Dandy, "Neural Networks for the Prediction and Forecasting of Water Resources Variables: a Review of Modelling Issues and Applications," Environmental Modelling & Software 15, pp. 39-42, 2000.

[73] Lachman. T and Mohamad T., "Neural Network Excitation Control System for Transient Stability Analysis of Power System," IEEE Region 10 Conference, January 2010.

[74] Laughlin and Sejnowski, "Communication in Neuronal Networks," Science, vol 301, pp. 1870-1874, September 2003.

[75] Stallard B. and Taylor J., "Quantifying Multivariate Classification Performance—the Problem of Overfitting," SPIE Annual Conference, Denver, 1999.

[76] Gelb, "Applied Optimal Estimation," MIT Press, Cambridge, 1979.

[77] Haykin S., "Neural Networks and Learning Machines," 3rd Edition, Prentice Hall, 2009.

[78] Kasabov N.K., "Foundations of Neural Networks, Fuzzy Systems, and Knowledge Engineering," The MIT Press, Cambridge, Massachusetts, London, second edition, 1996.

[79] Lawrence S., Giles C.L., and Tsoi A.C., "What Size Neural Network Gives Optimal Generalization?," Technical Report, Institute for Advanced Computer Studies, University of Maryland, 1996.

[80] Mohammad Daliri and Mehdi Fatan, "Improving the Generalization of Neural Networks by Changing The Structure of Artificial Neuron," Malaysian Journal of Computer Science, vol. 24, no. 4, 2001.

[81] Prechelt L., "Automatic Early Stopping Using Cross Validation: Quantifying the Criteria," Neural Networks, vol. 11, no. 4, pp. 761-767, 1998.

[82] Teixeira R.A., Braga A.P., and Takahashi R.H.C., Saldanha R.R., "Improving Generalization of MLPs with Multi-objective Optimization," Neurocomputing, vol. 35, no. 1-4, pp. 189-194, 2000.

[83] Demuth H. and Beale M., "Neural Network Toolbox for Use with MATLAB," user's guide version 4, 2000.

[84] Siraj F. and Osman W.R.S., "Improving Generalization of Neural Networks Using MLP Discriminant Based on Multiple Classifiers Failures," The 2nd Intl. Conf. on Computational Intelligence, Modelling and Simulation, Bali, 2010.

[85] Hua Q., Gao Y., Wang X.-Z., and Zhao B.-Y., "A New Approach to Improving Generalization Ability of Feed-Forward Neural Networks," Intl. Conf. on Machine Learning and Cybernetics (ICMLC), Qingdao, 2010.

[86] Horwill, C., Young, D.J., Wong, K.T.G., "A design for a relocatable tertiary connected SVC," IEE Conference on AC and DC power transmission, London, 1996.